

ISTANBUL TECHNICAL UNIVERSITY ★ GRADUATE SCHOOL OF SCIENCE
ENGINEERING AND TECHNOLOGY

**INVESTIGATION OF MECHANICAL PROPERTIES OF RANDOM CARBON
NANOTUBE NETWORKS USING MOLECULAR DYNAMICS METHOD**

M.Sc. THESIS

Alper Tunga ÇELEBİ

Department of Mechanical Engineering

Solid Mechanics Programme

Thesis Advisor: Prof. Dr. Ata MUĞAN

AUGUST 2013

ISTANBUL TECHNICAL UNIVERSITY ★ GRADUATE SCHOOL OF SCIENCE
ENGINEERING AND TECHNOLOGY

**INVESTIGATION OF MECHANICAL PROPERTIES OF RANDOM CARBON
NANOTUBE NETWORKS USING MOLECULAR DYNAMICS METHOD**

M.Sc. THESIS

Alper Tunga ÇELEBİ
(503111502)

Department of Mechanical Engineering

Solid Mechanics Programme

Thesis Advisor: Prof. Dr. Ata MUĞAN

AĞUSTOS 2013

İSTANBUL TEKNİK ÜNİVERSİTESİ ★ FEN BİLİMLERİ ENSTİTÜSÜ

**RASTGELE DAĞILMIŞ KARBON NANOTÜP AĞ YAPILARINDA MEKANİK
ÖZELLİKLERİNİN MOLEKÜLER DİNAMİK YÖNTEMİ İLE İNCELENMESİ**

YÜKSEK LİSANS TEZİ

**Alper Tunga ÇELEBİ
(503111502)**

Makina Mühendisliği Anabilim Dalı

Katı Cisimlerin Mekaniği Yüksek Lisans Programı

Tez Danışmanı: Prof. Dr. Ata MUĞAN

AĞUSTOS 2013

Alper Tunga ÇELEBİ, a **M.Sc.** student of **ITU Graduate School of Science Engineering and Technology** student ID **503111502** successfully defended the thesis entitled “**INVESTIGATION OF MECHANICAL PROPERTIES OF RANDOM CARBON NANOTUBE NETWORKS USING MOLECULAR DYNAMICS METHOD**”, which he prepared after fulfilling the requirements specified in the associated legislations, before the jury whose signatures are below.

Thesis Advisor : **Prof. Dr. Ata MUĞAN**
Istanbul Technical University

Co-advisor : **Assist. Prof. Dr.Cengiz BAYKASOGLU**
Hitit University

Jury Members: **Assoc. Prof. Dr. Serdar BARIŞ**
Istanbul University

Assist. Prof. Dr. Erdal BULĞAN
Istanbul Technical University

Assist. Prof. Dr. Hakan ERSOY
Akdeniz University

Date of Submission : 03 May 2013

Date of Defense : 13 August 2013

To my family and friends,

FOREWORD

This thesis is dedicated to my family, Sema – Osman - Deniz Çelebi, who have always been with me when I needed them and supported me always. I would like to thank each of them for their guidance, encouragement, support and love over the years.

I wish to sincerely thank my supervisor Prof. Dr. Ata Muğan for his suggestions, encouragements and guidance in writing and approaching the different challenges during the thesis. I also wish to thank my co-adviser Assist. Prof. Dr. Cengiz Baykasoğlu for his precious guidance, help and advice.

I want to thank Mesut Kırca for his valuable background, technical and practical support, vision, and help during my thesis. I would like to thanks Esra İçer who has always been a precious friend for years.

Thank you to my thesis committee members, Assoc. Prof. Dr. Serdar Barış and Assist. Prof. Dr. Erdal Bulğan and Assist. Prof. Dr. Hakan Ersoy for their considerations and directions.

Last but not the least, I would like to thank my dear friends Alptunç Çomak, Burak Tüzüner, Cihat Bora Yiğit, Gökçe Burak Tağlıoğlu, Mehmet Sait Özer, Şengül Arı for their support, help and advice.

August 2013

Alper Tunga ÇELEBİ
(Mechanical Engineer)

TABLE OF CONTENTS

	<u>Page</u>
FOREWORD	ix
TABLE OF CONTENTS	xi
ABBREVIATIONS	xiii
LIST OF TABLES	xv
LIST OF FIGURES	xvii
1. INTRODUCTION	1
2. CARBON NANOTUBES	9
2.1 Nanotechnology and Carbon-based Nanostructures	9
2.2 Essentials of Carbon Nanotubes.....	11
3. INTRODUCTION TO MOLECULAR DYNAMICS	Hata! Yer işareti tanımlanmamış.
3.1 Basics of Molecular Dynamics Simulation .Hata! Yer işareti tanımlanmamış.	
3.2 Statistical Ensembles.....	20
3.3 Periodic Boundary Conditions	21
3.4 Molecular Potentials.....	21
3.4.1 Bonded Interactions	22
3.4.2 Non-bonded Interactions.....	23
4. MANY BODY POTENTIALS	25
4.1 Bonded Potentials.....	25
4.1.1 Modified morse potential	25
4.1.2 Reactive empirical bond order potential	27
4.1.3 Adaptive intermolecular reactive empirical bond order potential	29
4.2 Non-bonded Potentials	29
4.2.1 Lennard-Jones potential	29
4.2.1 Columbic pairwise potentials.....	30
5. EVALUATING MECHANICAL PROPERTIES OF SWCNT USING MOLECULAR DYNAMICS SIMULATIONS	Hata! Yer işareti tanımlanmamış.
5.1 A Brief View to the Classical Structural Mechanics.....	Hata! Yer işareti tanımlanmamış.
5.2 Molecular Dynamics Simulations for SWCNT	33
5.3 Fracture Investigation.....	40
6. CARBON NANOTUBE NETWORKS	43
6.1 Network Generation	46
6.1.1 General concepts	46
6.1.2 General algorithm	47
6.1.2.1 Selection of CNTs from the library.....	48
6.1.2.2 Rotation and translation of candidate items	49
6.1.2.3 Implementation of design constraints	51
6.1.2.4 Decision of sub-loop	52
6.1.2.5 Generation of LAMMPS input data file:	53

6.1.2.6 Networks	53
6.2 Heat Welding of Junctions	54
6.3 Mechanical Loading Simulations	57
7. SIMULATION RESULTS	63
7.1 Mechanical Properties of 3D Random Carbon Nanotube Network	63
7.1.1 Young's modulus	64
7.1.2 Ultimate tensile strength.....	67
7.1.3 Yield strength	68
7.1.4 Poisson's ratio	69
7.1.5 Density	70
7.2 A Smaller Carbon Nanotube Network	71
8. CONCLUSION.....	73
9. REFERENCES	77
APPENDICES	87
CURRICULUM VITAE	89

ABBREVIATIONS

AFM	: Atomic Force Microscopy
AIREBO	: Adaptive Intermolecular Reactive Empirical Bond Order
CNT	: Carbon Nanotube
FEM	: Finite Element Methods
LAMMPS	: Large-scale Atomic/Molecular Massively Parallel Simulator
LJ	: Lennard-Jones
MD	: Molecular Dynamics
MSM	: Molecular Structural Mechanics
MWCNT	: Multi-walled Carbon Nanotube
REBO	: Reactive Empirical Bond Order
SEM	: Scanning Electron Microscopy
SWCNT	: Single-walled Carbon Nanotube
TEM	: Transmission Electron Microscopy
UTS	: Ultimate Tensile Strength
VdW	: Van der Waals

LIST OF TABLES

	<u>Page</u>
Table 2.1 : Some Comparative Mechanical Properties of Carbon nanotubes	11
Table 2.2 : Types of CNTs Based on Chiral Indices	13
Table 4.1 : Modified Morse Potential Parameters.....	26
Table 4.2 : Tersoff- Brenner Potential Constants.....	28
Table 5.1 : Comparative Investigations in Literature.....	38
Table 5.2 : Poisson's Ratios of Previous Studies	40
Table 7.1 : Parameters for Calculation of Density	73

LIST OF FIGURES

	<u>Page</u>
Figure 1.1 : Basic Approaches on Determining Mechanical Properties of CNTs.	1
Figure 2.1 : Presentation of Some Materials in Nanoscale World	9
Figure 2.2 : Carbon-based Nanostructures : a) C60: Buckminsterfullerene; b) Nested Giant Fullerenes; c) Carbon Nanotube; d) Nanocones; e) Nanotoroids; f) Graphene Surface; g) 3D Graphite Crystal; h) Haecelitic Surface; i) Graphene Nanoribbons; j) Graphene Clusters; k) Helicoidal Carbon Nanotube; l) Short Carbon Chains; m) 3D Schwarzite Crystals; n) Carbon Nanofoams o) 3D Nanotube Networks, and p) Nanoribbons 2D Networks	10
Figure 2.3 : a) A Two-dimensional Graphene Sheet, b) Single-walled CNT.....	11
Figure 2.4 : Nanotube Types: a) Armchair, b) Zigzag, c) Chiral.....	12
Figure 2.5 : Single-walled and Multi-walled Carbon Nanotubes	13
Figure 3.1 : Periodic Boundary Conditions.	21
Figure 3.2 : Interatomic Interactions	22
Figure 3.3 : Illustration of Van de Waals Interactions.....	23
Figure 3.4 : LJ Potential and Van der Waals Force versus Distance	24
Figure 4.1 : Force-strain curve of modified Morse Potential.....	26
Figure 4.2 : LJ force as the Distance between Two Interacting Atoms Changes	30
Figure 4.3 : Interaction of Two Separate Atoms.....	31
Figure 5.1 : Representation of Boundary and Loading Conditions.....	34
Figure 5.2 : Initial Situation of a (10,10) SWCNT.....	34
Figure 5.3 : Gradual Deformation Period of a SWCNT	36
Figure 5.4 : Schematic Representation of the SWCNT's Cross-section.....	37
Figure 5.5 : Strain Curves of a Single-walled Carbon Nanotube under Tensile Force by Using Adaptive Intermolecular Reactive Empirical Bond Order Potential	37
Figure 5.6 : Equivalent FE Model of the Defect-free and Defected SLGS Model; a) One Atom Vacancy, b) SW Defects	40
Figure 5.7 : Various Structural Defects on a (8,0) Nanotube.....	41
Figure 5.7 : The Brenner and The Modified Morse Potentials and Tensile Force Fields.....	41
Figure 6.1 : Images of Aerogels	43
Figure 6.2 : Ordered and Random CNTs	45
Figure 6.3 : Line Segment Representation.....	48
Figure 6.4 : Possible Segmentation of Target Item.....	49
Figure 6.5 : Rotation and Translation	50
Figure 6.6 : Mislocated Carbon Nanotubes.	52
Figure 6.7 : Increasing Number of CNTs in Design Space	53
Figure 6.8 : a) 3D CNT Network b) 2D CNT Network.....	54
Figure 6.9 : Images of Junction Regions.	55

Figure 6.10 : A Welded 2D Carbon Nanotube Network.....	56
Figure 6.11 : A Welded 3D Carbon Nanotube Network.....	56
Figure 6.12 : Initial CNT Network Without Any Deformation.	58
Figure 6.13 : Gradual Time Increase on Deformation Process (Isometric View). ...	59
Figure 6.14 : Gradual Time Increase on Deformation Process (Side View).	60
Figure 6.15 : Deformation under Exaggerated Tensile Force.....	61
Figure 7.1 : A Typical Engineering Stress-Strain Curve.....	64
Figure 7.2 : Units for “metal” and “SI” for MD Simulations.	66
Figure 7.3 : Stress-Strain Curve For 3D Random CNT Network.....	67
Figure 7.4 : Deformation of a Cube under Uniaxial Tensile Load	70
Figure 7.5 : A Smaller Carbon Nanotube Network Structure.....	70

INVESTIGATION OF MECHANICAL PROPERTIES OF RANDOM CARBON NANOTUBE NETWORKS USING MOLECULAR DYNAMICS METHOD

SUMMARY

Nanotechnology can be described as a very promising scientific field, which deals with design, production, fabrication and application of structures and materials in nanometer scales, and it enables to understand the unique physical properties of atoms, molecules and things with the size ranging from subnanometers to a couple of hundred nanometers. In particular, carbon-based nanostructures are considered to be in the center of many recent discussions on nanotechnology.

There are various carbon-based nanostructures including nanotubes, nanocones, fullerene, graphenes, nanoribbons, nanorods, nanotoroids etc. In this thesis, we study on carbon nanotube networks comprising of numerous carbon nanotubes (CNTs). Carbon nanotubes have particularly attracted researchers' interest for many years. Exceptional properties of carbon nanotubes are the main reasons of this interest of researchers in worldwide. The CNTs have the good combination of high stiffness, high strength, low density, small size, high fracture toughness, high electrical conductivity and good optical properties. However, these properties are generally practical in nanoscale applications. To transfer those features in continuum proportion, two-dimensional and three-dimensional network ideas are proposed.

In this thesis, a self-controlled algorithm is described to generate two-dimensional and three-dimensional networks consisting of numerous random intersected carbon nanotubes, which are distributed systematically in design space. The algorithm manipulates the length and chirality of individual nanotubes, junction density and angular position of cross-linked carbon nanotubes in order to obtain the best network. The control mechanism played an important role to avoid undesirable nanotube distribution. However, nanotubes randomly take positions through the control mechanism.

Afterwards, a molecular dynamics (MD) simulation is employed in order to create true junctions by heat welding method. Heating the system to a definite temperature enables formation of covalent bonds between intersected CNTs.

Finally, a tensile test using molecular dynamics simulations is carried out to investigate mechanical properties such as the Young's modulus, yield strength, ultimate tensile strength, and Poisson's ratio of current network. One side of network is fixed and tensile force is applied to the other side in the MD simulations. The analyses are implemented under certain parameters including temperature, thermostat, equilibration method, time etc. Results are calculated and discussed based on classical mechanic equations such as Hooke's law.

Optimum results are sought for the sake of better mechanical properties by altering the simulation parameters including temperature interval, welding temperature,

simulation time, timestep, displacement increment etc. Eventually, various simulations are conducted and results are compared. Moreover, two network structures having different tube density are analyzed and their mechanical properties are compared.

When we query the originality of the present study, it can be said that our thesis can be considered as a pioneering study. In literature, a previous study exists on random carbon nanotube networks and this study includes only generation process of carbon nanotube network. In our study, we updated current network generation algorithm in order to obtain better and more proper geometry and we tried to enable more optimum heat welding process at the same time. Then, we employed a tensile simulation to the generated geometry using molecular dynamics method in order to determine mechanical properties of current structure such as Young's modulus, ultimate tensile strength, yield strength or Poisson's ratio and any study is available on this subject. Moreover, mechanical properties of two different types of network having diverse nanotube density are compared and discussed. Besides, the effects of several simulation parameters on mechanical properties of CNT networks are investigated. For these reasons, our study has not only originality but also high quality.

RASTGELE DAĞILMIŞ KARBON NANOTÜP AĞ YAPILARINDA MEKANİK ÖZELLİKLERİNİN MOLEKÜLER DİNAMİK YÖNTEMİ İLE İNCELENMESİ

ÖZET

Nanoteknoloji, atomların, moleküllerin ve büyüklükleri metrenin milyarda biri boyutlarında olan yapıların ve malzemelerin üretimini, tasarımını, fiziksel ve kimyasal özelliklerini, hareketlerini, etkileşimlerini inceleyen ve birçok bilim adamı tarafından son derece gelecek vaat ettiği için sıkça çalışılan bir bilim dalı olmuştur.

Karbon bazlı nanoyapılar nanoteknoloji çalışmalarının daima merkezinde olmuşlardır. Bir çok karbon bazlı yapı mevcuttur. Bunlara örnek olarak karbon nanokoniler, karbon nanokirişler, karbon nanoçubuklar, karbon nanoküreler, grafenler, fullerenler, buckyballlar ve karbon nanotüpler verilebilir. Sahip oldukları mükemmel mekanik, elektrik ve ısı özellikleri ile karbon nanotüpler, karbon temelli nanoyapıların şüphesiz ki en önemlilerinden biri olarak adlandırılabilir. Fakat nanotüplerin bilinen üstün özelliklerini sadece nano ölçekte kullanmak mantıksız ve kullanışsızdır. Bu yüzden, karbon nanotüplerin üstün özelliklerini daha verimli kullanabilmek için onları nano boyuttan ziyade makro düzeyde kontrol edilmesi istenmektedir. Üstün nano ölçek özelliklerini sürekli boyuta kazandırmak gerekliliği böylece ortaya çıkmıştır. Bu doğrultuda, birçok karbon nanotüpün bir araya getirilmesi ile oluşturulabilen üç-boyutlu veya iki-boyutlu karbon nanotüp ağ yapıları ile nanotüplerin sadece kompozitlere takviye elemanı olmasından ziyade başlı başına bir hacim olarak kullanılması önerilmiştir.

Karbon nanotüp ağ yapıları yüzlerce nanotüpün bir araya getirilerek uygun sıcaklıkta kaynaştırılması sonucu oluşan yapılardır. Tek bir nanotüpün sahip olduğu özelliklerin ağ yapısında da gözlemlenmesi amaçlanmaktadır. Literatürde belli bir düzene sahip ağ yapıları ile ilgili çalışmalar çok sayıda olmasa da mevcuttur. Fakat daha gerçekçi bir model olan rastgele dağılışa sahip ağ yapıları ile ilgili çalışmalar yok denecek kadar azdır, çünküsaysalmodeli oluşturmak için elde hazır bir algoritma ya da ticari bir kod bulunmamaktadır. Kesişen karbon nanotüpleri birbirlerine bağlarken birçok farklı yöntem kullanılabilir iyon-kiriş irradiasyonu, kimyasal buhar biriktirme, metal sinterleme vb. Biz çalışmamızda ısı kaynağı yöntemini kullanarak daha güçlü bağlar tanımlama ihtiyacı duyduk. Sonrasında sistemimize moleküler dinamik yöntemini kullanarak uyguladığımız bir çekme deneyi simülasyonu ile malzemenin mekanik özellikleri incelendi. Gerek kullanılan geometri oluşturma algoritması, gerek kaynaklama yöntemleri açısından ve gerekse sonuçları elde etme teknikleri bakımından özgün bir çalışma olmuştur. Ayrıca sonuçlar açısından yani üç-boyutlu karbon nanotüp ağ yapılarının mekanik özelliklerini bularak literatüre yenilik kazandırılmıştır.

Bu çalışmada, karbon nanotüp ağ yapıların mekanik özellikleri moleküler dinamik yöntemi ile etraflıca incelenmiştir. Moleküler dinamik simülasyonlarını kesişen karbon nanotüplere ısı kaynağı yöntemi ile bağ oluşturmak için ve ayrıca sonrasında

oluşturulan üç-boyutlu veya iki-boyutlu karbon nanotüp ağ sistemine mekanik yükler uygulanmak için başvurulmuştur. Son zamanlarda güçlü ve hızlı bilgisayarların gelişmesiyle, simülasyon teknikleri bilimsel çalışmalarda kullanılan başlıca yöntemlerden olmuşlardır. Özellikle deneysel çalışmaların yetersiz kalması, çok maliyetli ya da tehlikeli olması gibi bir çok sebepten dolayı bilim adamları teorik hesaplamalara yönelmiştir ve bu yöntemleri sıkça kullanmaya başlamışlardır. Monte Carlo Yöntemi, Moleküler Dinamik Yöntemi ve Yoğunluk-Fonksiyonel Teorisi gibi yöntemler sıkça kullanılan teorik hesaplama tekniklerinden en önemlileridir. Kısaca değinmek gerekirse, Monte Carlo, zamandan bağımsız, yani, olasılıklara dayalı hesaplamalar için kullanılır. Moleküler Dinamik tekniği, klasik mekanik yaklaşımlarla açıklayabildiğimiz olayları simüle etmek için kullanılır ve Yoğunluk-Fonksiyonel Teorisi, kuantum mekaniksel hesaplamalar gerektiği durumlarda kullanılır. Moleküler Dinamik (MD), birbirleriyle etkileşimde olan çok parçacıklı sistemlerin zamana ve sıcaklığa bağlı davranışlarını istatistiksel mekanik ve yoğun madde fiziğine ve klasik Newton yasalarına dayanarak ilişkilendiren yöntemdir. Sistemin entropisine ve termodinamik özelliklerini kullanarak sayısal verilerle gözlenebilir veriler karşılaştırılabilir. MD simülasyonlarını sağlamak için sistemin hangi atomlardan oluştuğu, atomların başlangıç konumları ve hızları ve atomlar arası potansiyeller gibi parametreler bilinmelidir. Atomların birbirleriyle olan etkileşimlerini tanımlamak için literatürde birçok atomlar arası potansiyeller kullanılmaktadır. Biz çalışmamızda AIREBO (Adaptive Intermolecular Reactive Empirical Bond Order) adlı potansiyeli kullandık. Bu potansiyel, atomlar arası bağları kırılmasını ve yeni bağ oluşumunu hesaba kattığı ve REBO potansiyeline ek olarak burulma ve uzak-mesafe etkileşim parametrelerini de kullanabildiği için daha doğru bir yaklaşım sağlamaktadır.

Öncelikle tezin ilk bölümü kapsamında, iki boyutta ve üç boyutta ağ yapıları bir algoritma yardımı ile oluşturulmuştur. Literatürde karbon nanotüp ağ yapıları ile ilgili çok az sayıda çalışma olmasının en önemli nedenlerinden biri, bu yapıları oluşturacak hazır bir algoritmanın veya ticari bir yazılımının var olmaması olarak söylenebilir. Literatürde karbon nanotüp ağ yapıların iki farklı dağıtım şekline göre oluşturulabilmesi önerilmiştir. Bazı bilim insanları nanotüpleri düzgün bir şekilde bir araya getirerek kusursuz birleştirme yapmışlardır. Böylece ideal bir yapı elde edilmiştir. Fakat bu yapı olası kusurları ve bağlanma bölgelerindeki hataları içermediği için daha önce de belirtildiği gibi ideal yapı olarak nitelendirilebilirler. Diğer taraftan rastgele dağıtımla oluşturulan karbon nanotüp ağ yapıları ile gerçeğe daha yakın bir sistem elde edilebilmek mümkündür. Rastgele dağılmış karbon nanotüp ağ yapıları ile ilgili çalışma yok denecek kadar azdır. Bu yüzden, hem literatüre yenilik getirmek hem de buradaki eksikliği gidermek için, çalışmamızda rastgele karbon ağ yapılarını incelenmiştir.

Daha öncede belirtildiği üzere karbon nanotüpler, iki-boyutlu ve üç-boyutlu tasarım uzaylarına rastgele dağıtılarak bir ağ yapısı oluşturulmuştur. Fakat bu dağıtım işlemi yaparken, doğal olarak hiç bir tasarım kriteri koymadan yapılmamıştır. Çeşitli kısıtlamalar ve kontrol mekanizmaları getirilmiştir. Bu kısıtlamalar daha iyi ve gerçeğe yakın bir ağ yapısı elde etmek için uygulanmıştır. Çünkü üst üste çakışan onlarca nanotüpün olması, hedef nanotüpün üzerinde çok sayıda elemanın bulunması, çok yakın nanotüplerin birbirleri ile etkileşime girmesi, uygunsuz açılarda elemanların dağılımı, sistemin içinde gereğinden fazla parçacığın olması vb. birçok problemle karşılaşmak olasıdır. Bu olası tasarım eksiklikleri nedeniyle elde edilen sonuçların gerçeği yansıtamayabileceği düşünülmüştür. Dolayısıyla sistematik

bir network tasarımı yapmak sonuçların doğruluğu açısından mantıklıdır. Tabii bu ağ yapısının sistematik yapılması, rastgeleselliği bozmaz mı sorusunu akla getirebilir fakat bundaki amaç rastgeleselliği engellemek değil, karmaşıklığı engellemek amaçlanmıştır.

Çalışmanın ikinci bölümünde üst üste getirilmiş nanotüpler üzerinde bağlanma bölgeleri yaratılmıştır ve buralara moleküler dinamik simülasyonları ile bir nevi ısı kaynağı uygulanmıştır. Literatürde karbon nanotüpleri bağlarken pek çok yöntem mevcuttur ki bunlardan bazıları elektron-kiriş irradiasyon tekniği, iyon irradiasyon tekniği, kimyasal buhar biriktirme tekniği, atomik kuvvet mikroskobu ile mekanik manipülasyon, ısı kaynağı yöntemi olarak sayılabilir. Karbon nanotüpler arasında kuvvetli bağlar elde etmek amacıyla çalışmamızda ısı kaynağı yöntemi kullanılmıştır. Oda sıcaklığında olan yapı, yaklaşık 600-700K arası sıcaklığa kadar kısa sıcaklık aralıklarıyla artış yapılarak yükseltilmiştir ve sistemin kararlı hale getirilmesi için yeterli süre equilibration (dengeleme) uygulanmıştır. Önceki çalışmalarda karbon nanotüp kesişim bölgelerinde ısı kaynağı işlemi yaparken çok yüksek sıcaklıklara çıkıldığı gözlemlenmiştir. Fakat bu sıcaklığa ulaşmak hesaplama zamanını büyük ölçüde arttırdığı için çalışmamızda daha düşük sıcaklarda kaynak yapılmıştır. Burada daha kaliteli birleşme alanı oluşturmak amacıyla ilgili yerlerde bir bölge tanımlanarak buradaki bağ oluşturmaya atomlar silinmiştir. Böylece yüksek sıcaklıklardaki bağ davranışlarını simüle etmek amaçlanmıştır. Kaynak (referans) sıcaklığında bir müddet sistemi denge haline getirdikten sonra tekrar oda sıcaklığında bekletilerek denge konumuna ulaşması sağlanmıştır. Daha kararlı kesişim bölgeleri oluşturmak amacıyla dengeleme yapılmasındaki amaçtır. Sistemin termodinamik karakteristiğini temsil eden topluluk (ensemble) olarak mikrokantonik olarak belirlenmiştir ki bu topluluk sıcaklık, hacim ve toplam tanecik sayısını sabit kılacaktır. Ayrıca Nose-Hoover termostat ile ısı dengesi sağlanmıştır.

Tezin bir sonraki adımında ise moleküler dinamik yöntemi ile kullanılarak sisteme mekanik yükleme simülasyonları uygulanmıştır ve elastiklik modülü, Poisson oranı, akma dayanımı, çekme dayanımı ve kırılma dayanımı gibi karbon nanotüp ağ yapılarının mekanik özellikleri incelenmiştir. Mekanik test denilirken deneysel bir test yapılmamıştır, bilgisayar simülasyonları kullanarak tüm sisteme çekme gerilmesi uygulanmıştır. Çekme deneyini, yarattığımız ağ yapısına uygulamadan önce yazılan LAMMPS kodunun doğruluğunu kanıtlamak amacıyla, tek katmanlı bir nanotübe analiz yapılmıştır. Elde edilen değerlerle, literatürde daha önceki çalışmalarda tek katmanlı nanotüpler için bulunan sonuçlar karşılaştırılmıştır. Elde ettiğimiz sonuçların literatür ile uyumlu olması bu çekme kodunun doğruluğunu kanıtlamıştır. Bu işlem sonrasında, artık moleküler dinamik kodumuzu, üç-boyutlu karbon nanotüp ağ geometrimize küçük değişikliklerle uygulanması gerekmektedir. Yapının bir kenarı bütün serbestlik derecesinden kısıtlayacak şekilde sınır koşulları uygulanırken, aksi yönden çekme kuvveti uygulanmıştır. Bu kuvveti uygularken bir kenardaki tüm atomlara kritik uzama hızının altında olacak şekilde bir uzama hızı tanımlanmıştır. Ayrıca analizler oda sıcaklığında ve belirli basınç ve ısı koşulları altında malzemeye çekme uygulanarak yapılmıştır. Detaylı olarak NVT topluluğu ile sıcaklık, partikül sayısı ve hacim sabit tutularak ısı karakteristiği ve Langevin termostatla ise sıcaklık dengesi sağlanmıştır. Her çekme kuvveti artışı sonrasında malzemenin denge konumuna ulaşması için bir müddet bekletilmiştir. Sonucunda klasik mekanik yasaları baz alınarak malzemenin mekanik özellikleri incelenmiştir. Ayrıca birçok parametre değiştirilerek sonuçlardaki değişiklikler gözlemlenmiştir. Elde edilen bulgular karşılaştırılmış ve tartışılmıştır. Son olarak nanotüp yoğunluğu daha az bir

yapı için tüm analizler tekrarlanmıştır ve elde edilen yeni sonuçlarla eski sonuçlar karşılaştırılıp tartışılmıştır.

Çalışmamızın özgünlüğü sorgulanacak olursa, çalışmamız literatüre yenilik getirebilecek bir tez olarak adlandırılabilir. Daha önce rastgele dağılmış karbon nanotüp ağ yapısı çalışması bulunmaktadır fakat mevcut çalışmada sadece karbon nanotüp ağ geometrisinin oluşturulması yapılmıştır. Biz çalışmamızda ağ (network) oluşturma algoritmasını güncelleyerek daha düzgün yapılar oluşturmasını sağlarken aynı anda ısı kaynağı yöntemi ile oluşturulan bağlanma bölgelerini daha kaliteli ve daha optimum hale getirdik. Bu amaçta bir çok parametreyi değiştirdik ve etkisini inceledik. Sonrasında ise elde ettiğimiz geometrilere moleküler dinamik yöntemi ile çekme simülasyonları uygulayıp ağ yapısının elastisite modülü, akma dayanımı, kopma dayanımı gibi mekanik özelliklerini bulduk ki bu özellikte daha önce hiçbir çalışma bulunmamaktadır. Ayrıca çeşitli parametreler değiştirilerek yapının mekanik özellikleri üzerindeki etkileri incelendi. İki farklı nanotüp yoğunluğuna sahip ağ geometrilerin özellikleri karşılaştırıldı ve tartışıldı. Bu sebeplerden dolayı çalışmamız özgün olduğu kadar nitelikli bir çalışma olmuştur.

1. INTRODUCTION

Carbon based nanostructures such as graphenes, fullerenes, nanocones, nanorods and nanotubes have been accepted as very promising materials of near future. In particular, carbon nanotubes (CNTs), since their discovery in 1991 by Iijima [1], have drawn much attention of many scientists due to their excellent mechanical, electrical and thermal properties. To determine the exceptional properties of nanotubes, researchers in worldwide have conducted numerous studies by applying different approaches. These extensive studies on carbon nanotubes show that the CNTs have good combination of high stiffness, high strength, low density, small size high fracture toughness, high electrical and thermal conductivity and good optical properties [2-5].

Soon after realization of potential use of CNTs in material science, engineering, chemistry and physics, scientists have devoted their efforts on investigating mechanical properties of carbon nanotubes in distinct viewpoints. Many studies examined carbon nanotubes in different view of aspects. Figure 1.1 shows main approaches on determination of carbon nanotubes' mechanical properties.

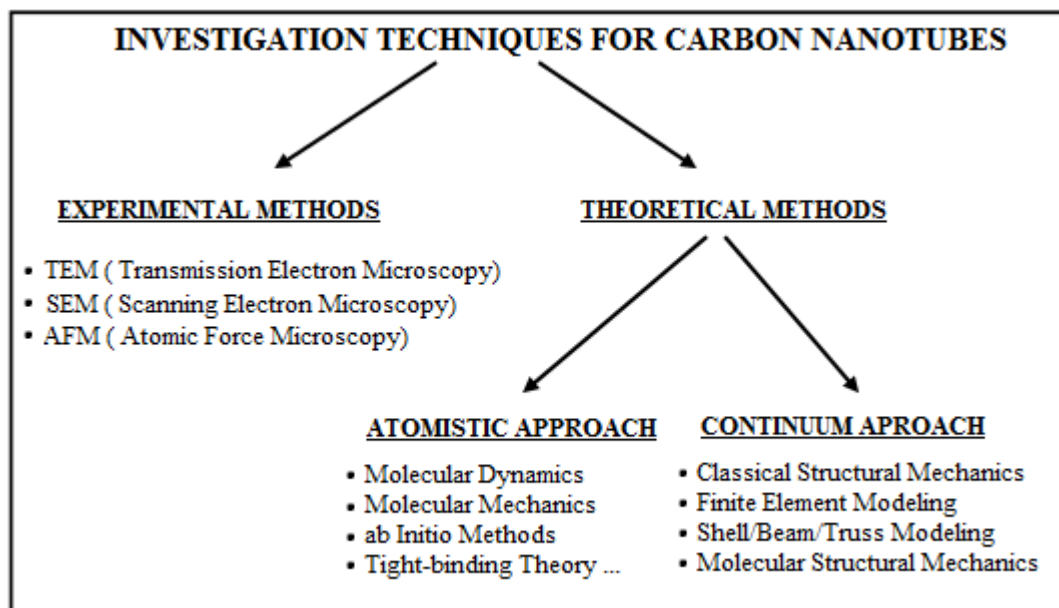


Figure 1.1 : Basic Approaches on Determining Mechanical Properties of CNTs.

In literature, experimental methods are mainly based on the usage of transmission electron microscopy (TEM), scanning electron microscopy (SEM) and atomic force microscopy (AFM). Treacy et al. [6] used the TEM by measuring thermal vibrations in order to estimate the Young's Modulus of multi-walled nanotubes (MWNT's) in 1996. Krishnan et al. [7] also used the TEM to observe single-walled nanotubes' (SWNT's) freestanding room temperature vibrations. Wong et al. [8] applied bending tests on cantilever beam models using the AFM. Elastic and shear moduli of different sized individual SWNT's and MWNT's were also investigated by Salvetat et al. [9,10] with simple support beam model in the AFM. Yu et al. [11,12] conducted tensile-loading experiment on both single-walled and multi-walled carbon nanotubes in AFM. Wei et al. [13] investigated natural frequencies, shear and Young's moduli of SWNT's by applying combination of electric-field-induced resonance method and nanoknife technique on Timoshenko beam model in the SEM and AFM. Guhados et al. [14] determined the Young's and shear moduli by measuring the tube compliance as a function of position along suspended tubes in the AFM. All these studies verify outstanding mechanical properties of carbon nanotubes and the results of the experiments can be considered as accurate. However, experimental methods are impractical due to CNTs' small size [5]. Moreover, the experimental process is an expensive procedure since tools like the TEM, AFM or SEM are needed.

Because of the challenges in experimental approaches, theoretical techniques have been also developed to determine the mechanical properties of nanotubes. Theoretical techniques are mainly based on the computer simulations and they can be investigated in two major categories: atomistic approaches and continuum approaches [5]. The continuum mechanics approach includes classical structural mechanics, finite element modeling, continuum shell/beam/truss modeling, etc. These techniques can be used in problems having a large number of atoms problems with affordable computational times and they are applicable to investigating both static and dynamic properties of CNT's. However, negligence of atomistic characteristic and interatomic forces is the main drawback of continuum mechanics approach and it causes accuracy problems. On the other side, the atomistic approaches include classical molecular dynamics (MD), molecular mechanics (MM), ab initio methods like density functional theory, tight-binding theory etc. The methods consider atomic or molecular motions of the system and eventually provide

better accuracy. However, problems are restricted in problems having a small number of atoms or molecules because they need huge computational tasks [5].

The accuracy of ab initio methods can be considered as better than the MD simulations. However, ab initio methods are both computationally expensive and limited to relatively small-scale models including just a few hundreds of carbon atoms. Although classical continuum approaches are effective for simulating large number of atoms, they do not give accurate results since the effects of time evaluation, temperature and interatomic forces are missing for continuum modeling. For these reasons, the MD is considerably advantageous method in terms of accuracy of the results and size of the simulation system.

There are extensive studies found in literature for continuum approach. Li and Chou [15, 16] calculated elastic moduli of beam elements by defining a linkage between classical structural mechanics and molecular mechanics. In their finite element model, beams represent the C-C covalent bonds and nodes represent the carbon atoms. Yakobson et al. [17] and Ru et al. [18, 19] investigated CNTs' mechanical properties by using continuum shell modeling approach. Odegard et al. [20] combined computational chemistry and solid mechanics on continuum truss model by equating strain energy of truss model with molecular potential energy of carbon nanotube in order to find effective bending rigidity. Meo and Rossi [21, 22] proposed a finite element model based on molecular mechanics theory and eventually evaluate the Young's modulus, ultimate strength and strain by using non-linear and torsional spring elements.

For atomistic approach, Hernandez et al. [23] used a nonorthogonal tight-binding formalism to determine and compare structural and elastic properties of carbon nanotubes and composite nanotubes. Sanchez-Portal et al. [24] applied pseudopotential-density-functional theory to determine structural, elastic and vibrational characteristics of single-walled carbon nanotubes in different radius and chirality. By using an empirical force-constant model, Lu [25] estimated the Poisson's ratio and elastic modulus of carbon nanotubes. Belytschko et al. [26] presented a study based on molecular mechanics and molecular dynamics methods in order to investigate carbon nanotubes' fracture characteristics. Gao et al. [27] also used molecular dynamics and molecular mechanics simulations separately to determine single-walled carbon nanotubes' mechanical and structural properties. Jin et al. [28]

investigated elastic properties of SWNT's using molecular dynamic simulations by obtaining dynamic response and mutual force interaction in case of small-strain deformation.

The CNTs are generally used as reinforcement for composite materials. However, it is impractical to use them only in nanoscale. Hence, it is desirable to produce solely the CNT-based material by aggregation and coalescence multiple intersected nanotubes to be used in the macro world applications. Eventually, the idea of combining numerous individual nanotubes may be the key of generation and improvement of new advanced materials [29, 30]. It is expected that superior properties of a single nanotube might be observed in a “carbon nanotube network” structure and thus nanoscale features of CNTs are observed in even continuum proportion [31]. The previous studies on junction generation techniques, experimental investigations of CNT network structures and computational approaches for CNT networks are summarized in the following paragraphs, respectively.

In order to obtain a carbon nanotube network with CNTs' desirable properties, it is intended to create true joints between intersected carbon nanotubes. Recently, many scientists have studied on joining methods of intersected nanotubes to generate multi-terminal junctions such as ‘Y’, ‘X’ and ‘T’ junctions. Roberts et al. [32] aligned several methods on joining carbon nanotubes and summarized previous studies in literature. Banhart [33], Terrones et al. [34] and Jang et al. [35] investigated electron beam irradiation techniques in their works. Ni et al. [36] and Krasheninnikov et al. [37] studied ion irradiation techniques. Lefebvre et al. [38] and Postma et al. [39] used mechanical manipulation using atomic force microscopy technique to generate junctions. Chiu et al. [40] applied chemical functionalization for interconnections of carbon nanotubes. Besides, heat-welding technique is particularly significant above all other methods. In the present study, a heat welding method is implemented with molecular dynamics (MD) simulations to generate desirable junctions between intersected CNTs. In literature, Meng et al. [41, 45] welded two defect-free ultrathin single-walled carbon nanotubes by heating at elevated temperature from 1300° K to 3500° K and then explored the mechanical properties of SWCNTs under uniaxial tensile loading. Stormer et al. [46] studied on two heat welded single-walled carbon nanotubes with X-junction via molecular

dynamics simulations and applied uniaxial tensile, shear and torsional loading to investigate the mechanical behaviors of X-junctions. Kirca et al. [31] also used heat welding technique on generating true junctions for random carbon network structure. Liu et al. [47] applied uniaxial and biaxial loadings to different sized ultrathin single-walled carbon nanotubes with five types of X-junctions. Yang et al. [48] also used heat welding techniques via molecular dynamics to generate non-orthogonal X-junctions in diverse crossed angle.

In literature, experimental studies embrace production process of the CNT networks or junction formation or investigation on mechanical, electrical or thermal features of CNT networks. Wang et al. [49] experimentally studied CNT networks and observed end-to-end, side-to-side and zigzag junctions of network in transmission electron microscope. Dimaki et al. [50] worked on temperature responses of CNT networks to safely integrate them into electronic devices. Rahatekar et al. [51] carried out a study that is based on length dependent mechanics of CNT networks. Gorassi et al. [52] investigated properties of multi-walled carbon nanotube network that is dispersed in a polymer matrix as a function of morphology under different experimental conditions. Another MWCNT network and polymer nanocomposite study is conducted by Chen et al. [53] where they examined the aspect ratio regarding supercritical CO₂ agent under different ambient conditions. Electrical conductivity of multi-walled carbon nanotube networks under monotonic stress and loading/unloading cycle are examined by Slobodian et al. [54]. Moreover, several studies [55-57] involves production process of CNT networks including chemical vapor deposition (CVD), spin coating, spray coating or vacuum filtration techniques

Computational studies using different approaches by different scientists are also available in literature. Some early studies on CNT networks investigate electrical behaviors and macroelectronic applications of random carbon nanotube networks due to possible utilization of CNTs' superior electrical properties [58-63]. There are several studies on the utilization of carbon nanotube networks in nanocomposite materials. Tai et al. [64] proposed a study on nanocomposites that include dispersed carbon nanotubes as reinforcing material and observed better mechanical properties. Li et al. [65] investigated damage sensing behaviors of a composite material with carbon nanotube networks reinforcement. Thostenson et al. [66] studied on the damage progression of fiber-epoxy composite containing CNT network

reinforcement. Following the studies on mechanical features of the carbon nanotube networks, it can be said that ordered CNT network studies dominate the literature. Coluci et al. [67, 68] explore stretching, twisting and rupture behaviors of ordered carbon nanotube networks using atomistic simulations. They also used molecular mechanics method for investigating mechanical properties of ordered networks. Li et al. [69] applied uniaxial tensile loading on ordered super square CNT network by using molecular structural mechanics approach in order to examine deformation behavior of a given structure. Liu et al. [70] used molecular structural method to examine deformation and failure mechanics of ordered super carbon nanotube network with X-junctions and Y-junctions considering the effects of chirality and size. Xie et al. [71] investigated multi-scale features of carbon nanotube networks by using molecular dynamics simulations. Li et al. [72] evaluated natural frequencies and specific heat for ordered CNT networks with different network configurations. However, ordered carbon nanotube networks are considered as ideal structures, which mean that they do not include geometrical irregularities and possible imperfections at junctions like bond re-arrangements. On the contrary, random carbon nanotube networks represent the real structure much better. Kirca [31] generated two and three dimensional carbon nanotube networks with a systematic algorithm and employed heat welding method to obtain networks by using molecular dynamic simulations.

Originality is an extremely significant matter for scientific researches. For this purpose, a pioneering study is targeted during this thesis. As mentioned above, a previous study exists on random carbon nanotube networks [31]. In this thesis, current algorithm is developed to generate better carbon nanotube network geometry and it is tried to enable more optimum heat welding process at the same time. Subsequently, different mechanical properties are obtained using molecular dynamics method for the tensile test simulations. Because no study is available on calculation of Young's modulus, ultimate tensile strength, yield strength and Poisson's ratio for random carbon nanotube networks, our study is original and has high quality.

In this thesis, a self-controlled algorithm is described to generate two-dimensional and three-dimensional networks consisting of numerous random intersected carbon nanotubes, which are distributed systematically in design space. The algorithm

manipulates length and chirality of nanotubes, junction density and angular position of cross-linked carbon nanotubes in to obtain the best network. Afterwards, a molecular dynamics simulation is employed in order to create true junctions by heat welding method. Heating the system to a definite temperature enables the formation of covalent bonds between intersected CNTs. Finally, a tensile test is carried out to investigate mechanical properties such as the Young's modulus, ultimate tensile strength, yield strength, Poisson's ratio or density of current network. The simulations are also implemented by using the MD simulations and results are calculated and discussed based on classical mechanic equations. Optimum solutions are sought for the best mechanical properties by altering the simulation parameters including temperature interval, welding temperature, simulation time, timestep, displacement increment etc. Eventually, various simulations are conducted and results are compared. Moreover, two network structures having different tube density are analyzed and their mechanical properties are compared.

General procedure of present thesis can be summarized in three main categories:

- **Matlab code for network models:** In this stage, carbon nanotube network is created with a MATLAB code and CNTs are selected, rotated, translated to design space if they are compatible with the constraints. Otherwise, candidate nanotube is abandoned.
- **Lammps script for implementation of junctions:** After the network is formed, molecular dynamic simulation is implemented with LAMMPS and junctions are obtained by heat welding regarding to potential functions, ensemble, thermostats etc.
- **Lammps script for mechanical test simulations:** A LAMMPS script is run to investigate mechanical properties of CNT networks. One side of the network is fixed as boundary conditions. After that, a reasonable strain rate is applied to bottom end region of the network structure under determined ambient conditions such as temperature and pressure.

2. CARBON NANOTUBES

2.1 Nanotechnology and Carbon-based Nanostructures

Nanotechnology can be described as a very promising scientific field, which deals with design, production, fabrication and application of structures and materials in nanometer scales, and it enables to understand the unique physical properties of atoms, molecules and things with the size ranging from subnanometers to a couple of hundred nanometers [73, 74]. It is an interdisciplinary field that has emerged from the collaboration of basic science physics, engineering, chemistry and biology.

Figure 2.1 gives a group of structures with their typical range of dimensions and provides opportunity to compare different structures with different scale.

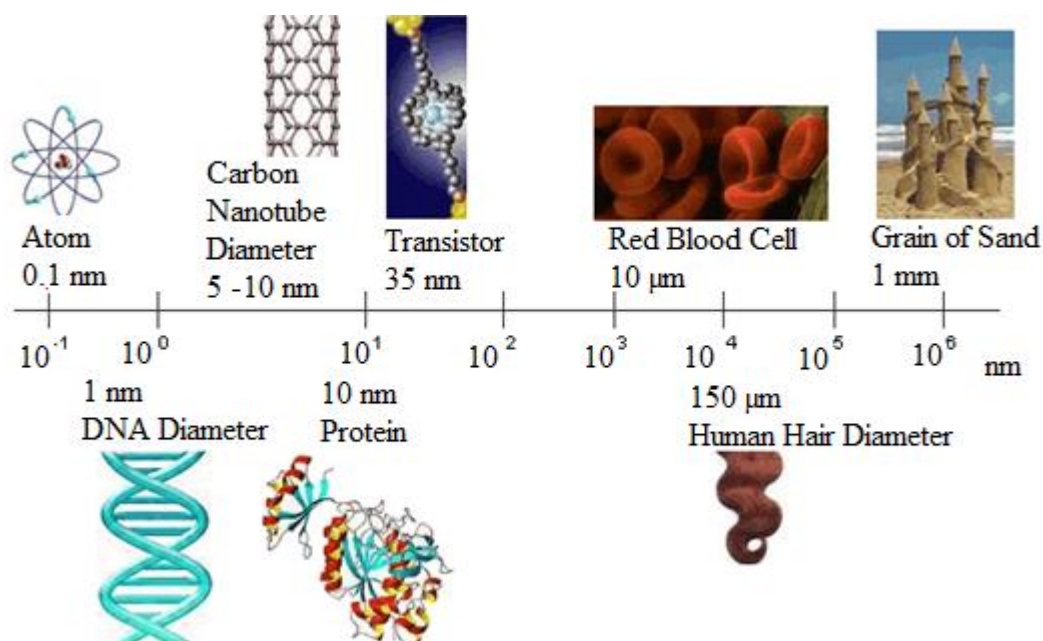


Figure 2.1 : Presentation of Some Materials in Nanoscale World [118].

As it can be clearly distinguished from the figure, the nanoscale contains engineering of the smallest structures, materials, devices and systems between 0.1 to 1000 nanometers. For instance, the diameter of a carbon nanotube varies approximately from 5 to 15 nanometers and the size of DNA can be considered around 1 nanometer. An Atom size is considered nearly 0.1 nanometer.

In recent years, carbon nanoscience is growing into an individual science field which investigate physical phenomena of carbon entities at the nanoscale within a unified framework, involving relationship of different nano carbon forms and condition of transformation from one carbon structure to another form or aggregating numerous single entities to a comprehensive structure or obtaining plausible combination of different types of carbon based nanostructures [75].

There are various types of carbon based nanostructures including fullerenes, nanotubes, graphenes, nanocones, nanowires, nanohorns, nanocrystalline diamonds, fullerites, etc. All carbon nanostructures can be classified based on their dimensionalities which are zero-dimensional structures such as fullerenes, one-dimensional structures such as nanotubes, nanohubs, two-dimensional structures such as graphene, nanoribbons, and three-dimensional structures such as nanocrystalline diamond, fullerite, 3D networks. Various types of carbon based nanostructures are demonstrated in Figure 2.2.

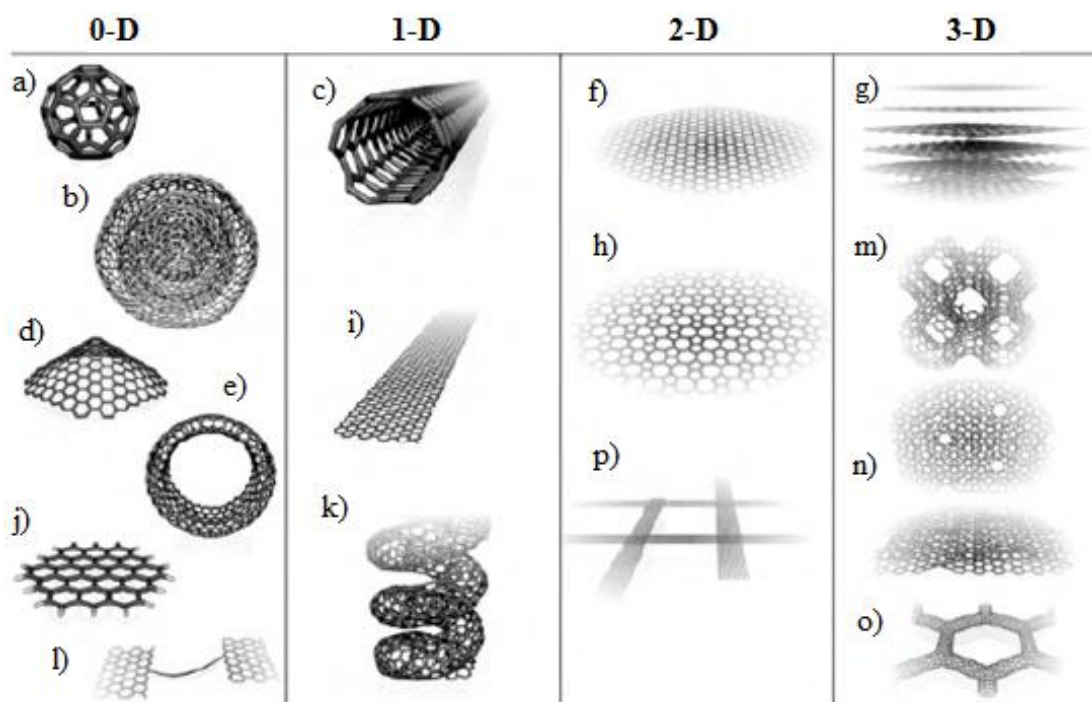


Figure 2.2 : Carbon-based Nanostructures : a) C60: Buckminsterfullerene; b) Nested Giant Fullerenes; c) Carbon Nanotube; d) Nanocones; e) Nanotoroids; f) Graphene Surface; g) 3D Graphite Crystal; h) Haecelite Surface; i) Graphene Nanoribbons; j) Graphene Clusters; k) Helicoidal Carbon Nanotube; l) Short Carbon Chains; m) 3D Schwarzite Crystals; n) Carbon Nanofoams o) 3D Nanotube Networks, and p) Nanoribbons 2D Networks [76].

2.2 Essentials of Carbon Nanotubes

Carbon nanotubes have particularly attracted researchers' interest for many years. Exceptional properties of carbon nanotubes are the main reasons of the exclusive interest of researchers in worldwide. The CNTs have the good combination of high stiffness, high strength, low density, small size, high fracture toughness, high electrical conductivity and good optical properties. Table 2.1 comparatively shows some advanced mechanical properties of carbon nanotubes by comparing different carbon based materials.

Table 2.1 : Some Comparative Mechanical Properties of Carbon Structures

Material	Young's Modulus	Tensile Strength	Density
Carbon Nanotubes	1000-1300 GPa	11-63 GPa	1.33-1.4 g/cm ³
Carbon Fibers	400-425 GPa	3.5-6 GPa	1.8-1.9 g/cm ³
High Strength Steel	180-220 GPa	0-2 GPa	7.7-7.85 g/cm ³

The Nanotube is best described as rolling up of a graphene sheet to form a tubular structure and this structure is comprised of benzene-type hexagonal carbon atom rings. Three neighbor carbon atoms bind with covalent bonds in periodic hexagonal pattern and the exceptional properties of CNTs highly depend on these strong covalent bonds. The bonding in carbon nanotubes is sp² hybridization, which contains three hybrid sp² orbitals at 120°. Figure 2.3 shows two-dimensional graphene sheet with roll-up vector and single walled carbon nanotube.

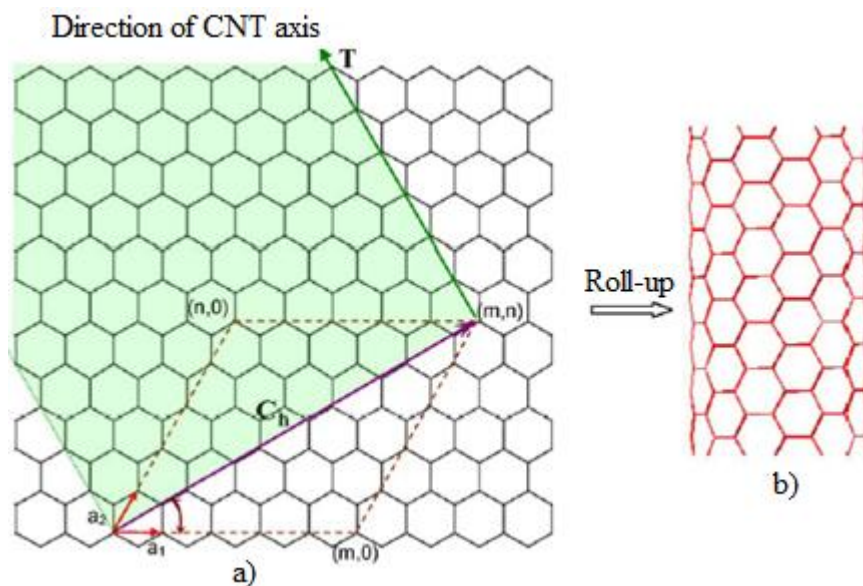


Figure 2.3 : a) A Two-dimensional Graphene Sheet, b) Single-walled CNT [30].

Chiral vector C_h and chiral angle θ are two main parameters that determine the atomic structure of carbon nanotube. A nomenclature (n, m) and graphene unit lattice vectors (a_1, a_2) are used to define chiral vector as follows.

$$C_h = ma_1 + na_2 \quad (2.1)$$

Carbon-carbon (C-C) bond length is considered to be equal to 1.421 Å and a is the unit lattice constant that is equal to $a = |a_1| = |a_2| = \sqrt{3}a_{C-C}$. The nanotube circumference and tube diameter can be respectively evaluated as:

$$d_t = \frac{|C_h|}{\pi} = \frac{a\sqrt{n^2 + mn + m^2}}{\pi} \quad (2.2)$$

Chiral angle is defined as the angle between the vectors C_h and a_1 . The chiral angle can be calculated with following equation:

$$\theta = \sin^{-1} \left[\frac{\sqrt{3}m}{2\sqrt{n^2 + mn + m^2}} \right] \quad (2.3)$$

The chiral angle describes three major categories of single walled carbon nanotube, which are shown in Figure 2.4.

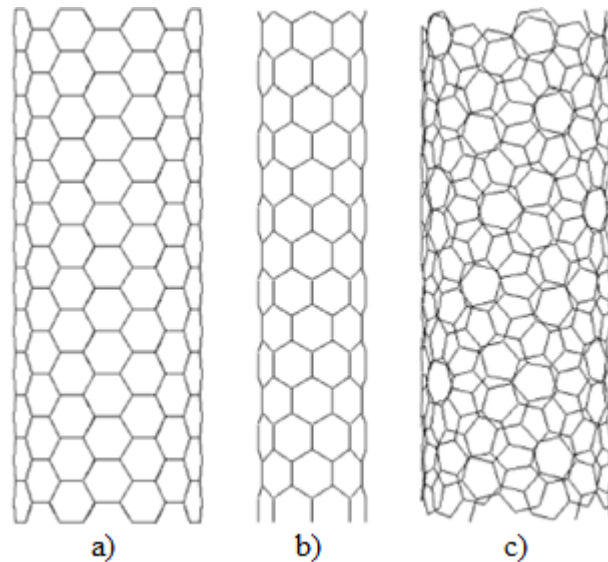


Figure 2.4 : Nanotube Types: a) Armchair, b) Zigzag, c) Chiral

If the chiral angle is 30° which means $m=n$ (m,m) , the nanotube is called as *armchair*; if the chiral angle is 0° which means $m=0$ $(m,0)$, the nanotube is called

zigzag; and finally if the angle is between 0° and 30° which means $m \neq n \neq 0(m,n)$, the nanotube is called *chiral*. Table 2.2 explains different types of CNTs.

Table 2.2 : Types of CNTs Based on Chiral Indices.

Nanotube type	Chiral indices (m,n)	Chiral angle, θ
Armchair	(m,m)	30°
Zig-zag	($m,0$)	0
Chiral	(m,n) $m \neq n \neq 0$;	$0 < \theta < 30^\circ$

As shown in Figure 2.5, there are two main types of carbon nanotubes in accordance with the number of layers that a CNT has. While single-walled carbon nanotubes (SWCNTs) contain only one layer, multi-walled carbon nanotubes (MWCNTs) are formed of multiple concentrically located SWCNTs in different radii. MWCNTs are not connected with covalent bonds; they are only related with Van der Waals forces so it is called non-bonded interaction.

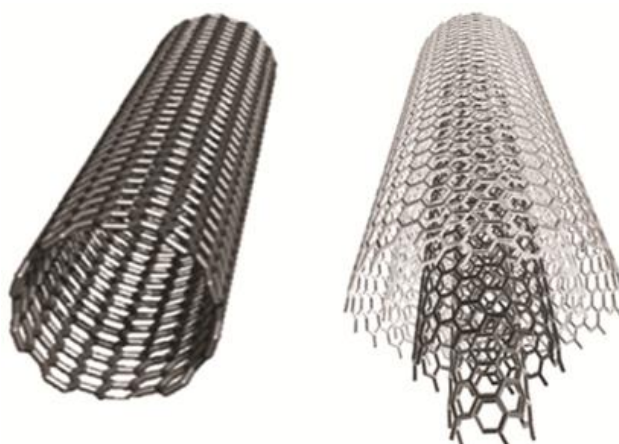


Figure 2.5 : Single-walled and Multi-walled Carbon Nanotubes [122].

3. INTRODUCTION TO MOLECULAR DYNAMICS

3.1 Basics of Molecular Dynamics Simulation

Computer simulations possess a privileged place in science recently. Some experiments can be impossible, dangerous or too expensive in order to implement. For some cases, simulations provide many advantages to researchers in terms of feasibility, expenses, time or safety. In molecular sense, computer simulations act as a bridge combining microscopic world to macroscopic world [77]. Molecular dynamics method and Monte Carlo method are two of the most common computer simulation techniques among all. Monte Carlo method is an indeterministic simulation method that relies on randomness of the system to compute the results. However, molecular dynamics is a deterministic technique that is fundamentally based on the principles of physic laws. Simulations are implemented depending on initial positions and velocities with time evolution [78]. Time-dependency so, accessible dynamic behavior of the system is the most significant advantage of molecular dynamics over Monte Carlo method. On the other hand, it is good to know that molecular dynamics is a stochastic method and the aim of an MD simulation is not to predict precisely what will happen to a system. We are always interested in statistical predictions and the average behavior of the system. In this study, molecular dynamic simulations are intensively used to predict nanostructures' time and temperature dependent behavior.

Molecular dynamics is a statistical mechanics method that has been become a widely used technique with powerful capability and great efficiency of computers in recent years. In other words, molecular dynamics can be defined as a computer simulation technique that calculates the equilibration and transport properties of set of interacting atoms with time evolution by integrating their Newton's equations of motions [79, 80]. The MD is an advantageous technique in contrast to other atomistic approaches due to its affordable computational expense, high accuracy acquisition and capability to simulate considerably large systems. A typical MD simulation

includes approximately thousands to millions particles ($10^4 - 10^7$) and simulation time takes picoseconds or a couple of hundreds nanosecond ($10^{-12} - 10^{-9}$).

In molecular dynamics simulations, atomistic simulation process can be investigated in three major steps: pre-processing, analysis and post-processing. Initial conditions such as pressure, temperatures etc. are determined at first. In numerical integrations, instant location and velocity of each atom in a definite system is determined applying Newton's dynamics. Then, energy and force calculations are conducted based on proper interatomic potentials under different thermodynamics conditions [77-80]. Finally, averages of measured quantities are printed and visualized.

The procedure of molecular dynamics simulations can be elaborated as follows:

1. Ambient conditions are determined that are initial temperature (T) and pressure (P) , number of particles (N) , volume (V) , external chemical potential (μ).
2. To begin simulation, initial positions and velocities have to be assigned for all particles of the system.
3. Periodic boundary conditions and interatomic potentials are defined.
4. Newton's equation of motions is solved.
5. Integration broken down to many small stages: δt . The total force on each particle in the configuration at a time t is the vector sum of its interactions with other particles. From the force, determine the acceleration of the particles and combine it with positions and velocities at time t to calculate at the current time. The force is constant during the time step $t + \delta t$.
6. New positions and velocities are determined with molecular dynamic algorithms such as Verlet, Velocity Verlet, Leap Frog etc.
7. Post processing (Evaluation or visualization of desired parameters at the end of current simulations).

Molecular dynamics obeys classical mechanic laws, particularly Newton's second law. Here, V is the atomic potential, F_i is the force due to interactions of atoms, which is also derived as the gradients of the potential, m_i is the atom's mass and a_i is atom's acceleration.

$$F_i = m_i a_i \quad (3.1)$$

$$a_i = \frac{d^2 r_i}{dt^2} \quad (3.2)$$

$$F_i = \nabla_i E = \nabla_{r_i} V(r_1, \dots, r_i) \quad (3.3)$$

If it is considered as the motion of a particle in one dimension with a given energy state, the basic dynamic progression of the simulation without taking account of temperature state.

The atomic force can be evaluated with Eq. (3.1) derivation of atomic potential and acceleration is easily found Eq. (3.2) since the atom's mass is known.

$$a = \frac{dv}{dt} \Rightarrow v(t) = at + v_0 \quad (3.4)$$

$$v = \frac{dx}{dt} \Rightarrow x(t) = vt + x_0 = \frac{1}{2}at^2 + v_0t + x_0 \quad (3.5)$$

After acceleration is found, positions and velocities are determined. To evaluate the equation as the function of time, Taylor Series of expansion is applied as given in Eq. (3.5) and $O(t^4)$ is the local truncation error parameter of the fourth order of time step.

$$x(t) = x_0 + v_0t + a_0t + a_0 \frac{t^2}{2} + \dot{a}_0 \frac{t^3}{3!} + O(t^4) \quad (3.5)$$

$$x(t + \Delta t) = x_0 + v(t)\Delta t + \frac{F(t)}{m} \frac{\Delta t^2}{2} + \frac{\dot{F}(t)}{m} \frac{\Delta t^3}{3!} + O(t^4) \quad (3.6)$$

As it can be seen from the given formula Eq. (3.6), it is carried out one time step of dynamics pass from $x(t)$ to $x(t + \Delta t)$. Velocities are calculated similarly and acceleration is recalculated from energy equation for each timestep.

In molecular dynamics simulations, there are prevalent algorithms such as Verlet algorithm, Leap Frog algorithm, Beeman algorithm and Velocity algorithm. But the

most common algorithm is Verlet algorithm which is mainly based on Taylor series of expansion of positions one step forward and one step backward in time. The reasons why Verlet algorithm is the most widely used and preferred algorithm that are versatile because of their simplicity, accuracy and stability. It comes from Taylor series expansion as follows.

$$x(t + \Delta t) = x(t) + v(t)\Delta t + \frac{1}{2}a(t)\Delta t^2 + \frac{1}{6}b(t)\Delta t^3 + O(\Delta t^4) \quad (3.7)$$

$$x(t - \Delta t) = x(t) - v(t)\Delta t + \frac{1}{2}a(t)\Delta t^2 - \frac{1}{6}b(t)\Delta t^3 + O(\Delta t^4) \quad (3.8)$$

Then,

$$x(t + \Delta t) = 2x(t) - x(t - \Delta t) + a(t)\Delta t^2 + O(\Delta t^4) \quad (3.9)$$

$$v(t) = \frac{x(t - \Delta t) - x(t - \Delta t)}{2\Delta t} \quad (3.10)$$

$$a(t) = -\frac{1}{m}\nabla V(r(t)) \quad (3.11)$$

As it can be seen, kinetic state of the system were not taken into consideration for the Newton's law of motion, only potential energies were considered. Hamiltonian formulations shall be also employed in the MD simulations besides the Newton's law of motion.

The Hamiltonian formulation is considered to evaluate total energy. In molecular dynamics simulation, Hamiltonian mechanic is used instead of Lagrangian mechanic. There is a just slight difference between these two major calculation methods, but it is a very significant difference. The Hamiltonian is mainly based on summation of potential and kinetic energy while the Lagrangian is based on the differences of energies as follows.

$$L = K - V \quad (3.12)$$

$$H = K + V \quad (3.13)$$

Potential energy description is given by

$$V(\mathbf{r}) = \sum_i^N V(\mathbf{r}_1, \dots, \mathbf{r}_i) = V_{\text{Bonded}} + V_{\text{Non-bonded}} \quad (3.14)$$

Kinetic energy description is given by

$$K = \frac{3}{2} N k_B T = \sum_i^N \frac{1}{2} m_i (v_i)^2 = \sum_i^N \frac{(p_i)^2}{2m_i} \quad (3.14)$$

The Hamiltonian expressions with position and linear momentum are given by

$$H(\mathbf{r}_1, \mathbf{r}_2, \mathbf{r}_3 \dots \mathbf{r}_N; \mathbf{p}_1, \mathbf{p}_2, \mathbf{p}_3 \dots \mathbf{p}_N) = \sum_i^N \frac{(p_i)^2}{2m_i} + V(\mathbf{r}_1, \mathbf{r}_2, \mathbf{r}_3 \dots \mathbf{r}_N) \quad (3.15)$$

$$\dot{\mathbf{p}}_i = -\frac{\partial H}{\partial \mathbf{r}_i} \quad (3.16)$$

$$\dot{\mathbf{r}}_i = -\frac{\partial H}{\partial \mathbf{p}_i} \quad (3.17)$$

So far, the effect of temperature has not been taken into account. It can be said that the temperature is directly related to average kinetic energy when equipartition theory of the gases and ideal gas theory are treated [77-80].

$$K = \frac{3}{2} N k_B T \quad (3.18)$$

Here K is instantaneous kinetic energy, T is the instantaneous temperature, $k_B = 1.38066 \times 10^{-23}$ J/K is the Boltzmann constant and N is the number of the particles. 3 comes from that there are three velocity components of the whole system.

Eq. (3.18) can be written with classic kinetic energy theorem including temperature as follows:

$$K = \frac{3}{2} N k_B T = \left\langle \sum_i^N \frac{1}{2} m_i (v_i)^2 \right\rangle \quad (3.19)$$

Then, the temperature is given by

$$T = \frac{1}{3Nk_B} \left\langle \sum_i^N m_i (v_i)^2 \right\rangle \quad (3.20)$$

3.2 Statistical Ensembles

The MD simulations give knowledge about microscopic state of the system including atomic positions, velocities and accelerations. Statistical mechanics act as a bridge that integrates the microscopic state of the system with observable macroscopic data such as pressure, temperature or energy condition. By this way, macroscopic conditions of an atomic system can be examined in a molecular viewpoint.

In molecular dynamic simulations, a system could be stated in a definite temperature, pressure, density, total energy or number of particles, [78]. These parameters describe thermodynamics state of the system and are controlled by statistical ensembles.

An ensemble is defined as all possible quantum state of N identical particle system. It is idealization of large number of particles in a system considered all at once; each represents possible a state. Main statistical ensembles can be given as following alignment:

- **Microcanonical ensemble (NVE):** Each possible state of the system has the same energy, volume and number of particles. The ensemble indicates that N-V-E are constant quantities.
- **Canonical ensemble (NVT):** Each possible state of the system has the same temperature, volume and number of particles. The ensemble indicates that N-V-T are constant quantities.
- **Isothermal-isobaric ensemble (NPT):** Each possible state of the system has the same temperature, pressure and number of particles. The ensemble indicates that N-P-T are constant quantities.
- **Isoenthalpic-isobaric ensemble (NPH):** Each possible state of the system has the same enthalpy, pressure and number of particles. The ensemble indicates that N-P- H are constant quantities.

- **Grand canonical ensemble (μVT):** Each possible state of the system has the same chemical potential, volume and number of particles. The ensemble indicates that μ -V-T are constant quantities.

3.3 Periodic Boundary Conditions

Molecular dynamics simulations are carried out for N-particle systems in a simulation cell with a definite volume. Periodic boundary conditions enable the systems total number of particles and total volume to remain constant [81, 82]. According to periodic boundary conditions, when a particle moves out of simulation box, another particle replaces as an incoming image in order to conserve total number of particles as it is shown in the Figure 3.1. In molecular dynamics simulators, for which LAMMPS is used in the present study, periodic boundary conditions have to be introduced during the initialization step. Because, there is a size limitation of defined simulation box. Otherwise, extensive simulations can cause great increase in computational time.

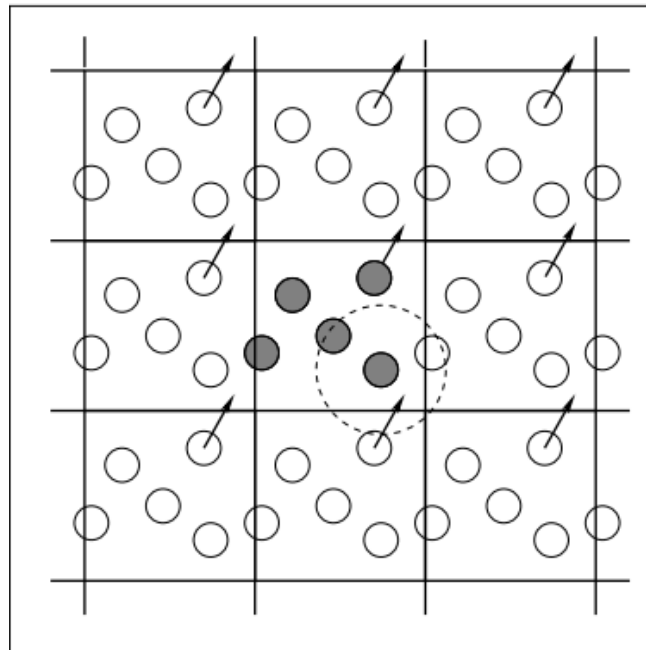


Figure 3.1 : Periodic Boundary Conditions [82].

3.4 Molecular Potentials

Carbon nanotubes are large molecules including carbon atoms, which are bonded together with covalent bonds. The motion and displacement of independent atoms

are set up by a molecular force field which is created by nucleus-nucleus or electron-nucleus interactions. Molecular force field can be explained in terms of steric potential energy that depends on only relative position of the nuclei [83]. This energy is directly linked with previous equations.

For molecular dynamics and molecular mechanics evaluations, the total steric potential energy of the force field can be explained as the sum of the energies because of the bonded and non-bonded interactions as it is given in Eq. (3.21).

$$V = \sum V_r + \sum V_\theta + \sum V_\phi + \sum V_\omega + \sum V_{vdw} + \sum V_{es} \quad (3.21)$$

where V_r is the bond stretching energy, V_θ is the bond angle bending energy, V_ϕ is the dihedral angle torsion energy, V_ω is the out-of-plane torsion energy, V_{vdw} is the van der Waals interaction energy and V_{es} is the electrostatic interaction energy.

3.4.1 Bonded interactions

Eq. (3.21) shows all types of interactions constituting total steric potential energy. However, the first four terms, which are represented as bonded potentials, contribute more. A sketch demonstration of above mentioned interatomic interactions is given in Figure 3.2 as follows:

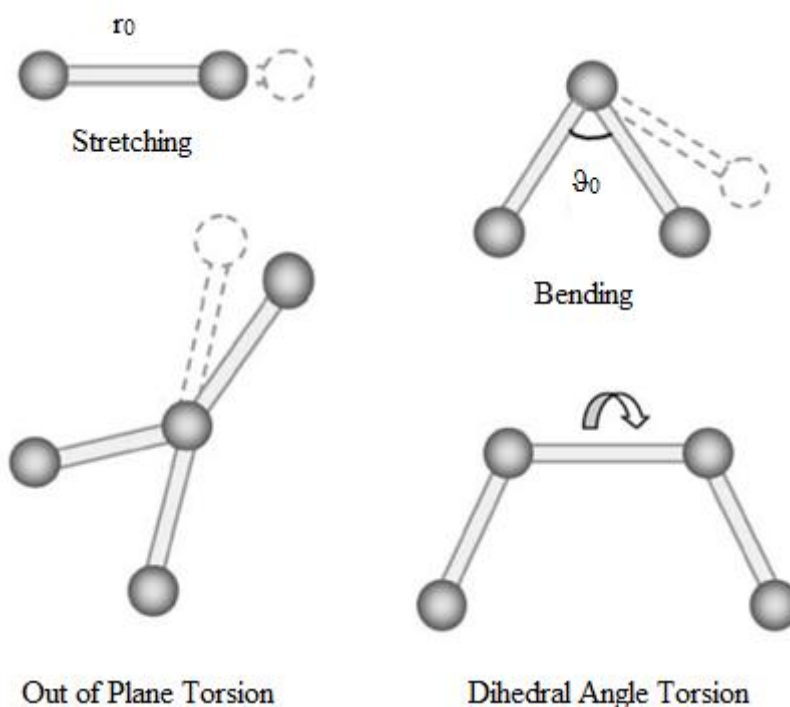


Figure 3.2 : Interatomic Interactions [15].

To define total potential energy of an atomic system, following simple harmonic small deformation theory assumption may be convenient [5]. Dihedral angle torsion and out of plane torsion are merged into a single term in order to simplify the equation.

$$V_r = \frac{1}{2}k_r(r-r_0)^2 = \frac{1}{2}k_r(\Delta r)^2 \quad (3.22)$$

$$V_\theta = \frac{1}{2}k_\theta(\theta-\theta_0)^2 = \frac{1}{2}k_\theta(\Delta\theta)^2 \quad (3.23)$$

$$V_\tau = V_j + V_\omega = \frac{1}{2}k_\tau(\Delta\varphi)^2 \quad (3.24)$$

where k_r , k_θ and k_τ symbolize the bond stretching, angle bending and torsional force constant and Δr , $\Delta\theta$ and $\Delta\varphi$ denote the bond stretching increment, bond angle change and twisting angle change, respectively.

3.4.2 Non-bonded interactions

Non-bonded potentials are significantly essential for the sake of atomistic simulation accuracy despite the fact that they contribute less effect during evaluations. Van der Waals (vdW) and Coulomb are two main type non-bonded interactions. The multiple layers of CNTs are held together thorough Van der Waals forces. Van der Waals effects are being active if two atoms are separated at least two bonds distance. As it can be seen from the Figure 3.3 that the atom I is not far enough from the J, K, N and M atoms to observe in-layer vdW effects. However, Van der Waals interaction can be considered for the atoms L, I', K' and J' because they have the distance more than 2 bonds from the atom I [2].

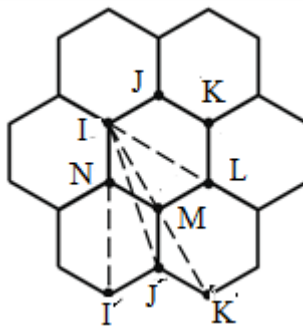


Figure 3.3 : Illustration of Van der Waals Interactions [2].

Van der Waals interaction can be expressed with Lennard-Jones potential as given in the following equation where, r is the distance between interacting atoms; ϵ is the minimum energy parameter and σ cutoff distance between two atoms. For carbon atoms, the LJ parameters are $\epsilon=0.0556$ kcal/mole and $\sigma=3.4$ Å

$$V_{\text{vdw}} = 4\epsilon \left[\left(\frac{\sigma}{r} \right)^{12} - \left(\frac{\sigma}{r} \right)^6 \right] \quad (3.23)$$

The relation between van der Force and Lennard-Jones potential for two atoms with a certain distance is depicted in the Figure 3.4.

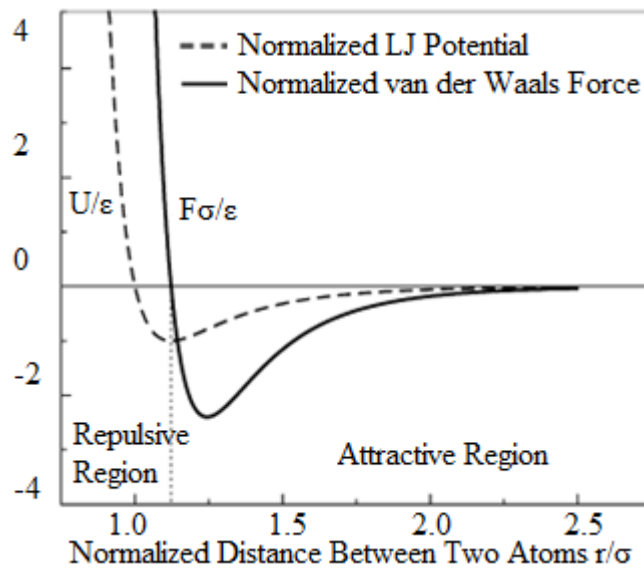


Figure 3.4 : LJ Potential and Van der Waals Force versus Distance [16].

If the electrostatic charges are present, it is convenient to employ Coulomb potentials being taken into account where Q_1 and Q_2 are electrostatic forces and ϵ_0 is the permittivity of free space [83].

$$V_{\text{es}} = \frac{Q_1 Q_2}{4\epsilon_0 \pi r} \quad (3.24)$$

4. MANY BODY POTENTIALS

4.1 Bonded Potentials

A potential energy function depends on atomic locations that generate forces in molecular dynamics simulations. Different potential functions existed for describing the carbon nanotubes C-C bonds.

4.1.1 Modified morse potential

Morse potential is one of the most significant potential to describe the atomic interaction between carbon-carbon atoms. Generally, this potential is used in atomistic based continuum approaches of CNT fracture and growth for both small and large deformation problems [4, 5, 20]. In this approach, covalent bonds are presented by beam elements such as Euler-Bernoulli (EB) or Timoshenko beams. Euler-Bernoulli or Timoshenko beam elements can be used to find out the behavior of atomic interaction under small deformation theory. However, large deformation criteria and geometric nonlinear effects must be taken into account for failure behavior. Timoshenko beam element is not preferred for large deformation problems because it is more complex than the EB beam element to be adapted for the modified Morse potential energy terms. In this manner, an extensive iterative implementation might be applied for large deformation problems by using the modified Morse potential.

A modified Morse potential function is based on bond stretching and bond angle bending terms under small strain hypothesis [84-88]. Stretching and bending movements are calculated similar to beam theories. Continuum mechanic equations are directly related to molecular mechanics parameters. Similar to all interatomic potentials, the equations are equalized with system energy terms. The modified Morse potential energy can be expressed as follows

$$V(\mathbf{r}_{ij}) = V_R(\mathbf{r}_{ij}) - B_{ij} V_A(\mathbf{r}_{ij}) \quad (4.1)$$

$$V_r = D_e \left\{ \left[1 - e^{-\beta(r-r_0)} \right]^2 - 1 \right\} \quad (4.2)$$

$$V_\theta = \frac{1}{2} k_\theta (\theta - \theta_0)^2 \left[1 + k_{\text{sextic}} (\theta - \theta_0)^4 \right] \quad (4.3)$$

where U_r is the bond stretching energy, U_θ is the angle bending bond energy, D_e is dissociation energy, β is fitting parameter, r and θ respectively are the current bond length and current angle of the adjacent bonds.

Table 4.1 : Modified Morse Potential Parameters [26].

Parameter	Value	Parameter	Value
r_0	1.421 Å	θ_0	2.094 rad
β	2.625 Å ⁻¹	k_θ	0.9×10^{-8} NÅ/rad ²
D_e	6.03105×10^{-9} NÅ	k_{sextic}	0.754 Å ⁴

According to the Morse potential, carbon nanotube has inflection point at 19% strain which is shown in Figure 4.1.

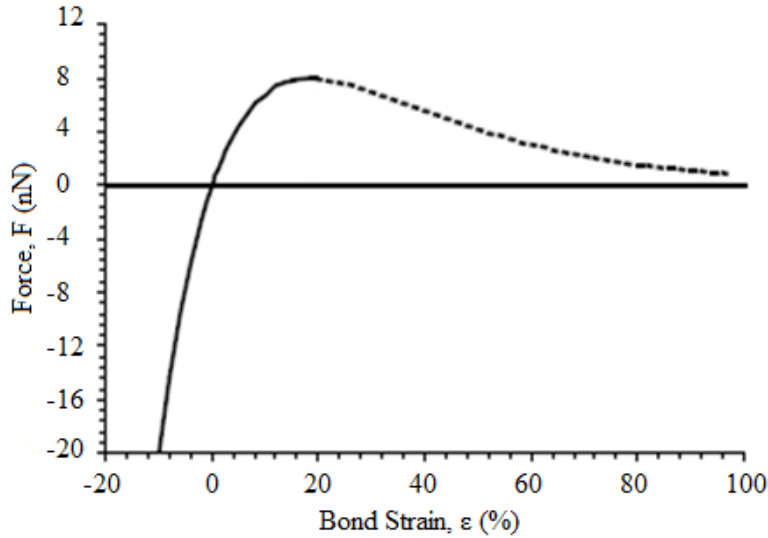


Figure 4.1 : Force-strain Curve of The Modified Morse Potential [88].

The modified Morse potential function is not capable of describing the bond breaking and formation behaviors of carbon-carbon bonds and it does not consider many-body interactions so these drawbacks limit the accuracy of crack propagation. It is desired to develop a better approach on both bond behavior and multi-body interactions to obtain more accurate results.

4.1.2 Reactive empirical bond order potential

Reactive empirical bond order potential is also called REBO potential or Tersoff-Brenner potential. Primitive formulation of this potential was proposed by Tersoff [89, 90]. Then, Brenner [91, 92] provided significant improvements by suggesting first-generation reactive empirical bond order. Due to the several drawbacks of first-generation REBO potential, Brenner et al. [93] proposed the second-order REBO potential in 2002. The second-order REBO includes improved analytic function and extensive database relative to an earlier version [41].

The REBO potential is a widely used many body interatomic potential to characterize C-C bonds in carbon nanostructures. Despite the complexity in implementation, it is accepted that the Brenner potential function is more accurate and more versatile than the Morse potential function since Brenner function describes formation and deformation of the Carbon-carbon bonds [26]. A second-generation reactive empirical bond order (REBO) potential provides a finer approach on mechanical deformation behavior of hydrocarbon molecules as allowing bond breaking and forming mechanics for covalent bonds [41-45]. Eventually, a better approximation in contrast to Morse potential is proposed.

It can be expressed as:

$$V(r_{ij}) = V_R(r_{ij}) - B_{ij} V_A(r_{ij}) \quad (4.4)$$

where r_{ij} is the distance between the linking atoms i and j , V_R and V_A are the repulsive and attractive pair terms:

$$V_A(r) = \frac{S D^{(e)}}{S-1} e^{-\sqrt{\frac{2}{S}} \beta (r-R^{(e)})} f_c(r) \quad (4.5)$$

$$V_R(r) = \frac{D^{(e)}}{S-1} e^{-\sqrt{2S} \beta (r-R^{(e)})} f_c(r) \quad (4.6)$$

where $D^{(e)}$, S , β , and $R^{(e)}$ are carbon, graphite and diamond known properties. The function f_c is merely a Smooth cutoff function f_c is used to limit the range of the potential as follows [121]. The smooth cutoff function is controlled and it takes certain values of the following equations.

$$f_c(r) = \begin{cases} 1 & r < R^{(1)}, \\ \frac{1}{2} \left\{ 1 + \cos \left[\frac{\pi(r - R^{(1)})}{R^{(2)} - R^{(1)}} \right] \right\} & R^{(1)} < r < R^{(2)}, \\ 0 & r < R^{(2)} \end{cases} \quad (4.7)$$

which is continuous and has a cutoff of $R^{(2)} = 0.2$ nm and $R^{(1)} = 0.17$ nm to include only the first-neighbor shell for carbon atoms. A multi-body coupling between the bonds from the atom i to the atom j and the local environment of atom I , are parameters of B_{ij} as follows.

$$B_{IJ} = \left[1 + \sum_{k(i,j)} G(\theta_{ijk}) f_c(r_{ik}) \right]^{-\delta} \quad (4.8)$$

where r_{ik} is the distance between the atoms i and k , f_c is the cutoff function in Eq. (4.8), θ_{ijk} is the angle between bonds $i-j$ and $i-k$, and the function G is given by

$$G(\theta) = a_0 \left[1 + \frac{c_0^2}{d_0^2} - \frac{c_0^2}{d_0^2 + (1 + \cos\theta)^2} \right] \quad (4.9)$$

Certain values for the Tersoff-Brenner potential constants are elaborated in the following table.

Table 4.2 : Tersoff- Brenner Potential Constants [26].

Parameter	Value	Parameter	Value
$D^{(e)}$	6.000 eV	Δ	0.5
$R^{(e)}$	0.139 nm	a_0	0.00020813
S	1.22	c_0	330
β	21 n/m	d_0	3.5

As it mentioned earlier, the second-generation REBO potential do not include long-range interactions and torsional terms in addition to complexity of computation. It can be stated that REBO is short ranged and quickly evaluated potential. However, it neglects non-bonded interactions and torsional terms which [91-93].

4.1.3 Adaptive intermolecular reactive empirical bond order potential

The adaptive intermolecular reactive empirical bond order also called AIREBO is a multi-body potential that contains long-range atomic interactions and torsional terms in addition to REBO potential terms. To describe CNT deformation under mechanical loading, AIREBO potential is accepted as an accurate atomic potential for hydrocarbons molecules [94].

It is similar to Brenner potential but AIREBO potential also allows atomic torsion and non-bonded interactions through an adaptive treatment of intermolecular interactions as shown in Eq. (4.10).

$$V_{\text{AIREBO}} = \frac{1}{2} \sum_i \sum_{i'j} \left[V_{ij}^{\text{REBO}} + V_{ij}^{\text{LJ}} + \sum_{i'k} \sum_{j'l} V_{kijl}^{\text{Torsion}} \right] \quad (4.10)$$

where the total interaction energy V^{AIREBO} , V_{ij}^{REBO} is REBO interactions, V_{ij}^{LJ} is LJ terms and $V_{kijl}^{\text{Torsion}}$ is the torsion interactions.

AIREBO potential presents reactive capabilities of the atomic system and only describes short-ranged C-C, C-H and H-H interactions. These interactions depends strictly on the position through a bond order parameter that adjusts the attraction between the I, J atoms.

4.2 Non-bonded Potentials

4.2.1 Lennard-Jones potential

Lennard-Jones(LJ) potential is used to simulate of van der Waals forces which occur in a certain distance between two neighbor atoms. Lennard-Jones potential is also named as "6-12 potential" and it enables a proper linkage to attraction and repulsion forces [16, 95]. The general LJ formulation is given by

$$V_{\text{LJ}} = 4\epsilon \left[\left(\frac{\sigma}{r} \right)^{12} - \left(\frac{\sigma}{r} \right)^6 \right] \quad (4.11)$$

where r is the distance between interacting atoms, ϵ and σ are LJ parameters that are minimum energy parameter and cutoff distance between two atoms, respectively. For

carbon atoms, the LJ parameters are $\epsilon=0.0556$ kcal/mole and $\sigma=3.4 \text{ \AA}$ [95, 96]. The potential $V(r)$ is usually truncated at an interatomic distance of 2.5σ without a significant loss of accuracy.

Based on the general expression for Lennard-Jones potential, which is shown in Eq. (4.11), Van der Waals force can be stated in detail as given in the following equation [16].

$$F_{\text{vdw}}(r) = -\frac{dV_{\text{LJ}}(r)}{dr} = 24 \frac{\epsilon}{r} \left[2 \left(\frac{\sigma}{r} \right)^{13} - \left(\frac{\sigma}{r} \right)^7 \right] \quad (4.12)$$

The variations of the LJ potential and Van der Waals force with the distance between two interacting atoms are shown in Figure 4.2.

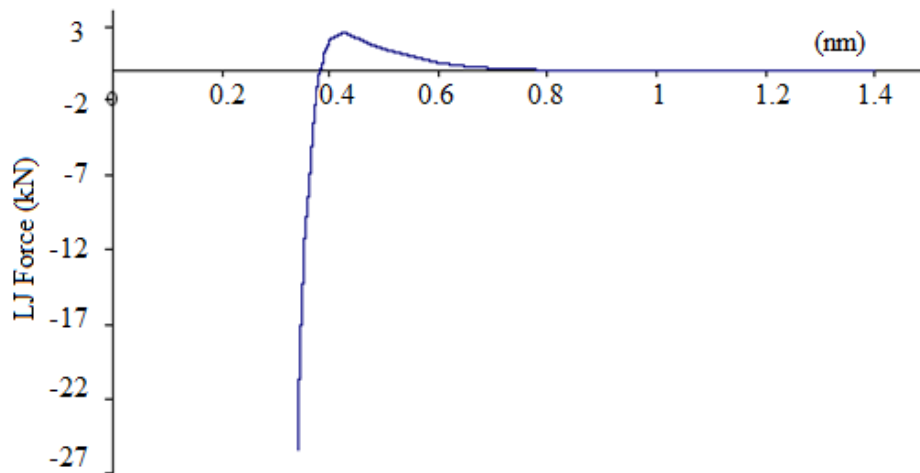


Figure 4.2 : LJ Force as the Distance between Two Interacting Atoms Changes [121].

4.2.1 Columbic pairwise potentials

Figure 4.3 represents the Columbic interactions of two atoms. Charge of atoms may cause repulsive/impulsive forces and their distance directly affects potential energy. Columbic pairwise interaction between two different atoms can be expressed by the following equation.

$$V_{\text{coulombic}} = \frac{CQ_i Q_j}{\epsilon r} \quad (4.13)$$

where C is an energy-conversion constant, Q_i and Q_j are the charges on the 2 atoms, and ϵ is the dielectric constant and r is the radius that must be smaller than r_c which

is the cut off distance. If the radius is smaller than the cut off distance of, r_c no interaction is observed in the system.

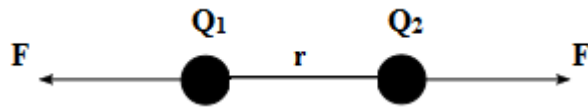


Figure 4.3 : Interaction of Two Separate Atoms.

5. EVALUATING MECHANICAL PROPERTIES OF SWCNT USING MOLECULAR DYNAMICS SIMULATIONS

5.1 A Brief View to the Classical Structural Mechanics

Potential usage of CNTs for advanced materials, as it mentioned in the previous section, caused to extensive investigation of their mechanical properties in particular elastic behavior. Both theoretical and experimental studies exist for determining the Young's modulus of nanotubes.

The Young's Modulus is also known as Modulus of Elasticity which is a quantity to describe elastic characteristics of a material. The Young's modulus can be experimentally identified by taking the slope of stress-strain curve under tensile load

From the Hooke's Law in one-dimension, the Young's modulus is evaluated with the following equation:

$$E = \frac{\sigma}{\varepsilon} = \frac{FL_0}{A_0\Delta L} \quad (5.1)$$

where E is the Young's modulus, σ is one-dimensional normal stress, ε is one-dimensional strain, F is the total applied force under tension, A_0 is the initial cross-sectional area, L_0 is the initial length, ΔL is the changes in the length.

5.2 Molecular Dynamics Simulations for SWCNT

In this part of the present study, a tensile load simulation is implemented to a single-walled carbon nanotube by using LAMMPS in order to determine the Young's modulus of SWCNT. There are previous studies estimating SWCNT Young's modulus, but the original aim is not only determination of the Elastic modulus, tensile strength, Poisson's ratio or density. If calculated Young's modulus is in a good agreement with literature data, the tensile code proves that the LAMMPS script works properly. Eventually, it means that LAMMPS code can be used for the mechanical test simulations of carbon nanotube network structure.

In principle, the atoms at the bottom end are fixed as both translational and rotational degree of freedoms as boundary conditions and atoms at the upper end are subjected to a tensile force as represented in Figure 5.1. Then,

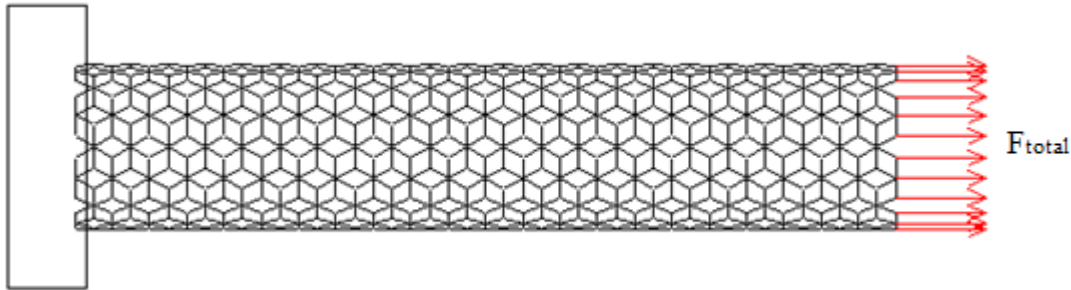


Figure 5.1 : Representation of Boundary and Load Conditions [121].

As it can be clearly indicated from given formula, elastic modulus of single-walled carbon nanotube highly depends on chirality, diameter and wall-thickness of nanotube. In the present simulations, an armchair nanotube with $(n,m)=(10,10)$ nomenclature is considered in the MD simulations which is shown in Figure 5.2. The length and wall-thickness are determined as 23.382 \AA and 3.4 \AA respectively, and the diameter is evaluated as 13.57 \AA .

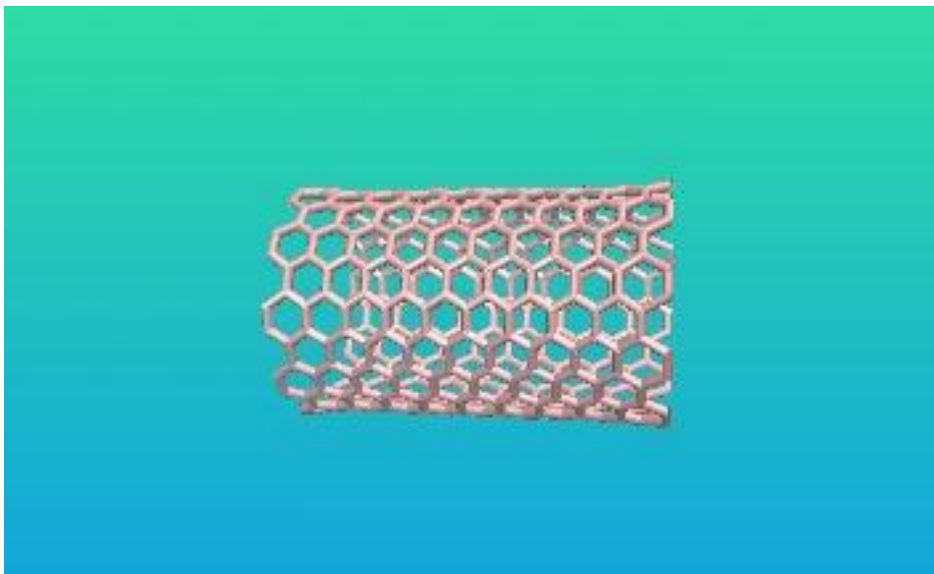


Figure 5.2 : Initial Situation of a $(10,10)$ SWCNT

Large-scale Atomic/Molecular Massively Parallel Simulator (LAMMPS) is employed to apply a tensile load to selected $(10,10)$ carbon nanotube for molecular dynamics simulations. The AIREBO potential with a 2.5 \AA cutoff distance is applied to the system and energy minimization is obtained by using conjugate-gradient method.

$$V_{\text{AIREBO}} = \frac{1}{2} \sum_i \sum_{i'j} \left[V_{ij}^{\text{REBO}} + V_{ij}^{\text{LJ}} + \sum_{i'k} \sum_{j'l} V_{kijl}^{\text{Torsion}} \right] \quad (5.2)$$

All simulations are carried out at 300° K temperature with a Langevin thermostat, which provides that the structure stays unaffected at the temperature 300° K during simulations. Besides, NVE ensemble keeps total number of particles, total energy and total volume constant regarding periodic boundary conditions. As the boundary condition, the bottom end of the nanotube is clamped which means all degrees of freedom are constrained. Then, the region having a set of atoms from upper end of CNT is introduced so as to apply a displacement increment of 0.25 Å. Time step is kept fixed at 0.001 ps to minimize dynamical effect of force response. One increment occurs in 1000 runs for present time step, consequently total time is evaluated for 1 ps.

$$t = \Delta t \times N = 0.001 \times 1000 = 1 \text{ ps} \quad (5.3)$$

$$\varepsilon = \frac{\Delta L}{L_0} = \frac{0.25}{23.4} \approx 0.01 \quad (5.4)$$

$$\dot{\varepsilon} = \frac{\varepsilon}{t} = \frac{0.01}{10^{-12}} \approx 10^{10} \text{ s}^{-1} \quad (5.5)$$

In molecular dynamics simulations, the strain rate is a highly substantial parameter that is directly related to simulations results. To obtain accurate results, a rational strain rate must be chosen. Mylvaganam et al. [97] determined the strain rate for MD simulations of carbon nanotubes as $1.3 \times 10^9 \text{ s}^{-1}$ which is a reasonable value.

However, this value depends on temperature, nanotubes length or chirality. Liu et al. [47] stated in their study that specified strain rate has to be lower a critical strain rate value of 10^{10} s^{-1} , because higher strain rate values cause problems such as hardening. Therefore, they selected the strain rate as $1 \times 10^8 \text{ s}^{-1}$ to avoid these artifacts.

Eventually, it can be clearly seen from the evaluations that applied strain rate is lower than the critical rate. Moreover, varied strain rates under critical values give similar and logical results in the MD simulations of single-walled carbon nanotubes.

Whole simulation process is carried out on powerful workstations, after essential arrangements, commands and variables are set inside the LAMMPS input file.

Figure 5.3 shows a gradual deformation of the (10, 10) SWCNT during the tensile loading simulations

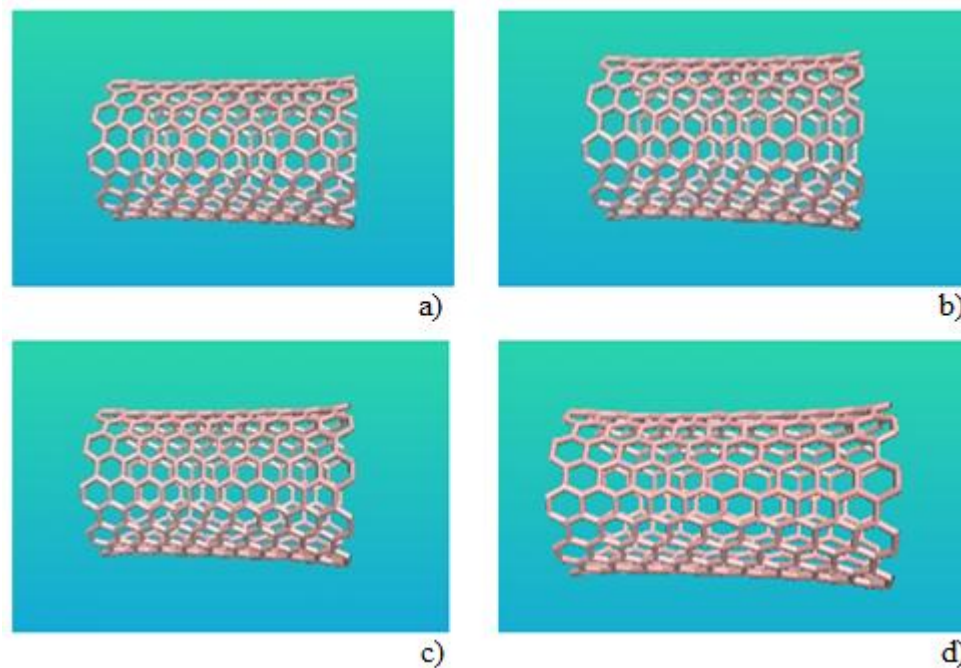


Figure 5.3 : Gradual Deformation Period of a SWCNT.

Note that, view d is the last step just before the fracture of carbon nanotube. It can be realized that regular hexagonal rings distorts due to the tensile force. As it mentioned before, displacement increment is applied to a group of atoms in the upper end of carbon nanotube where average forces per atom in the z direction are calculated in every few timesteps for long time scales. Then, average forces per atom are summed up to evaluate the total applied force in z direction.

Young's modulus of SWCNT is calculated using the same formula given in Eq. (5.1). However, definitions of some parameters are a bit different from that formula. E is the Young's modulus, σ is one-dimensional normal stress, ϵ is one-dimensional strain, F is the total applied force under tension, A_0 is the initial cross-sectional area of tube, L_0 is the initial length of nanotube, ΔL is changes in the tubes length., ΔL is the displacement increment, D is mean diameter that depends on the chirality of nanotube and t is the wall thickness of CNT which can be taken as 3.4 \AA .

Figure 4.4 shows schematic representation of the cross-section of SWCNT. As it can be clearly seen, there is an outer and inner radius of the tube. But an averaged diameter is calculated as follows:

$$A_0 = \pi Dt \quad (5.6)$$

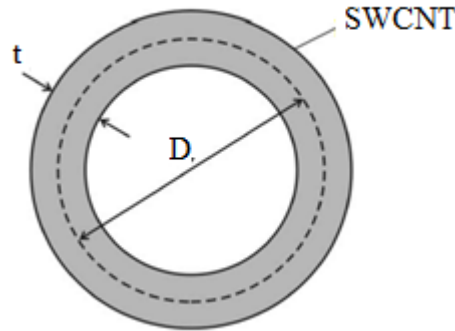


Figure 5.4 : Schematic Representation of the SWCNT's Cross-section [5].

Eventually, an Excel code is used to apply general Hooke's law for calculating the Young's modulus of nanotube and to plot strain-stress curves. Figure 5.5 shows stress-strain curves of the present nanotube.

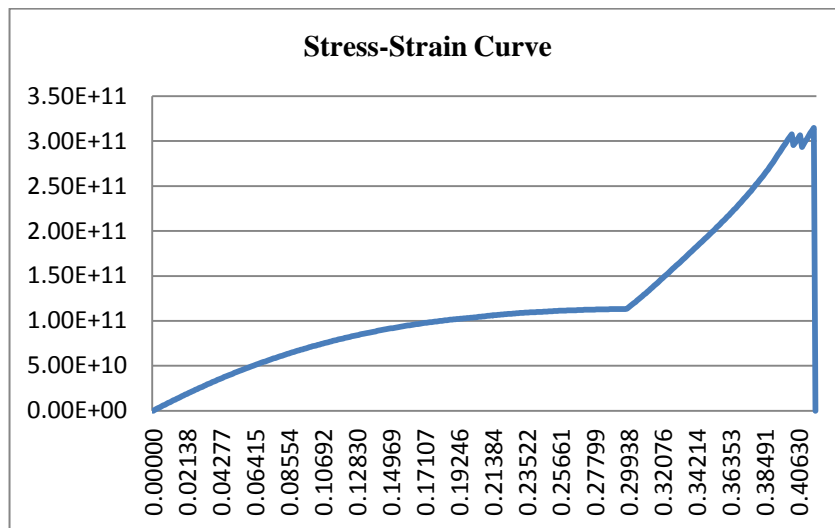


Figure 5.5 : Strain Curves of a Single-walled Carbon Nanotube under Tensile Force by Using Adaptive Intermolecular Reactive Empirical Bond Order Potential.

Consequently, modulus of elasticity is determined around 0.982 *TPa* from current calculations. This value is in agreement with the previous studies on estimation of SWCNTs Young's modulus.

Table 5.1 gives the axial Young's Moduli of single-walled Carbon nanotubes, which were reported by different scientists using different approaches as mentioned in the previous sections. Besides, values of chirality and current wall-thickness changes results.

Table 5.1 : Comparative Investigations in Literature.

Study	Method	Chirality (n,m)	Wall- Thickness <i>t</i>-nm	Young's Modulus <i>E</i> -TPa
Present work	Molecular Dynamics	10,10	0.34	0.984
Lu [25]	Molecular Dynamics	10,10	0.34	0.975
Jin and Yuan [28]	Molecular Dynamics	10,10	0.34	1.235
Yakobson et al. [17]	Molecular Dynamics	Xxx	0.066	5.5
Li and Chou [15]	Structural Mechanics Approach	Xxx	0.34	1.002
Tserpes and Papnikos [5]	Molecular Structural Mechanics	8,8	0.147	2.377
Giannapoulos et al. [101]	Molecular Structural Mechanics	8,8	0.34	1.3069
Fan et al. [2]	Molecular Structural Mechanics	10,10	0.34	1.0363
Lu et al. [4]	Molecular Structural Mechanics	Xxx	0.34	0.989 - 1.058
To [103]	Molecular Structural Mechanics	Xxx	0.34	1.03
Ávila et al. [104]	Molecular Structural Mechanics	Xxx	0.34	0.978 - 1.057
Wernik et al. [98]	Atomistic Continuum Modeling	9,9	0.34	0.944
Pantano et al. [22]	Continuum Shell Modeling	13,0	0.075	4.84
Tu and Ou-Yang [100]	Local Density Approximation	Xxx	0.075	4.7
Kudin et al. [99]	Ab Initio Methods	10,10	19.6	3.859
Hernandez et al. [23]	Tight-binding Theory	10,10	0.34	1.24
Gupta et al. [102]	Molecular Mechanics	10,10	0.34	1.23
Krishnan et al. [8]	Experimental Method	Xxx	Xxx	1.35-0.35/+0.45
Yu et al. [12]	Experimental Method	Xxx	Xxx	1.02 (Av)

For mechanical properties of CNT networks, we are also going to investigate Poisson's ratio for carbon nanotube network. Thus, we need to find the Poisson's ratio for a SWCNT. For a 1D tensile test simulation, the Poisson's ratio can be found from the following equation.

$$v = -\frac{\varepsilon_y}{\varepsilon_x} = \frac{\frac{\Delta D}{D_0}}{\frac{\Delta L}{L_0}} \quad (5.7)$$

where v is the resulting Poisson's ratio, ε_x is transverse strain (negative for axial tension (stretching), positive for axial compression), ε_y is axial strain (positive for axial tension, negative for axial compression), D is diameter and L is length.

Table 5.2 : Poisson's Ratios of Previous Studies [105].

Study	Method	Poisson's Ratio
Present work	Molecular Dynamics	0.16
Shitna and Nrita (2003)	Molecular Dynamics	0.15
Sanchez-Portal et al. (1999)	Ab Initio Methods	0.12-0.16
Hernandez et al. (1998)	Tight-binding Theory	0.24-0.26
Lu (1997)	Empirical Potentials	0.282
Popov et al. (2000)	Lattice-dynamical Model	0.21
Chang and Gao (2003)	Molecular Mechanics	0.16
Li and Chou (2003)	Molecular Structural Mechanics	0.06
Chen et al. (2010)	Molecular Structural Mechanics	0.1
Krishnan et al. (1998)	Experimental Method	0.3
Treacy et al. (1996)	Experimental Method	0.3
Salvetat et al. (1999)	Experimental Method	0.16
Guo, Wang and Zhang (2005)	Continuum Modeling Theory	0.55

Similar to the Young's modulus, the Poisson's ratio may be calculated. Thus, it is reasonable to determine the Poisson's ratio for a single-walled carbon nanotube. When a uniaxial tensile loading is applied to a tube, the biggest shrinkage is observed in the middle of the tube. Therefore, we shall create a region in the middle of the carbon nanotube and consider related atoms in this region. After applying the tensile loading, the final positions of atoms can be easily found and final diameter can be calculated from the positions. Since we know initial and final diameters, initial and final lengths, we are able to evaluate Poisson's ratio from Eq. (5.7). After all, the

Poisson's ratio is obtained as 0.16. This value is in a good agreement with previous studies in literature. Similar molecular dynamics studies indicate that the Poisson's ratio is found around 0.16.

5.3 Fracture Investigation

Different fracture mechanisms may cause undesirable changes on the mechanical, electrical or thermal properties of carbon nanostructures. Incomplete bonding defects such as one atom vacancy and topological defects such as Stone-Wales transformation are the most common and frequently investigated defects mechanisms for carbon nanostructures. The finite element representation of these defects are shown in Figure 5.6.

Electron irradiation or oxidative purification process may cause missing atoms in a carbon nanotube and generate vacancy defects. The 90° rotation of a carbon bond about its center is introduced as a Stone-Wales transformation. After rotation, two pentagons and two heptagons are obtained instead of four hexagons [106].

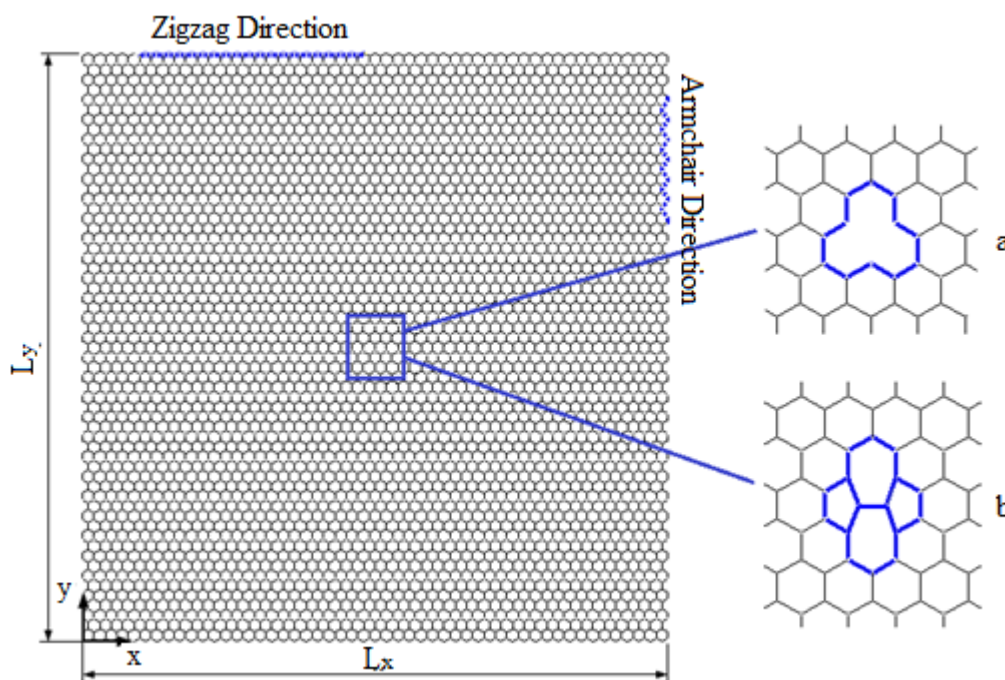


Figure 5.6 : Equivalent FE Model of the Defect-free and Defected SLGS Model; a) One Atom Vacancy, b) SW Defects [121].

In Figure 5.7, various defects for carbon nanotubes are demonstrated and it can be emphasized that most significant ones are vacancy and Stone-Wales defects [90].: a) defect-free tube; b) vacancy (V) c) interstitial (I); d) straight Stone–Wales defect

(SW1); e) O₂ molecule pre-dissociated at SW1 (SW1_O_O); and f) slanted Stone–Wales defect (SW2). The atoms in the vicinity of the defects are shown in stick representation.

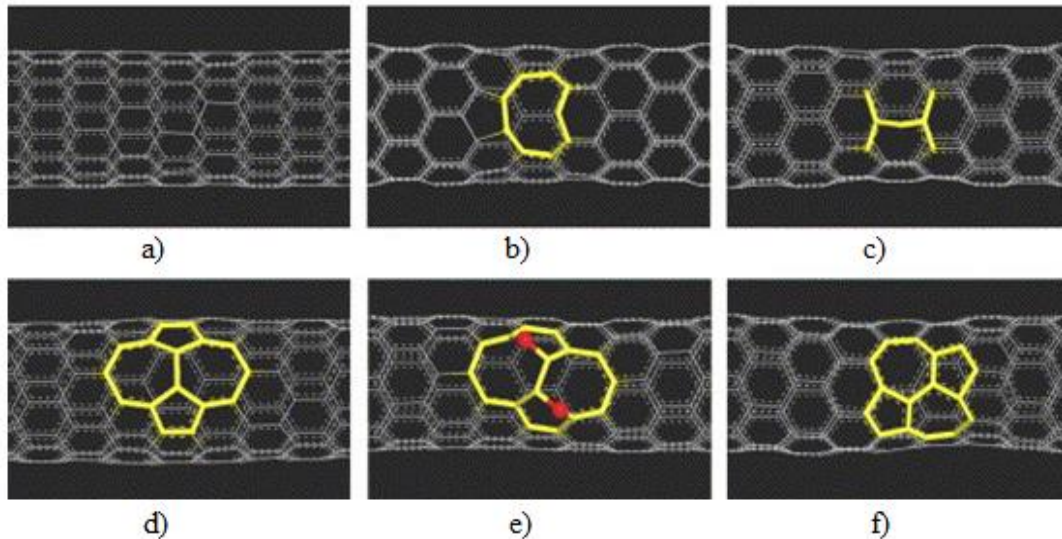


Figure 5.7 : Various Structural Defects on a (8,0) Nanotube [107]

Based on the selected potential functions, in carbon nanotubes the reconfiguration of bonds and structural transformations may occur after the C-C bonds are broken. The modified Morse potential function is not capable of describing the bond breaking and formation behaviors of carbon-carbon bonds and it does not consider many-body interactions; thus, these deficiencies limit the accuracy of nanotubes crack propagation. However, the Brenner formulations allow bond breakage and bond reconstruction.

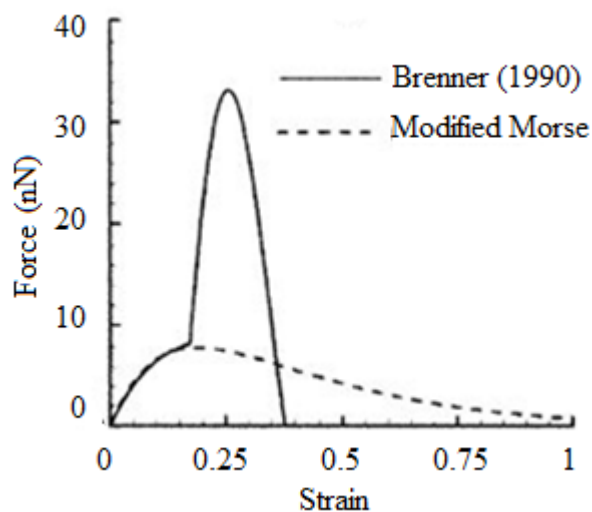


Figure 5.8 : The Brenner and The Modified Morse Potentials and Tensile Force Fields [26].

Carbon-carbon bonds of the nanotube begin fracture, when the strain reaches a threshold value. Inflection point of the interatomic potentials affects the fracture behavior most and influence of separation energy is inconsiderable [26]. After the inflection point, strain occurs with bond breaking where bond formation is expected and the shape of the potential function is not important since material damage occurs.

It is predicted from molecular mechanics and dynamics simulations of single-walled carbon nanotubes that the strain at a tensile failure should be around % 30. However, experimental studies present the strain has generally value between %10 and %16.

An interatomic force-strain curve describes fracture behavior of carbon nanotubes properly. The strain is named as the inflection strain and the force is named as the peak force when the interatomic force reaches the peak point. The rest is called bond-breaking strain. In Figure 5.7, the interatomic force is investigated for the Brenner and modified Morse potentials under tension. As it can be clearly seen from the Figure, both potentials show the similar force behaviors until a definite strain value around %19 which is the inflection strain for the modified Morse potential. But, a sharp increase is observed in the interatomic force of the Brenner potential due to its cut off function $f_c(r)$ as elaborated in Eq. (4.7) and then the cut-off distance is a bond-breaking criteria which is frequently applied in atomistic simulations. The increase can be depicted as a camelback on the force curve and reaches to its top value around 30% strain. Consequently, this figure reasonably explains similar sharp slope on the stress-strain curve in Figure 5.5 Belytschko et al. [26] indicates that carbon nanotube fails at %28 strain and tensile strength is 110 GPa similar to the computational results of the previous studies presented by Campell, Brabec and Bernholc (%30). In the present study, similar values as %28,9 and 113 GPa values are observed for strain and tensile strength, respectively.

6. CARBON NANOTUBE NETWORKS

Exceptional properties of carbon nanotubes lead to the idea that combining numerous nanotubes may be the key for generation and improvement of new advanced materials. Thus, individual CNTs will be used as building blocks of new materials and their nanoscale properties might be observed even in continuum scale [31]. Consequently, the idea of CNT networks has been born to use, the unique properties of CNTs more efficiently.

CNTs are generally used as the reinforcement for composite materials. However, it is impractical to use them only in nanoscale. Hence, it is proposed to produce solely CNT-based materials without any reinforcement in order to utilize superior properties of CNTs in macro scale. In this sense, a recent study based on generation of a bulk material composed of carbon nanotube ensembles, which is called "Carbon Aerogels" can be considered as one of the most adequate and significant example [108].

In Figure 6.1, an example of carbon aerogels in electron microscope is demonstrated. Aerogels are synthetic porous ultralight materials generally produced by extracting liquid component without destroying network structures through lyophilization (freeze-drying) or critical-point drying (CPD) methods.

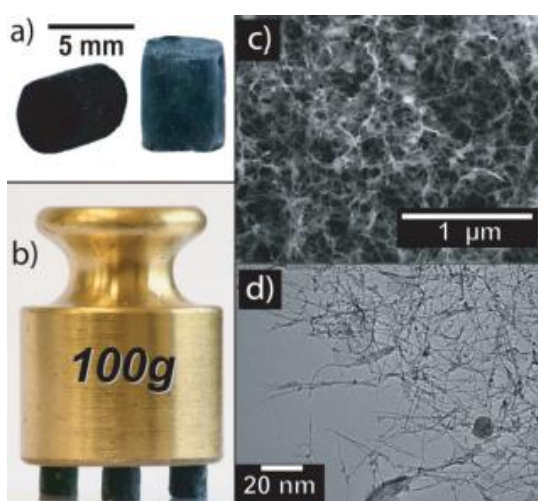


Figure 6.1 : Images of Aerogels.

Some of the main types of aerogels are silica, alumina, organic and most significantly carbon [108, 109]. Carbon aerogel is a novel material consisting of a great number of carbon nanotube networks with unusual properties such as high strength, high surface-area-to-volume ratios, low density, good electrical properties and highly porous structure. In Figure 6.1, images of carbon aerogels are given with different scale demonstrations obtained by using transmission electron microscope. Details are given in: a) Macroscopic pieces of 7.5 mg mL⁻¹ CNT aerogels.; Pristine CNT aerogel (left) appears black, whereas the aerogel reinforced in 1 wt % PVA bath (right) is slightly gray. b) Three PVA-reinforced aerogel pillars (total mass = 13.0 mg) supporting 100 g, orca. 8000 times their weight. c) This scanning electron microscopy image of a critical-point-dried aerogel reinforced in a 0.5 wt % PVA solution (CNT content = 10 mg mL⁻¹) reveals an open, porous structure. d) This high-magnification transmission electron microscopy image of an unreinforced aerogel reveals small-diameter CNTs arranged in a classic filamentous network.

Carbon nanotube networks are composed of numerous self-intersected carbon nanotubes in two or three-dimensional space. The coalescence of network structure is obtained with production of covalent bonds between intersecting CNTs. To maintain exceptional properties of an individual carbon nanotube in a network structure, true joints are intended between intersected CNTs. These joints are provided by using various methods including electron beam welding, ion beam irradiation, and mechanical manipulation with atomic force microscopy, spark plasma sintering, bonding through chemical modification, pressure treatments, nanotube soldering and heat welding [32]. In addition to junction quality, nanotube length distribution, chirality of nanotubes, presence of surface defects, junction types and their density are some other parameters that affect network behavior.

In theory, it can be said that the idea of network is extremely charming in order to observe nanoscale features of carbon nanotubes in macro world applications. In this viewpoint, every single property of carbon nanotubes can be easily utilized in our practical studies with the help of network structure. However, it is not as easy as in thought to generate a proper network model since there is not a prepared method to build a network. Before all, scientists have categorized networks to have a better understanding. In this matter, carbon nanotube networks can be classified in two main categories: the ordered networks and random networks. Two major types of

carbon nanotube network structures can be shown in Figure 6.2 in two-dimensional space.

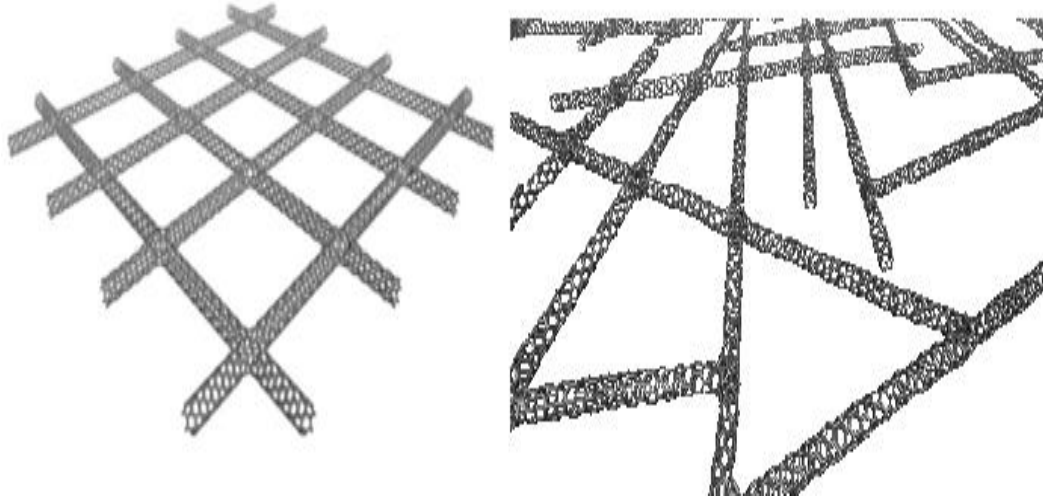


Figure 6.2 : Ordered and Random CNTs.

When nanotubes are arranged and coalesced with a proper system as it is shown in Figure 6.2, it is called "Ordered CNT network". These networks can be considered as ideal structures. On the contrary, an arbitrary distribution of individual carbon nanotubes in a two or three dimensional design space is named as "Random CNT network".

Most of studies about carbon nanotube networks in literature consider ordered CNT network structures [66-69,109-112]. However, these studies do not contain geometrical irregularities and possible imperfections at junctions like bond rearrangements. On the other hand, the numbers of studies about random networks are very limited since there is no appropriate computational method or numerical model algorithm to create random structure [31].

In the present thesis, the general procedure can be summarized in 3 main categories as it is mentioned in previous sections. First, a self-controlled algorithm is described to generate two-dimensional or three dimensional network models comprising of random intersected carbon nanotubes which are distributed systematically in design space and then a molecular dynamics simulation is employed to create true junctions by heat welding method in the following stage. In the final step, a tensile load simulation is applied to investigate and discuss mechanical properties such as the Young's modulus, Poisson's ratio, ultimate tensile strength, yield strength or density of current network.

6.1 Network Generation

In the first stage of the study, an extensive MATLAB algorithm is employed to generate carbon nanotube networks. There are 2 loops in this procedure. The first loop is for continuation of the generation of the CNT items while the second loop is the sub-loop for generation and validation of candidate CNTs. When one of the CNT candidates satisfies all the design constraints in the sub-loop, the generation process continues with the selection of a CNT from the library in the main loop.

6.1.1 General concepts

The present algorithm aims at generation and validation of CNT networks by selecting randomly rotated and translated candidate nanotubes in a design space if they obey to specified design constraints. However, some definitions should be clarified before giving the details of network generation procedure.

- **Design space:** The design space can be described as a working domain for generating CNT networks where individual nanotubes are translated into this domain randomly. For 3D network applications, nanotubes can be placed in all three dimensions. For 2D applications, nanotubes are placed in a plane with a definite thickness introducing the diameter of nanotubes.
- **Library:** As it is mentioned earlier, network properties highly depend on lengths and chiralities of selected nanotubes. The library is a cognitive concept that stores all types of carbon nanotubes in different lengths and diameters where candidates are picked and placed into the design space if they satisfy design constraints.
- **Candidate:** Every CNT in the library is defined as a candidate before being located in the design space. If a candidate CNT satisfies the constraints, it can join to a target element to form a proper junction.
- **Target:** The interconnections of a CNT network are implemented on the target element considering the number of cross-linked CNTs. When a candidate satisfies the design constraints, it is placed to the target element very closely to obtain covalent bonding in that region.
- **Cross-linked CNTs:** Appropriate nanotubes to obtain interconnections on the target item are called cross-linked CNTs. A certain number of cross-

linked carbon nanotubes exist on a target element, which is determined in the algorithm.

- **Design constraints:** To obtain proper and realistic network structures, some design limitations are defined in terms of angles and intervals between cross-linked CNTs and distance of intersection points.

6.1.2 General algorithm

Present algorithm encapsulates two loops during the network generation process. The first loop is the main loop, which provides permanence and maintenance of individual CNT's translation into the design space. The other loop is a sub-loop that controls the candidate CNTs' compatibility with the design constraints. The design parameters are determined in accordance with reasonable settlement of cross-linked CNTs on the target element. After a candidate CNT is selected in main loop, sub-loop seeks if the candidate fulfills the design constraints. Consequently, nanotube is placed in the design space providing that all design constraints are satisfied. Otherwise, the candidate is abandoned with a great number of trials. Finally, the procedure returns the main loop and selecting of new CNTs from the library begins. As it can be clearly distinguished, there is a self-controllable systematic cycle in network generation process. And this procedure can be explained in five major steps:

1. **Selection of CNTs from the library:** The library may include various nanotubes in distinct lengths and chiralities. Candidate nanotubes are randomly selected from this library.
2. **Rotation and translation of candidate items:** Random rotation and translation of chosen CNTs in the design space are implemented in this step.
3. **Implementation of design constraints:** Candidate CNTs are tested with certain design conditions until an appropriate item is determined.
4. **Decision of sub-loop:** Two decisions are made in this step. The candidate item is located into the design space if design constraints are satisfied. If not, current candidate is abandoned and new one is tested
5. **Generation of LAMMPS input data file:** To use in subsequent steps such as welding process or tensile loading simulations atomic locations are saved into different files. Then, a LAMMPS script read the atomic coordinates.

These significant steps of network generation procedure are explained in detail consecutively in the following paragraphs.

6.1.2.1 Selection of CNTs from the library

A carbon nanotube is a cylindrical hollow structure with various diameters. In the present algorithm, a line representation is preferred while generating network structure in order to provide better computational time efficiency. A line segment located through centerline direction between two ends of the hollow cylinder symbolizes three-dimensional nanotube item. The center points of circles at each nanotubes end are the essential and sufficient coordinates to build the line segment. Figure 6.3 shows the line representation of nanotubes.

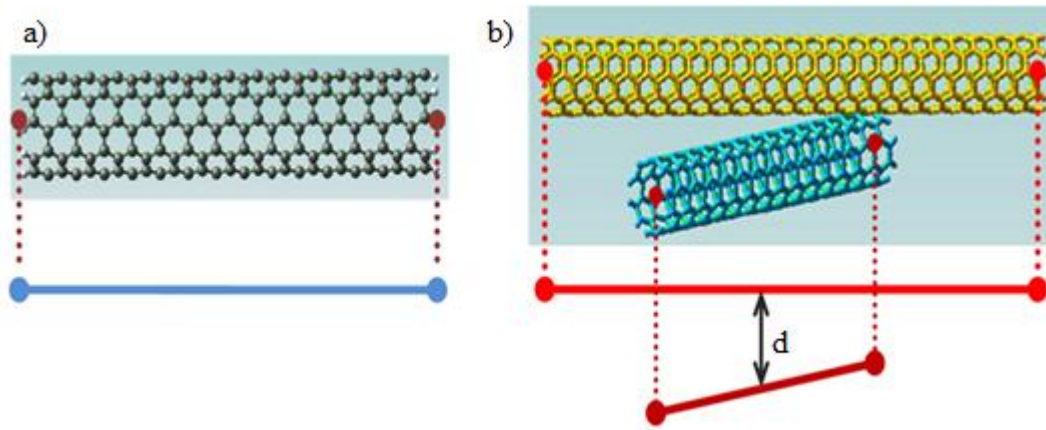


Figure 6.3 : Line Segment Representation [31].

The tip coordinates are very significant concepts because they are not only used during selection of nanotubes from the library but also used during rotation and translation process of chosen candidates since these motions are applied to end points. Subsequently, random interconnection points on a line representation are determined as function of tip coordinates. Eq. (6.1) determines the random points on the line segments.

$$\begin{aligned}
 x &= x_0 - t(x_1 - x_0) \\
 y &= y_0 - t(y_1 - y_0) \\
 z &= z_0 - t(z_1 - z_0)
 \end{aligned}
 \tag{6.1}$$

where $\{x_0y_0z_0\}$ and $\{x_1y_1z_1\}$ are end coordinates, t is line segment parameter which has a varying value between 0 and 1. The line representation is two-dimensional but it is obvious that the nanotube has a thickness.

Figure 6.4 demonstrates a possible settlement of candidate CNTs on a target depending on line segment parameter and number of cross-linked carbon nanotubes. As it can be clearly distinguished from the figure below, there are total 4 cross-linked CNT's that are located on the target CNT. The cross-linked CNT's are settled in certain distance, which is also controlled by the algorithm similar to the total number of cross-linked CNT's.

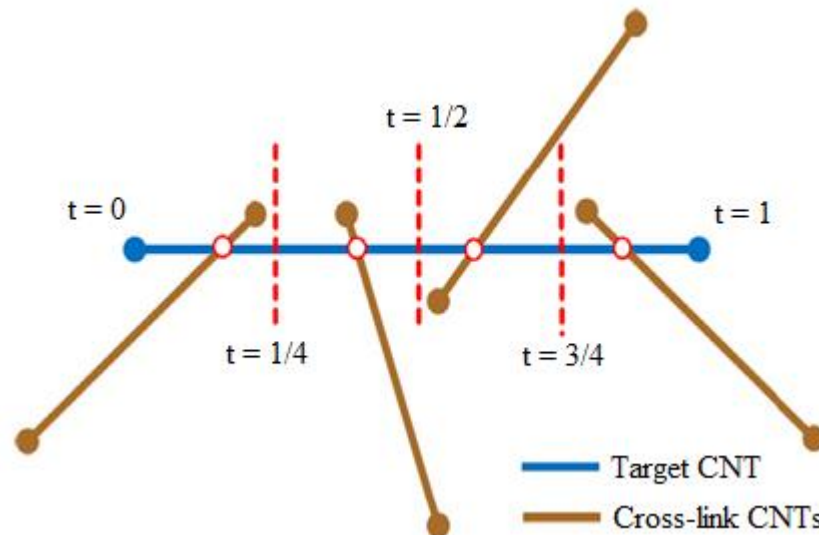


Figure 6.4 : Possible Segmentation of Target Item [31].

The number of cross-linked CNTs is a predefined parameter in the algorithm which is represent with n . Based on the parameter n , the interval of the k_{th} cross-linked item is found as $[(k-1)/n, k/n]$.

6.1.2.2 Rotation and translation of candidate items

As it is mentioned earlier, a definite number of cross-linked CNTs are placed on target items to generate interconnected networks, which is illustrated in Figure 6.5. Initially, a target item is located in the design space. Then, first cross-linked nanotube is placed on the target element considering line segment interval and the process carries on consecutively settling the other cross-linked CNTs until it reaches to the maximum value. Finally, a new target is assigned after the settlements of cross-linked CNTs are accomplished to the previous target item. Not all these arrangements are likely to be an arbitrary procedure; there is a comprehensive and systematic logic behind all operations. Because, we desire to create a fine structure without impossible overlapping or mistakes.

The correct order of building network structure is demonstrated in Figure 6.5 that explains the logic behind the generation of a two-dimensional network. Rotation arrangements of candidate nanotube in library, selection of random intersection points on target and translation of cross-linked carbon nanotube are represented in the figure, respectively,

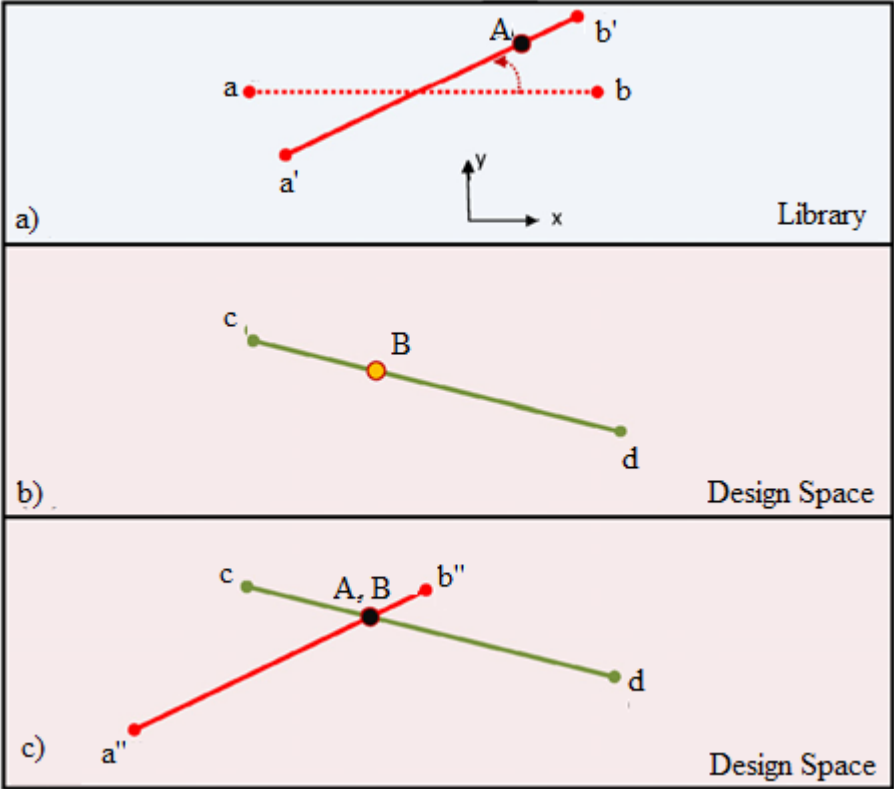


Figure 6.5 : Rotation and Translation [31].

Candidate CNTs are rotated in the library with a random angle and their current tip coordinates changes eventually. As it can be clearly seen from Figure 6.6, the positions a and b go to the new positions a' and b' with rotation. After, intersection point of candidate CNT that is represented here with A is specified. The Intersection points of selected carbon nanotubes are introduced randomly depending line segment parameter given in Eq. (6.1). Then, the candidate nanotube is translated to the design space and matched here with another CNT, which is also similarly rotated in the same plane inside the library earlier. The intersection points of both nanotubes are aligned closely. Because the given system is two dimensional, an additional direction has to be defined here to prevent the overlapping of selected carbon nanotubes. In this way, individual nanotubes will have adequate distance from the other ones.

6.1.2.3 Implementation of design constraints

To obtain proper and realistic network structures, some design limitations are defined in terms of angles and intervals between cross-linked CNTs and locations of intersection points. Therefore, each candidate CNT is checked with certain design rules until an appropriate item is accepted. When it is found, the candidate is considered as cross-linked nanotube anymore and saved to a different file with its own identification number.

In order to have regular and stable junction regions, a certain distance is described between the candidate CNT and target item, and other CNTs already existed. The candidate cannot be closed under this definite value. Moreover, the angle between candidate and target is randomly determined in accordance with predefined values in the algorithm. The angle between the candidate and target items should not be out of a specified range since the angle determines junction types and junction types highly affect the properties of CNT networks [112-119]. If we do not constrain the angles or relative orientations between target and candidate CNTs, they tend to be parallel which produces an ugly network with undesirable properties. Furthermore, a reasonable distance must be defined between intersection points, which are determined by line segment parameter as it is shown in Figure 6.4. Parameter t controls the proper and homogenous distribution of cross-linked CNTs on target items. In this way, carbon nanotubes can be placed to the design space easier and more flexible way. If it is supposed to fail of this constrain, it can be said that a complexity in locating nanotubes on the target element begins since the other constraints limits placement and consequently the network fails. What is more, the number of cross-linked carbon nanotubes also has to be defined as a constraint in algorithm. If it is too many, complicated and unsystematic network structure is obtained at the end. Thus, possible crossed-linked CNTs cannot be located in the design space anymore because of the constraint crowd of existed CNTs hinder settlement. On the other hand, a weak network with undesirable properties are generated if the number of cross-linked candidate is not sufficiently large. Consequently, a reasonable number for cross-link CNTs must be selected. Because, the networks begin to be too crowded when the number of cross-link is too many.

All these constraints enable to construct more stable, more homogenous, more regular carbon nanotube network with desirable mechanical, electrical or thermal

properties. It is not intended to break these rules during the network generation process. If the constraints were not active in the present algorithm, similar violations of constraints in two dimensional design space would be noticed as represented in Figure 6.6.

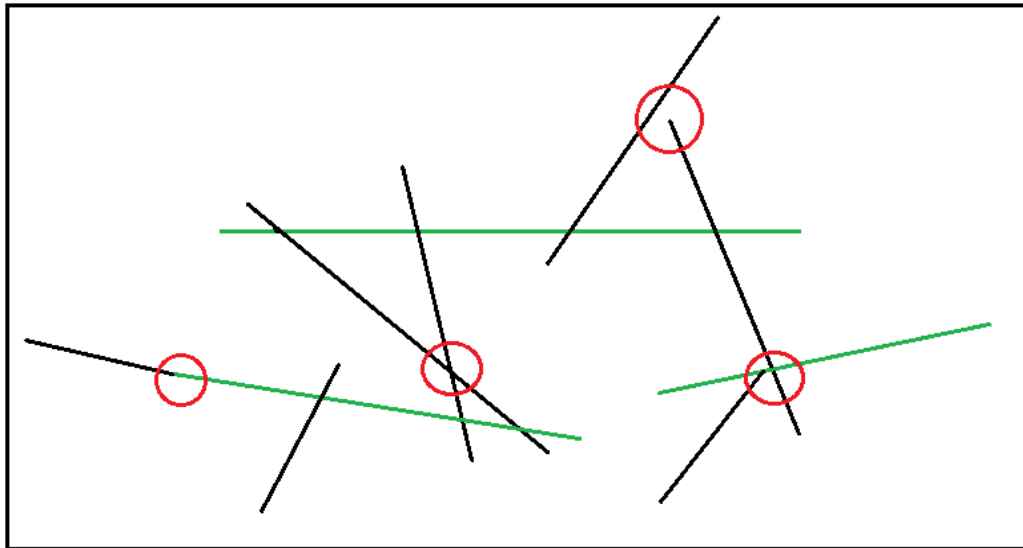


Figure 6.6 : Mislocated Carbon Nanotubes.

All the constraints that will affect the topology of the network can be arranged in the future according to the detailed characterization results of CNT network materials. Therefore, the proposed method allows experimental characterization data to be employed in computer simulations of the materials' behavior. Alternatively, the constraints can be set independently to investigate the effects of several topological parameters such as CNT lengths between two intersection points, the frequency of intersections through the network or the angularity of the intersecting CNTs.

6.1.2.4 Decision of sub-loop

As it is explained in previous sections, the sub-loop controls the candidate CNTs' compatibility with design constraints. However, cross-linked CNTs cannot always be placed on a target CNT because of that the geometrical restrictions or existing constraints impede the settlement of cross-linked element. After certain number of trials by different cross-linked nanotubes, vacancy on the target nanotube remains empty and a new target carbon nanotube from the library is assigned to the design space. In other words, if a candidate fails from current constraints, another nanotube is summoned to design space from the library until a proper item accomplishes the definite limitations.

6.1.2.5 Generation of LAMMPS input data file:

Generating a network is not the end of study; it is just the initial step on the contrary. Because, a heat welding procedure should be applied to the interconnected carbon nanotubes via molecular dynamics simulations after the network generation is done. Then, mechanical loads have to be implemented using MD simulations again. Before all, the network coordinates data is written to a separate file in order to be used subsequently.

6.1.2.6 Networks

In the present study, only carbon nanotubes with a (5,0) chirality and a constant length are used during the network generation process. It is planned to include various types of carbon nanotubes with different length and chirality for further investigations. It is highly important because network properties depend on design parameters such as the number of junctions, length and diameter of CNTs, interval of intersection points, junction type, and range of extra distance beyond the cut-off or distance between cross-linked CNTs.

Figure 6.7 shows increasing number of carbon nanotubes in two dimensional design space.

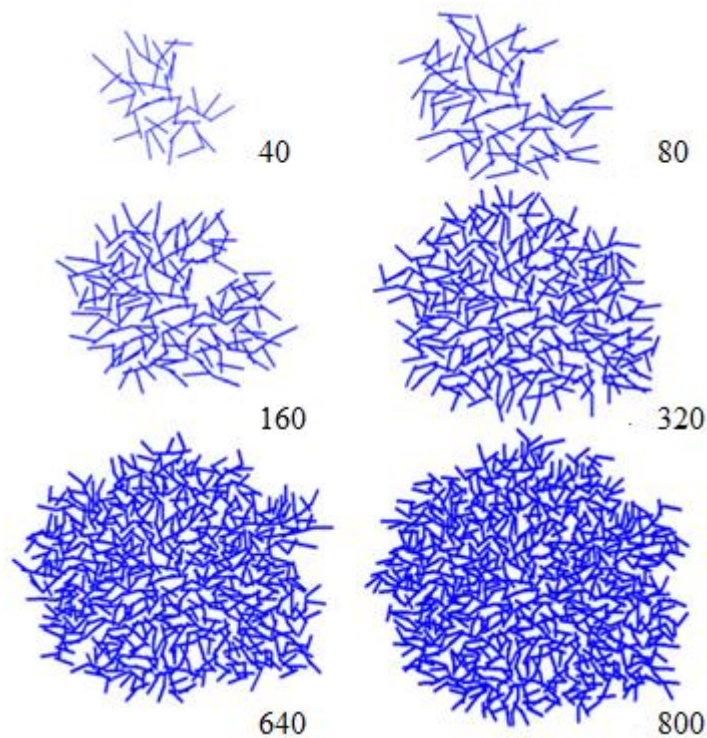


Figure 6.7 : Increasing Number of CNTs in Design Space [31].

Both two-dimensional and three-dimensional numerical models are created in our study. However, junctions and numerical tests are implemented for three-dimensional model since it can be considered as more realistic for a bulk structure. Figure 6.8 shows created two-dimensional and three-dimensional carbon nanotube networks.

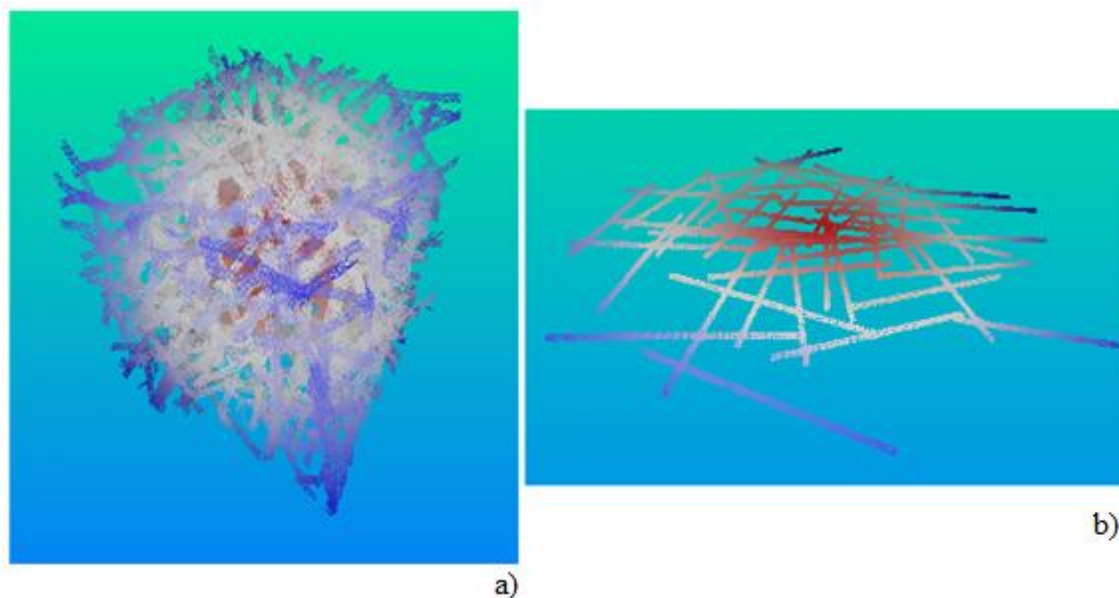


Figure 6.8 : a) 3D CNT Network, b) 2D CNT Network.

6.2 Heat Welding of Junctions

In this stage of the present study, an open source classical molecular dynamics code LAMMPS (Large-scale Atomic/Molecular Massively Parallel Simulator) is extensively used for implementation of junctions. An Adaptive Intermolecular Reactive Empirical Bond Order (AIREBO) potential is selected which provides a finer approach on mechanical deformation behavior of hydrocarbon molecules as allowing bond breaking and forming mechanics for covalent bonds. The AIREBO is a multi-body potential contains long-range atomic interactions and torsional terms in addition to REBO potential terms; thus it gives a better accuracy. The AIREBO potential with a 2 \AA cutoff distance is applied and energy minimization is obtained by using conjugate-gradient method. Sufficient coordinates data which is created in MATLAB stage are summoned from a separate file in order to be processed in LAMMPS. When the CNT network is summoned, it is placed in an appropriate simulation box. All molecular dynamics simulations are performed under periodic boundary conditions in the simulation box.

In the beginning, the system has 300° K initial temperature and a Nose-Hoover thermostat provides the thermal equilibrium to the system. Thermodynamic characteristic of the system is determined by NVT canonical ensemble, which keeps total number of particles, temperature and total volume constant during the equilibration. In order to weld the intersected carbon nanotubes to form proper junctions, temperature of the system has to be increased gradually. The range of referenced temperature for heat welding procedure is a disputable subject. In the previous studies, referenced temperature values are chosen between 2000 - 3000° K degrees [41-47]. Although welding at high temperatures enhances bonding characteristics of interaction regions, the number of topological defects including dangling bonds or idle atoms around the current region immensely proliferated and more importantly, a huge increase on the computational time is observed. Due to these drawbacks, it is aimed to create a novel welding procedure at the lower reference temperatures such as 600 - 800° K in the present study. Eventually, significant save on the computational time and stable junction regions without topological defects are attained. In the MD script, a spherical region is introduced in order to remove dangling bonds and free atoms around the junction region so this provides a better welding spot. For the sake of stability in junction regions, the temperature maintains at 600 K° initially. Then, the structure is relaxed between 600-300° K within a sufficient time. Finally, thermostating is applied at room temperature. After this extensive process, junctions are formed successfully.

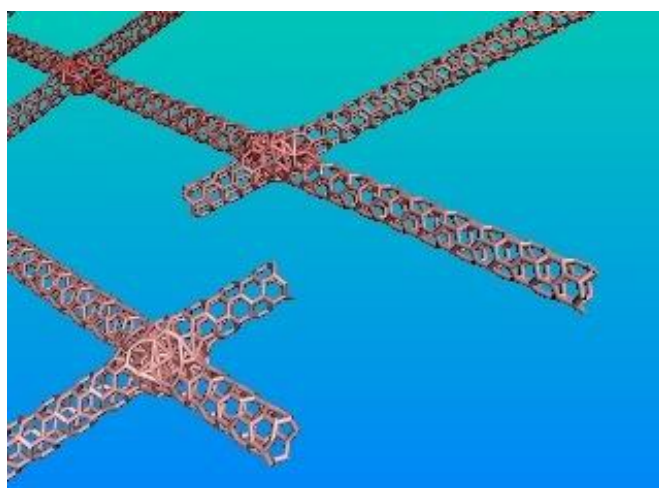


Figure 6.9 : Images of Junction Regions.

As it is mentioned before, heat welding process is applied around 600° K, that range is not as much as 2000-3000° K.

After welding process, we obtained two different types of networks as given in the figures below. The algorithm manipulates the number of carbon nanotubes, size and shape of the network structure.

Figure 6.10 shows the created network in two-dimension:

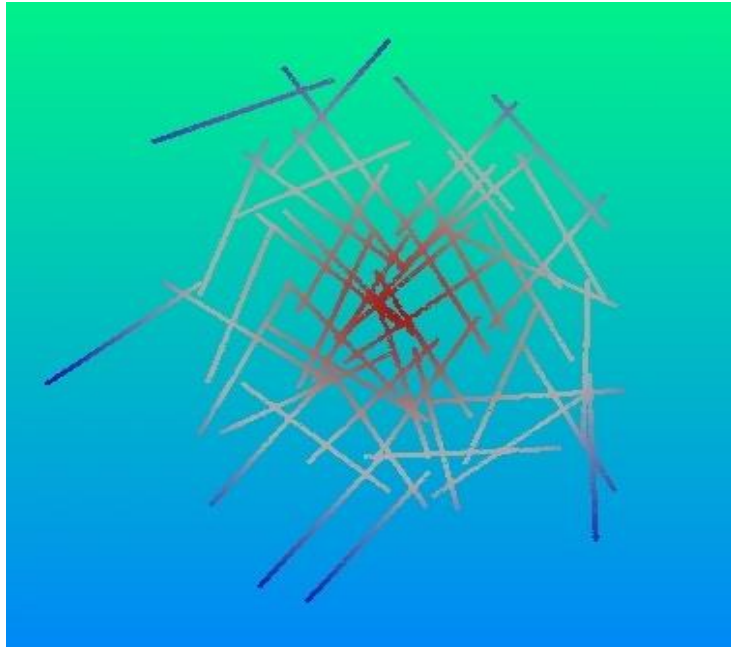


Figure 6.10 : A Welded 2D Carbon Nanotube Network.

Figure 6.11 shows the created network in three-dimension:

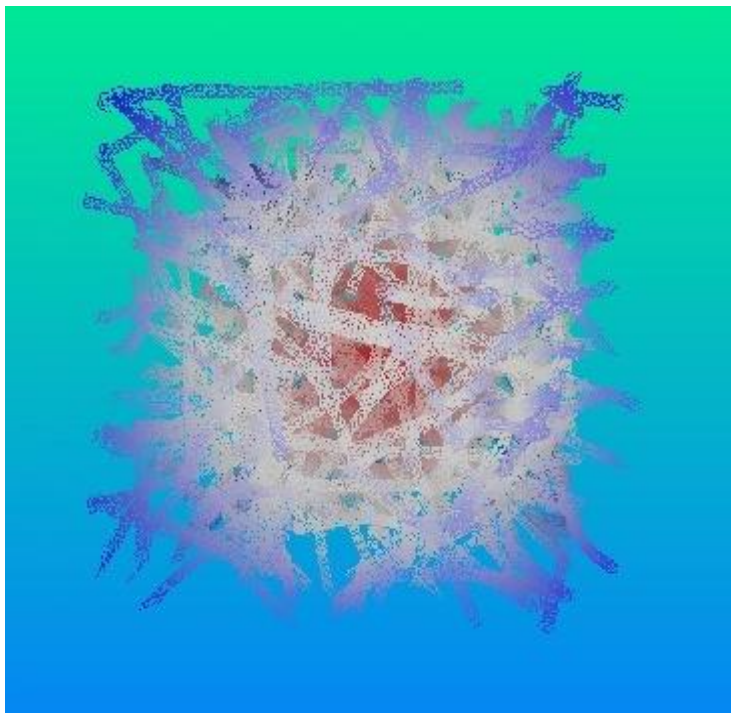


Figure 6.11 : A Welded 3D Carbon Nanotube Network.

6.3 Mechanical Loading Simulations

In this stage of the present study, an open source classical molecular dynamics code LAMMPS (Large-scale Atomic/Molecular Massively Parallel Simulator) is extensively used in implementation of mechanical loads. A tensile force is applied at the bottom end of the carbon nanotube network structure to investigate deformation behavior and find out the Young's modulus.

As settings, the atoms at the bottom end are fixed in both translational and rotational degree of freedoms as boundary conditions and atoms at the upper end are subjected to tensile force. In the present simulations, ultrathin zigzag nanotubes with (n,m)=(5,0) nomenclature are performed in the MD simulations. The wall-thickness is taken as 3.4 Å .

All simulations are carried out at 300° K temperature with a Langevin thermostat, which provides that the structure stays unaffected at temperature 300 K° during simulations. Besides, NVT ensemble keeps total number of particles, total temperature and total volume constant under periodic boundary conditions. Initially, a region containing a set of atoms from the upper end is introduced so as to apply a displacement increment 0.25 Å. Time step is kept fixed at 0.001 ps to minimize dynamical effect of force response. One increment occurs in 1000 runs for present time step, total time is evaluated as 1 ps. Total simulation time, strain rate and strain are evaluated from the same formula as given in Eqs. (5.3), (5.4), (5.5).

$$t = \Delta t \times N = 0.001 \times 1000 = 1 \text{ ps}$$

$$\varepsilon = \frac{\Delta L}{L_0} = \frac{0.25}{23.4} \approx 0.01$$

$$\dot{\varepsilon} = \frac{\varepsilon}{t} = \frac{0.01}{10^{-12}} \approx 10^{10} \text{ s}^{-1}$$

To be under critical strain rate value, lower displacement increment is chosen for further analysis. If the displacement increment is kept as 0.025 Å then total run increases to 10000 instead of 1000. A more reasonable strain rate is obtained similar to literature [47]. However, computational time extends, so the simulation process become more expensive.

In Figure 6.12, the initial form of carbon nanotube network structure is given before tensile load is applied to. It can be clearly seen that the present network is a porous three-dimensional structure that consists of numerous carbon nanotubes located randomly in the design space. In this stage, any mechanical test such as tensile or compression has not applied yet. Before all, an energy minimization and thermal equilibrium should be implemented.

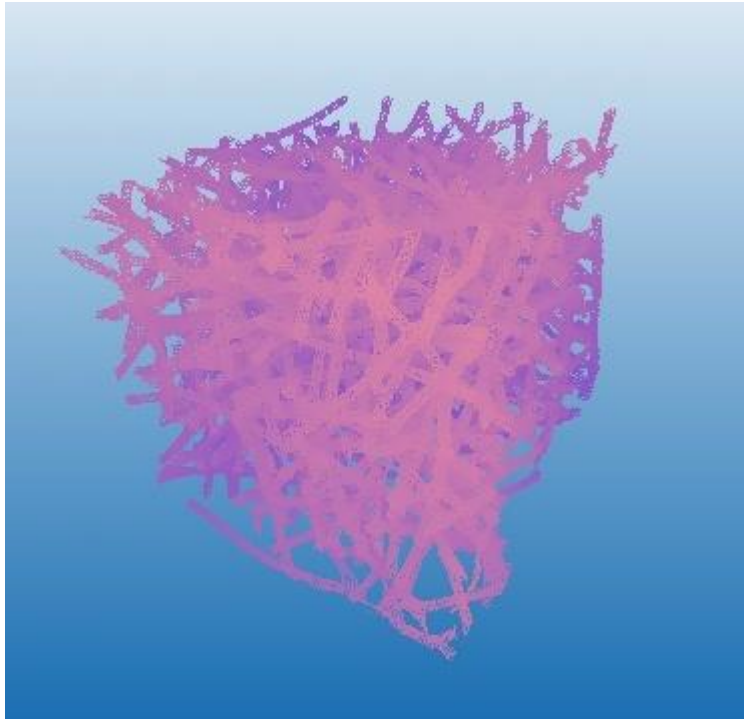


Figure 6.12 : Initial CNT Network without any Deformation.

In Figure 6.13, gradual deformation range with time is demonstrated, and side view of same deformation procedure is given in Figure 6.14. The deformation of cubic structures can be clearly seen in the figures.

As it can be seen from Figures 6.13 and 6.14, structure deforms more as time increases and after a certain inflection point, which is mentioned in previous sections, bond breaking starts to occur. Due to the used potential of AIREBO, bond formation is also happening besides bond breakage. However, the network cannot resist the tensile load after a certain value, and the failure begins in the carbon nanotube network. This behavior can be distinguished easily in the deformation under an exaggerated tensile force as given in Figure 6.15.

The aim of showing this exaggerated circumstance is demonstrating how the present network structure will react under a sudden and massive loading condition.

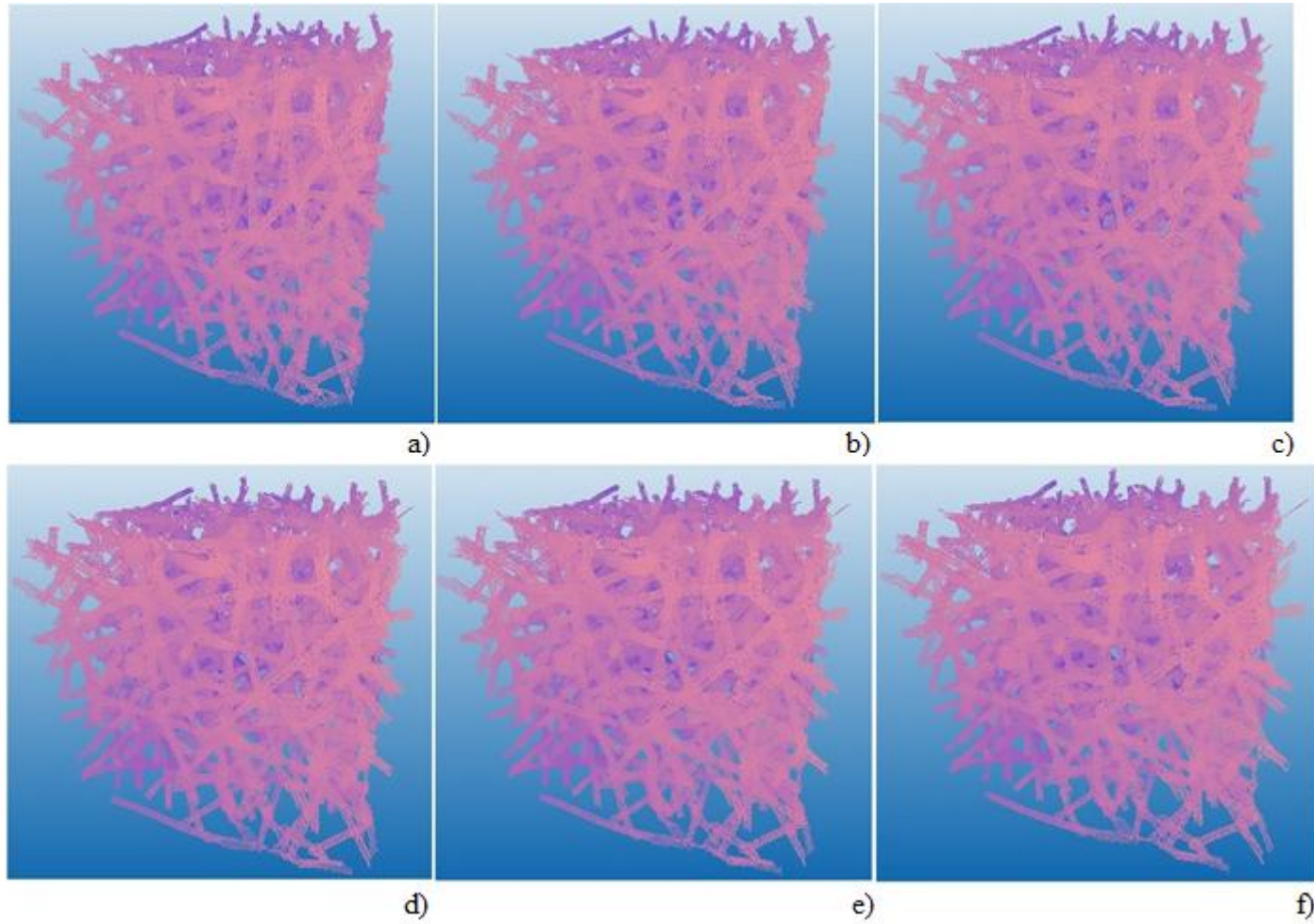


Figure 6.13 : Gradual Time Increase on Deformation Process (Isometric View).

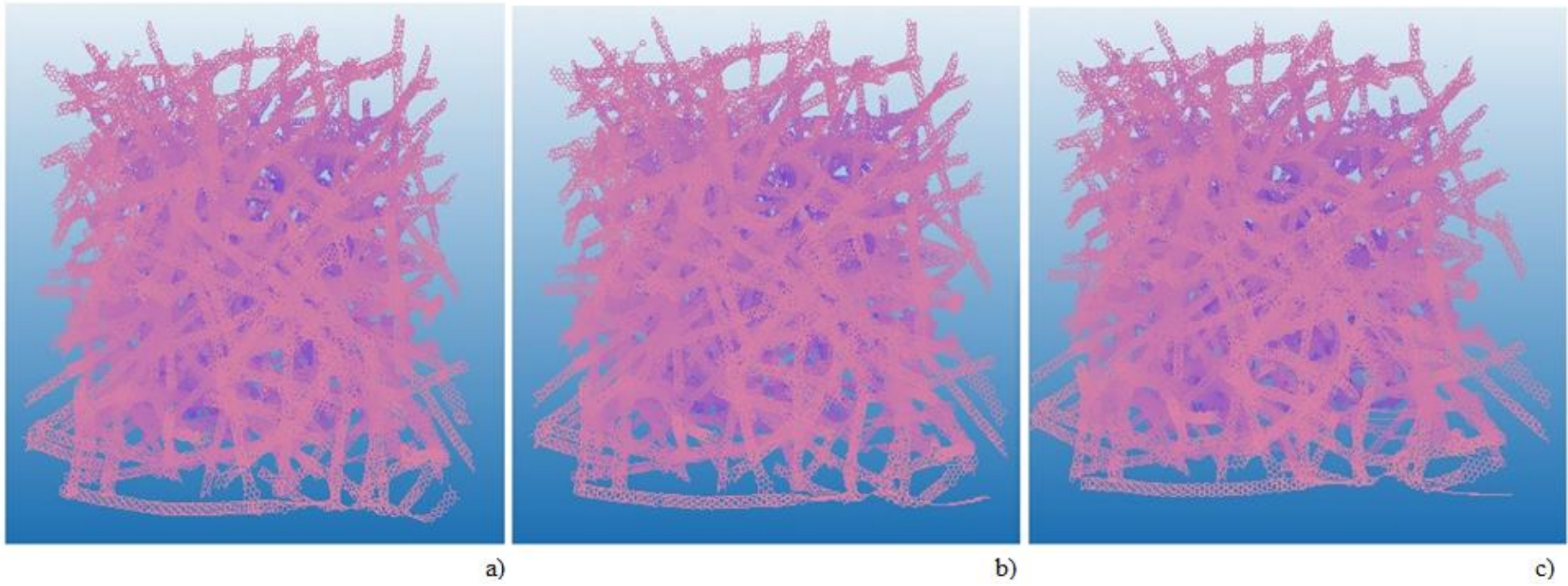


Figure 6.14 : Gradual Time Increase on Deformation Process (Side View).

Instead of logical strain rate, if we apply a tremendous deformation increment above the normal rate, we obtain the deformation shown in Figure 6.15. A quick breakage between covalent bonds is observed.

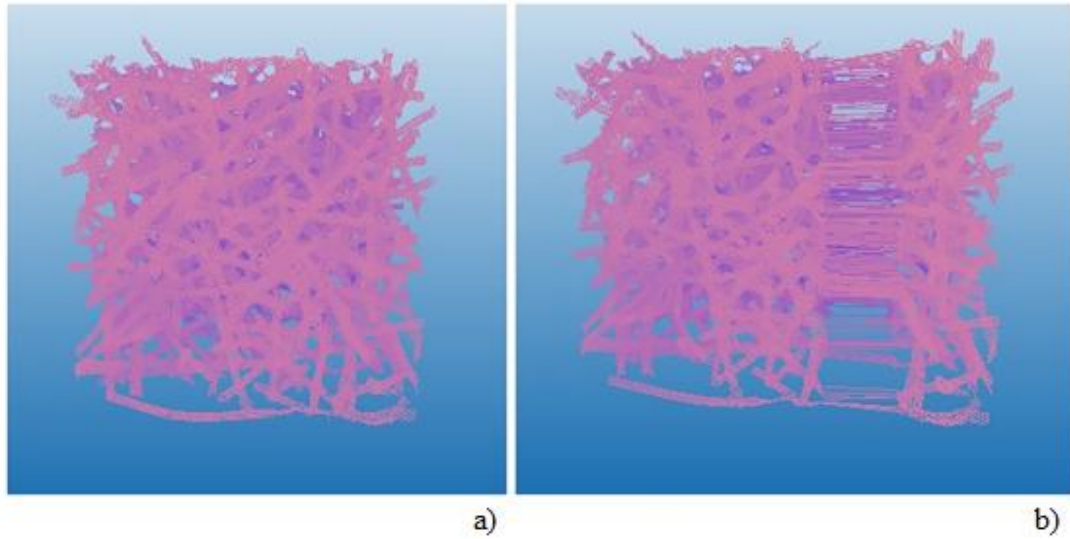


Figure 6.15 : Deformation under Exaggerated Tensile Force.

7. SIMULATION RESULTS

7.1 Mechanical Properties of 3D Random Carbon Nanotube Network

CNT networks are very promising novel materials and determination of their mechanical properties are extremely important matter for a better understanding on CNT networks. However, there is no study available for mechanical properties of “**Random Carbon Nanotube Networks**” and a very limited number of studies exist on mechanical properties of “**Ordered Carbon Nanotube Networks**” in literature. Eventually, our study can be accepted as pioneering work due to the absence of relevant studies.

It can be indicated that investigation of mechanical properties such as the elastic properties of our 3D random carbon nanotube network became an essential and necessary issue because no study is available in literature that investigates the mechanical properties of “random CNT networks”. In addition, a very limited number of studies exist on mechanical properties of “ordered CNT networks”. Coluci et al. [67] investigated mechanical properties of ordered crossbar CNT network and ordered hexagonal CNT network in different chiralities and various size. Axial Young’s Modulus are found between 130-280 GPa, 10-50 GPa and 10-30 GPa for Cb@(6,0), Hex@(8,0) and Hex@(6,0) carbon nanotube networks, respectively. Wang et al. [118] examined mechanical properties of carbon nanotube super honeycomb network structure and indicated the Young’s Modulus between 70-120 GPa. In another study, Coluci et al. [68] investigated rupture behavior of ordered single walled carbon nanotube network in tubular forms (super carbon nanotubes – STs). Under stretching deformation, ultimate tensile strength is obtained between the range of 36.5-92.6 GPa for different CNTs radii. These studies are the only relevant studies of the present work and these values are only parameters for a healthy comparison of our results.

As mechanical properties of our random carbon nanotube network, we estimated the Young’s Modulus, ultimate tensile strength, yield strength, Poisson’s ratio and

density. All these parameters and the obtained results are briefly explained in the following paragraphs.

7.1.1 Young’s modulus

The Young's modulus also known as Modulus of Elasticity is a quantity to describe elastic characteristics of a material. The Young's modulus measures the resistance of a material to elastic (recoverable) deformation under loads.

To determine the elastic properties of materials including Young’s modulus, elastic limit, elongation, proportional limit, reduction in area, tensile strength, yield point, yield strength, tensile loads are implemented. The main outcome of a tensile loading is a load versus elongation curve, which is then converted into a stress versus strain curve as it is shown in Figure 7.1. The stress-strain curve relates the applied stress to the resulting strain and each material has its own unique stress-strain curve.

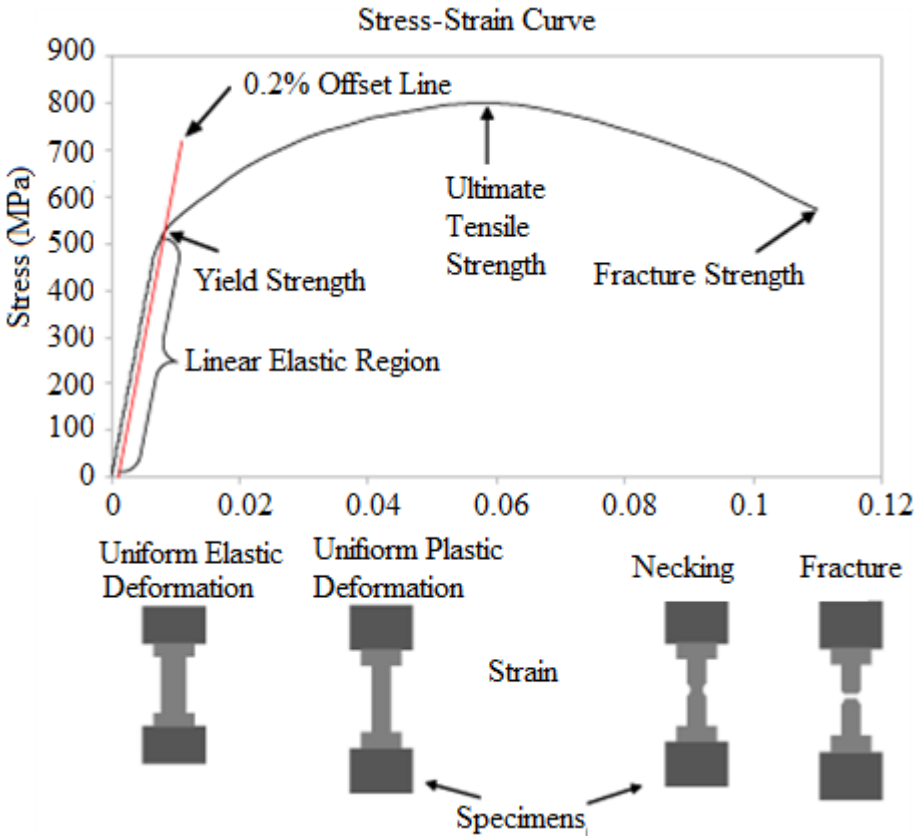


Figure 7.1 : A Typical Engineering Stress-Strain Curve [124].

As it is previously mentioned, Young’s modulus determines the elastic behavior of specimen. A stiff material has a high Young's modulus and changes its shape only slightly under elastic loads (e.g., diamond). A flexible material has a low Young's

modulus and changes its shape considerably (e.g., rubbers). A stiff material requires high loads to elastically deform it - not to be confused with a strong material, which requires high loads to permanently deform (or break) it.

The stiffness of a component means how much it deflects under a given load. This depends on the Young's modulus of the material, but also on how it is loaded (tension or bending) and the shape and size of the component. The stiffness is important in designing products, which can only be allowed to deflect by a certain amount (e.g., bridges, bicycles, furniture). Stiffness is important in springs, which store elastic energy (e.g. vaulting poles, bungee ropes). In transport applications (e.g. aircraft, racing bicycles), the stiffness is required at minimum weight. In these cases, materials with a large specific stiffness are the best.

As it can be realized from the previous paragraphs that there are not sufficient former studies even for mechanical properties of ordered CNT networks. Therefore, we worked to find out these desirable features. If we consider our random carbon nanotube network structure, we evaluate the Young's modulus by applying classical Hooke's equation.

As explained in previous section, the Young's modulus is obtained from the Hooke's Law. Hooke's Law in one-dimension is evaluated with the following equation:

$$E = \frac{\sigma}{\varepsilon} = \frac{FL_0}{A_0\Delta L} \quad (7.1)$$

where E is the Young's modulus, σ is one-dimensional normal stress, ε is one-dimensional strain, F is the total applied force under tension, A_0 is the cross-sectional area, L_0 is the initial length, ΔL is the change in the length.

For Eq. (7.1), we know the displacement increment for every step, initial length and cross-sectional area of the tube. The problem is determining the tensile force values on atoms which is evaluated and averaged via MD simulations (in LAMMPS). All mechanical properties of current carbon nanotube network structures and essential graphics are calculated with the help of an EXCEL script.

In MD simulations, our unit is specified as unit "Metal" which is represented in Figure 7.2. However, they are all converted to SI system in our Excel code to avoid confusion.

For style <i>metal</i> , these are the units:		For style <i>si</i> , these are the units:
mass = grams/mole		mass = kilograms
distance = Angstroms		distance = meters
time = picoseconds		time = seconds
energy = eV		energy = Joules
velocity = Angstroms/picosecond		velocity = meters/second
force = eV/Angstrom	→	force = Newtons
torque = eV		torque = Newton-meters
temperature = Kelvin		temperature = Kelvin
pressure = bars		pressure = Pascals
dynamic viscosity = Poise		dynamic viscosity = Pascal*second
charge = multiple of electron charge		charge = Coulombs
dipole = charge*Angstroms		dipole = Coulombs*meters
electric field = volts/Angstrom		electric field = volts/meter
density = gram/cm ^{dim}		density = kilograms/meter ^{dim}

Figure 7.2 : Units for “metal” and “SI” for MD Simulations [127].

In MD simulations, force component of each carbon atom in the z direction computed for every displacement increment. Then, obtained force values are averaged and reduced to a single value for every many timesteps.

$$1 \frac{\text{eV}}{\text{A}^\circ} = 1.60217 \times 10^{-19} \frac{\text{N.m}}{\text{A}^\circ} = 1.60217 \times 10^{-9} \text{ N} \quad (7.2)$$

After unit conversions, forces in each displacement increment are divided with cross-sectional area of the cube in order to obtain stress values. It is important to remark that electron volt / Angstrom force unit has to be arranged in Newton type force value.

Since the present structure is in a cubic form, initial length and cross-sectional area can be written in the following equations. As it can be seen, metal units are transformed to SI units.

$$l_0 = a = 200 \text{ A}^\circ = 200 \times 10^{-10} \text{ m} \quad (7.3)$$

$$A_0 = a^2 = 40000 \text{ A}^\circ = 40000 \times 10^{-20} \text{ m} \quad (7.4)$$

Finally, the Young’s modulus is calculated by taking the proportion of stress and strain values for each increment from Eq. (7.1).

In Figure 7.3, stress-strain curve of 3D random carbon nanotube network is given. It can be clearly noticed that present figure resembles a typical engineering stress-strain curve which is similar to Figure 7.1. An observable linear region, yield strength, ultimate tensile strength, fracture point can be easily distinguished from the figure.

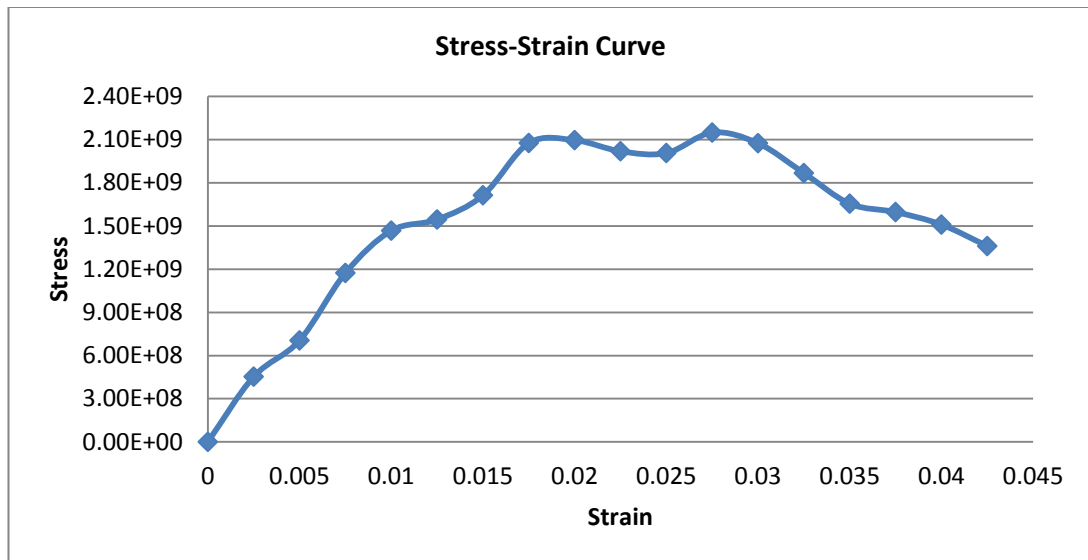


Figure 7.3 : Stress-Strain Curve For 3D Random CNT Network.

From the slope of the present strain-stress curve, the Young's modulus is obtained between 110 – 230 GPa. Besides, the average value of Young's modulus in elastic region can be calculated as 145 GPa. This value is bigger than the most of the metals including Steel, Titanium, Copper etc.

7.1.2 Ultimate tensile strength

The ultimate tensile strength (UTS) or tensile strength can be defined as the maximum engineering stress level reached in a tension loading or maximum stress level that material withstands external forces without breaking, necking or failing. In brittle materials, the UTS will occur at the end of the linear-elastic portion of the stress-strain curve or close to the elastic limit. In ductile materials, the UTS will be well outside of the elastic portion into the plastic portion of the stress-strain curve.

As shown in Figure 7.1, the material begins to fail after ultimate tensile point until the fracture point. Some materials will break sharply, without deforming, what is called a brittle failure. Others, which are more ductile, including most metals, will stretch some - and for rods or bars, shrink or neck at the point of maximum stress, that area is stretched out. Since the UTS is based on the engineering stress, it is often

not the same as the breaking strength. In ductile materials, strain hardening occurs and the stress will continue to increase until fracture occurs, but the engineering stress-strain curve may show a decline in the stress level before fracture occurs. This is the result of engineering stress being based on the original cross-sectional area and not accounting for the necking that commonly occurs in the test specimen [124].

If we investigate Figure 7.3, it can be stated that ultimate tensile strength is obtained approximately 2.15 GPa which is also 2150 MPa. Comparatively, this value is 7 times bigger than ASTM A36 steel, 3 times bigger than Titanium 11 alloy, 20 times bigger than Cast Iron, 5 times bigger than high strength low alloy Steel, 2 times bigger than carbon nanotube composites. Besides, the network begins to failure at 3% strain. The fracture occurs at 4.25% strain.

7.1.3 Yield strength

The yield strength or yield point of a material is defined in engineering and materials science as the stress at which a material begins to deform plastically. Prior to the yield point, the material will deform elastically and will return to its original shape when the applied stress is removed. Once the yield point is passed, some fraction of the deformation will be permanent and non-reversible [125]. The yield strength is defined as the stress required to produce a small amount of plastic deformation. The offset yield strength is the stress corresponding to the intersection of the stress-strain curve and a line parallel to the elastic part of the curve offset by a specified strain (in the US, the offset is typically 0.2% for metals and 2% for plastics).

To determine the yield strength using this offset, the point is found on the strain axis (x-axis) of 0.002, and then a line parallel to the stress-strain line is drawn. This line will intersect the stress-strain line slightly after it begins to curve, and that intersection is defined as the yield strength with a 0.2% offset. A good way of looking at offset yield strength is that after a specimen has been loaded to its 0.2 percent offset the yield strength; when unloaded, it will be 0.2 percent longer than before the test. Even though the yield strength is meant to represent exact point at which the material becomes permanently deformed, 0.2% elongation is considered to be a tolerable amount of sacrifice for the definition of the yield strength [124].

As described in previous paragraph, we obtained yield strength of our random CNT network structure when we draw a parallel line to stress-strain line from 0.2% offset

in the x direction. The yield strength value is estimated around 1.5 GPa which is 1500 MPa. Comparatively, this value is 7 times bigger than ASTM A36 steel, 2 times bigger than Titanium 11 alloy, 13 times bigger than Cast Iron, 3 times bigger than high strength low alloy Steel, 2 times bigger than carbon nanotube composites. Moreover, we can say that plastic deformation starts after 1.5-2% strain value.

7.1.4 Poisson's ratio

Axial strain is always accompanied by lateral strains of opposite sign in the two directions mutually perpendicular to the axial strain. Strains that result from an increase in length are designated as positive and those that result in a decrease in cross section are designated as negative. The Poisson's ratio can be defined as the shrinkage of the cross section under an axial stress. For three-dimensional deformation, this shrinkage occur in two different direction except. The Poisson's ratio of a stable, isotropic, linear elastic material cannot be less than -1.0 nor greater than 0.5 due to the requirement that the Young's modulus, the shear modulus and bulk modulus have positive values (Lame equation).

$$\lambda = -\frac{E \cdot \nu}{(1 + \nu) \cdot (1 - 2\nu)} \quad (7.5)$$

For a 1D tensile test, Poisson's ratio can be found from following equation.

$$\nu = -\frac{\varepsilon_y}{\varepsilon_x} = \frac{\frac{\Delta D}{D_0}}{\frac{\Delta L}{L_0}} \quad (7.6)$$

where ν is the resulting Poisson's ratio, ε_x is transverse strain (negative for axial tension (stretching), positive for axial compression), ε_y is axial strain (positive for axial tension, negative for axial compression), D is the diameter, L is the length.

If the logic is true for the SWCNT in Section 5, so it must be also true for our random CNT network. Thus, it is reasonable to determine the Poisson's ratio for a single-walled carbon nanotube. In consequence, the Poisson's ratio is obtained 0.16. We also proved that this value is in a good agreement with literature data. However, we are not dealing with a SWCNT.

In the present case, our 3D random CNT network will be similarly deformed as the case pictured in Figure 7.4. The uniaxial deformation of cubic structure under uniaxial tensile is demonstrated exaggeratedly in the figure. The shrinkage occurs in two different directions.

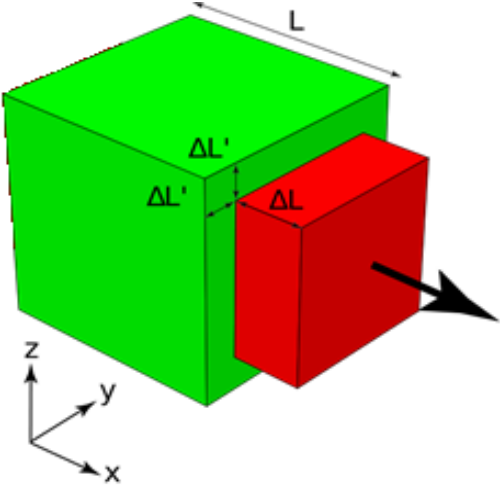


Figure 7.4 : Deformation of a Cube Under Uniaxial Tensile Load [126].

As a result, a very small Poisson’s ratio is obtained around 0.00138. Slight deformations in radial directions are observed in the simulations and this causes a very small Poisson’s ratio.

7.1.5 Density

Recently, lightweight materials have become a very essential and important issue in terms of lowering cost, increasing ability to be recycled, having advanced mechanical and electrical properties, enabling the integration into products and maximizing fuel economy benefits. Therefore, it is desirable to have both light and strong materials.

Density is a well-known parameter that provides better understanding on weight, composition and morphology of materials. Basically, it is defined as material weight per volume.

$$\rho = \frac{m}{V} \tag{7.7}$$

where \$\rho\$ is the density, \$m\$ is the mass, and \$V\$ is the volume.

In our case, we have a cubic form structure, which means that volume is known. The cubic structure has numerous intersected individual carbon nanotubes and each nanotube consists of only carbon atoms. Besides, we know the mass of Carbon atoms and the total number of atoms in the whole system. Eventually, the density of the system can be calculated easily. Table 7.1 expresses the essential parameters for calculation of density.

Table 7.1 : Parameters for Calculation of Density

Parameter	Value
1 Carbon Atom Mass	12. 011 akb
1 gram	6.022x10 ²³ akb
Total Number of Atoms	232089
Volume	8× 10 ⁻¹⁸ cm ³

We can evaluate the density of our random carbon nanotube network from Eq. (7.7) and (7.8).

$$\rho = \frac{m}{V} = \frac{12 * 232089}{6.0221 \times 10^{23} * 8 \times 10^{-8}} = 0.578 \frac{\text{g}}{\text{cm}^3} \quad (7.8)$$

As shown in Eq. (7.8), the density of our system is calculated around 0.578 g/cm³. Comparatively, this value is 14 times lower than ASTM A36 steel, 8 times lower than Titanium 11 alloy, 13 times lower than Cast Iron, 2 times lower than graphene, 3 times lower than carbon fiber and we can say that it is in the range of density of an individual carbon nanotube.

7.2 A Smaller Carbon Nanotube Network

It can be obviously said that the size of current structure and the number of carbon nanotubes directly affect the mechanical properties of our carbon nanotube network. In this sense, we can say that density of the structure decreases with increasing number of atoms. However, this also causes decrease in strength.

As we stated earlier, we generated a three-dimensional structure having nearly 240.000 Carbon atoms. In this study, we also analyzed a smaller cubic form three-dimensional CNT network having approximately 85.000 atoms in order to compare the differences of mechanical properties and understand the effects of size for each

CNT network form. Figure 7.5 shows our current smaller CNT network form. A less crowded and more regular structure can be clearly seen.

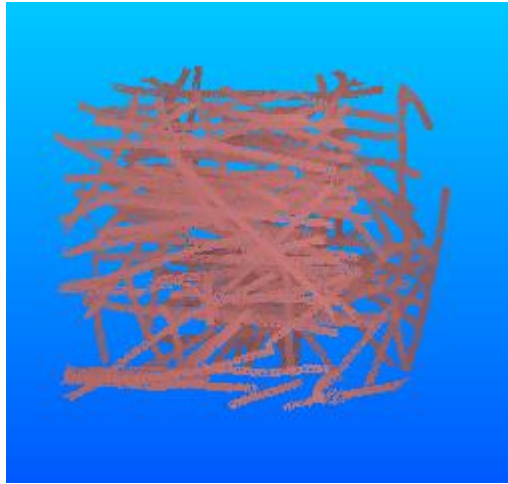


Figure 7.5 : A Smaller Carbon Nanotube Network Structure.

We obtained a lighter material and its density is determined around 0.196 g/cm^3 . The Young's modulus is calculated as between 30-70 GPa. The Yield strength and ultimate tensile strength are found as 250 MPa and 600 MPa, respectively.

8. CONCLUSION

In this thesis, mechanical properties of three-dimensional random carbon nanotube networks are investigated using molecular dynamics simulations. The thesis includes an extensive theoretical atomistic approach on mechanical properties of related carbon based nanostructure including the Young's modulus, ultimate tensile strength, yield strength, Poisson's ratio and density.

Before beginning the study, a comprehensive literature investigation has been presented on both carbon nanotubes and carbon nanotube networks in order to learn the essentials of the topic, understand and compare the previous studies and give the right direction to our study. As a result, we realized that there is no previous study on mechanical properties of random carbon nanotube networks. Besides, a very limited number of studies exist for even ordered carbon nanotube networks. In this matter, we aimed at doing an innovative study to literature. Thus, this study can be accepted as pioneering on mechanical properties of random CNT networks.

This thesis can be investigated in three main stages.

First, a self-controlled algorithm is described to generate three-dimensional networks consisting of numerous random intersected carbon nanotubes, which are distributed systematically in the design space. The algorithm manipulates the length and chirality of nanotubes, junction density and angular position of cross-linked carbon nanotubes to obtain the best network. The control mechanism plays an important role to avoid undesirable nanotube distribution but nanotubes randomly take positions considering the control mechanism. Afterwards, a molecular dynamics simulation is employed in order to create true junctions via heat welding method. Heating the system to a definite temperature enables formation of covalent bonds between intersected CNTs. Finally, a tensile loading is applied to investigate mechanical properties such as the Young's modulus, ultimate tensile strength, yield strength, Poisson's ratio or density of current network. The loading is implemented by using MD simulations. For mechanical loading simulations, one side of the network is

fixed and tensile force is applied to the other side. The analyses are implemented under certain parameters including temperature, thermostat, equilibration method, time etc. Results are calculated and discussed based on classical mechanics viewpoint.

Molecular dynamics simulations are applied by using LAMMPS (Large-scale Atomic/Molecular Massively Parallel Simulator). Before implementation of an MD script to our network structure, mechanical properties of a single-walled carbon nanotube is verified for the purpose of validation of the code. It is observed that obtained results are in a good agreement with previous works in the literature. After all, the script can be applied to the bulk structure.

For the final step, the Young's modulus, ultimate tensile strength, yield strength, Poisson's ratio and density are calculated in the last part of our study, respectively. The outputs of molecular dynamics simulations are arranged by an Excel code and the desirable properties of random CNT networks are evaluated with this code regarding suitable units and equations. The results are calculated with classical mechanics equations like the Hooke's Law. Plenty of simulations were conducted by varying parameters because optimum results are sought for the sake of more comprehensive results. Therefore, we altered several parameters in the molecular dynamics simulations including deformation increment, timestep, run size, equilibration time, temperature level, thermostat type, temperature interval. In each simulation, just one parameter is varied and the others remain constant in order to distinguish the effects of that one more clearly. If we summarize the results, the Young's Modulus is obtained in the range of 100-230 GPa regarding the elastic region of the stress-strain curve and the average value is evaluated as 145 GPa. These results can be considered as reasonable when we compare them with relevant studies and several other materials in literature. For the maximum engineering stress level, which means ultimate tensile strength, 2150 MPa value is determined. To obtain the Yield strength, a parallel line is drawn to current stress-strain curve from 0.2% strain value until the intersection point. Then, the intersection point indicates that the yield value is obtained approximately as 1500 MPa. Because very slight displacements occur in the Y and Z directions, Poisson's ratio is found a very low value around 0.002. Finally, the density are found with proportion of total mass of atoms with total volume of system. We know all essential parameters such as total number atoms,

total size of our system, eventually density is calculated as 0.576 g/cm^3 . This shows that our structure is a highly lightweight material.

When we compare our results with known materials, we found that our carbon nanotube network has quite reasonable properties. For instance, our CNT network is as stiff as ASTM A36 steel and has 6 times bigger ultimate tensile strength and yield strength, 14 times lower weight than ASTM A36. It has 2 times bigger stiffness, 5 times bigger ultimate tensile strength, 8 times bigger yield strength and 8 times lighter than pure titanium. For aluminum, It has 3 times bigger stiffness, 11 times bigger ultimate tensile strength, 12 times bigger yield strength and 12 times lighter than cast iron (4.5% C, ASTM A-48). It can be stated that our CNT network has 8 times stronger than steel, 16 times stronger than titanium, 36 times stronger than cast iron for the strength per unit volume. Indeed, the outputs are not equal as mechanical properties of a SWCNT. However, we can indicate from all results that our random carbon nanotube network structure has high stiffness, high tensile, fracture and yield strength and low density.

For the three-dimensional network, we designed a cubic form structure, which consists of approximately 230.000 Carbon atoms. The density and stiffness highly depends on the porosity of the structure, which is directly related number of our carbon atoms, e.g., the number of carbon nanotubes distributed in design space. If we would like to arrange these parameters, we must change the number of carbon nanotubes. If we design more crowded structure, we shall obtain more stiff and strong material. If we design more porous structure we shall obtain light weight material. In this study, we aimed at an optimized material including both lightweightness and high strength.

Carbon nanotube networks are very promising materials because of their advanced mechanical, thermal and electrical properties. There is a huge demand for extensive researches on the random carbon nanotube networks. For further investigations, we can study on the other mechanical properties of random CNT networks such as shear modulus and bulk modulus. The behavior of CNT network structure can be also examined under different loading conditions such as shear or compression loading. Moreover, there is no previous study on the electrical and thermal properties of random CNT networks. In addition, a perfect numerical model for generation of structure provides better and desirable mechanical properties. Therefore, the

construction algorithm should be improved for further investigations and perhaps more desirable results shall be obtained. Besides, we are planning to investigate the effects of porosity (number of CNTs in the network) on the mechanical properties of network structures and effects of nanotubes' chirality. For the sake of validation, the results can be best verified with experimental investigations; therefore experimental studies on this topic are extremely needed. We also would like to validate our results by applying other methods such as molecular structural mechanics approach. As we mentioned before, CNTs networks are porous the structures. The porosity can be coated with different materials and eventually a novel composite may be generated. This may be even a major, individual subject of random CNT networks. Similarly, numerous unstudied topics on random CNT networks may be proposed.

9. REFERENCES

- [1] **Iijima, S.** (1991). Helical microtubules of graphitic carbon, *Nature*, **354**, 56-58.
- [2] **Fan, C.W., Liu, Y.Y., Hwu, C.** (2009). Finite element simulation for estimating the mechanical properties of multi-walled carbon nanotubes, *Appl Phys A*, **95**, 819–831
- [3] **Cheng, H.C., Liu, Y.L., Hsu, Y.C. and Chen, W.H.** (2009). Atomistic-continuum modeling for mechanical properties of single-walled carbon nanotubes, *Inter Journal Solids and Structures*, **46**, 1695-1704.
- [4] **Lu, X., Hu, Z.** (2012). Mechanical property evaluation of single-walled carbon nanotubes by finite element modeling, *Composites:Part B*, **43**, 1902-13
- [5] **Tserpes, K.I. and Papanikos, P.** (2005). Finite element modeling of single-walled carbon nanotubes, *Composites Part B*, **36**, 468–477.
- [6] **Treacy, M.M.J., Ebbesen, T.W., Gibson, J.M.** (1996). Exceptionally high Young's modulus observed for individual carbon nanotubes, *Nature*, **38**, 678–680.
- [7] **Krishnan, A., Dujardin, E., Ebbesen, T.W., Yianilos, P.N., Treacy, M.M.J.** (1998). Young's modulus of single-walled nanotubes, *Phys. Rev. B*, **58**, 14013–14019.
- [8] **Wong E.W., Sheehan, P.E., Lieber, C.M.** (1997). Nanobeam mechanics: elasticity, strength, and toughness of nanorods and nanotubes. *Science*, **277**, 1971–1975.
- [9] **Salvetat, J.P., Kulik, A.J., Bonard, J.M., Briggs, G.A.D., Stockli, T., Metenier, K.** (1999). Elastic modulus of ordered and disordered multiwalled carbon nanotubes, *Adv Mater*, **11**, 161–165.
- [10] **Salvetat, J.P., Briggs, G.A.D., Bonard, J.M., Bacsá, R.R., Kulik, A.J., Stockli T,** (1999). Elastic and shear moduli of single-walled carbon nanotube ropes, *Phys Rev Lett*, **82**, 944–947.
- [11] **Yu, M.F., Files, B.S., Arepalli, S., Ruoff, R.S.** (2000). Tensile loading of ropes of single wall carbon nanotubes and their mechanical properties, *Phys Rev Lett*, **84**, 5552–5554.
- [12] **Yu, M.F., Lourie, O., Dyer, M.J., Kelly, T.F., Ruoff, R.S.** (2000). Strength and breaking mechanism of multiwalled carbon nanotubes under tensile load. *Science*, **287**, 637–640.
- [13] **Wei, X.L., Liu, Y., Chen, Q., Wang, M.S., Peng, L.M.** (2008). The very low shear modulus of multi-walled carbon nanotubes determined simultaneously with the axial Young's modulus via in situ experiments. *Adv Funct Mater*, **18**, 1555–1562.

- [14] **Guhados, G., Wan, W.K., Sun, X.L., Hutter, J.L.** (2007). Simultaneous measurement of Young's and shear moduli of multiwalled carbon nanotubes using atomic force microscopy, *J Appl Phys*, **101**, 033514.
- [15] **Li, C., Chou, T.W.**, (2003). A structural mechanics approach for the analysis of carbon nanotubes. *Int J Solid Struct*; **40**, 2487–2499.
- [16] **Li, C., Chou, T.W.**, (2003) Elastic moduli of multi-walled carbon nanotubes and the effect of van der Waals forces, *Composite Science and Technology*, **63**, 1517–1524.
- [17] **Yakobson, B.I., Brabec, C.J., Bernholc, J.** (1996). Nanomechanics of carbon tubes: instabilities beyond linear response, *Phys Rev Lett*, **76**, 2511-44.
- [18] **Ru, C.Q.** (2000). Effective bending stiffness of carbon nanotubes, *Phys Rev B*, **62**, 9973–9976.
- [19] **Ru C.Q.** (2000). Elastic buckling of singlewalled carbon nanotube ropes under high pressure. *Phys Rev*, **2(15)**:10405–8.
- [20] **Odegard, G.M., Gates, T.S., Nicholson, L.M., Wise, K.E.** (2002). Equivalent-continuum modeling of nano-structured materials, *Compos Sci Technol*, **60**, 1869–1880.
- [21] **Meo, M., Rossi, M.** (2007). A molecular-mechanics based finite element model for strength prediction of single wall carbon nanotubes, *Mater Sci Eng A*, 454–455, 170–7.
- [22] **Rossi, M., Meo, M.** (2009). On the estimation of mechanical properties of single-walled carbon nanotubes by using a molecular-mechanics based FE approach, *Compos Sci Technol*, **69**, 1394–1398.
- [23] **Hernandez, E., Goze, C., Bernier, P., Rubio, A.** (1998). Elastic properties of C and BxCyNz composite nanotubes, *Phys Rev Lett*, **80**, 4502–4505.
- [24] **Sanchez-Portal, D., Artacho, E., Soler, J.M., Rubio, A., Ordejon P.** (1999). Ab initio structural elastic and vibrational properties of carbon nanotubes, *Phys Rev B*, **59**, 12678–12688.
- [25] **Lu, J.P.** (1997). Elastic properties of carbon nanotubes and nanoropes, *Phys Rev Lett*, **79**, 1297–1300.
- [26] **Belytschko, T., Xiao, S.P., Schatz, G.C., and Ruoff, R.S.** (2002). Atomistic simulations of nanotube fracture, *Physical Review B*, **65**, 235430
- [27] **Gao, G., Cagin, T., Goddard, W.** (1998). Energetics, structure, mechanical and vibrational properties of single-walled carbon nanotubes, *Nanotechnology*, **9**, 184-191
- [28] **Jin, Y., Yuan, F.G.** (2003). Simulation of elastic properties of single-walled carbon nanotubes, *Compos Sci Technol*, **63**, 1507–1515
- [29] **Dresselhaus, M.S., Dresselhaus, G., Eklund, P.C.** (1996). Science of fullerenes and carbon nanotubes, Academic Press, New York.
- [30] **Kalamkarov, A.L., Georgiades, A.V., Rokkam, S.K., Veedu, V.P., Ghasemi Nejjhad M.N.** (2006). Analytical and numerical techniques to predict carbon nanotubes properties, *International Journal of Solids and Structures*, **43**, 6832–6854.

- [31] **Kirca, M., Yang, X., To, A.C.** (2013). A stochastic algorithm for modeling heat welded random carbon nanotube network, *Comput. Methods Appl. Mech. Engrg*, **259**, 1–9
- [32] **Roberts, G., Singjai, P.** (2011). Joining carbon nanotubes, *Nanoscale*, **3**, 4503–4514
- [33] **Banhart, F.** (2001). The formation of a connection between carbon nanotubes in an electron beam, *Nano Lett*, **1**, 329–332.
- [34] **Terrones, M., Banhart, F., Grobert, N., Charlier, J.C., Terrones, H., Ajayan, P.M.** (2002). Molecular junctions by joining single-walled carbon nanotubes, *Phys. Rev. Lett.* **89**, 075505.
- [35] **Jang, I., Sinnott, S.B., Danailov, D., Keblinski, P.** (2004). Molecular dynamics simulation study of carbon nanotube welding under electron beam irradiation, *Nano Lett.*, **4**, 109–14.
- [36] **Ni, B. Andrews, R., Jacques, D. Qian, D., Wijesundara, M.B.J., Choi, Y., Hanley, L., Sinnort, S.B.A.** (2001). A combined computational and experimental study of ion-beam modification of carbon nanotube bundles, *J. Phys. Chem. B*, **105**, 12719–12725.
- [37] **Krasheninnikov, A.V., Nordlund, K., Keinonen, J., Banhart, F.** (2002). Ion irradiation-induced welding of carbon nanotubes, *Phys. Rev. B*, **66**, 245403.
- [38] **Lefebvre J., Lynch J.F., Laguno, M., Radosavljevic, M., Johnson, A.T.** (1999). Single-wall carbon nanotube circuits assembled with an atomic force microscope, *Appl. Phys. Lett.* **75**, 3014–3016.
- [39] **Postma, H.W.C., de Jonge, M., Yao Z., Dekker, C.** (2000). Electrical transport through carbon nanotube junctions created by mechanical manipulation, *Phys. Rev. B*, **62**, 10653.
- [40] **Chiu, P.W., Duesberg, G.S., Weglikowska, U.D., Roth S.** (2002). Interconnection of carbon nanotubes by chemical functionalization, *Appl. Phys. Lett*, **80**, 3811–3813.
- [41] **Meng, F.Y, Shi, S.Q., Xu, D.S, Yang, R.** (2004). Multiterminal junctions formed by heating ultrathin single-walled carbon nanotubes, *Phys. Rev. B*, **70**, 125418.
- [42] **Meng, F.Y, Shi, S.Q., Xu, D.S, Chan, C.T.** (2006). Mechanical properties of ultrathin carbon nanotube junctions, *Modelling Simul Mater Sci Eng*, **14**, 1–8.
- [43] **Meng, F.Y, Shi, S.Q., Xu, D.S, Yang, R.** (2006). Size effect of X-shaped carbon nanotube junctions, *Carbon*, **44**, 1263–1266.
- [44] **Meng, F.Y, Shi, S.Q., Xu, D.S, Chan, C.T.,** (2006). Surface reconstructions and stability of X-shaped carbon nanotube junction, *J. Chem. Phys.* **124**, 024711.
- [45] **Meng, F.Y., Liu, W.C., Shi, S.Q.** (2009). Tensile deformation behavior of carbon nanotube junctions, *NSTI-Nanotech 3 Nano Science and Technology Institute*, 450–453.

- [46] **Stormer, B.A. Piper, N.M., Yang, X.M., Tao, T., Fu, Y., Kirca, M., To, A.C.** (2012). Mechanical properties of SWNT X-Junctions through molecular dynamics simulation, *International Journal of Smart and Nano Materials*, **3**, 33–46
- [47] **Liu, W.C., Meng, F.Y., Shi, S.Q.** (2010). A theoretical investigation of the mechanical stability of single-walled carbon nanotube 3-D junctions, *Carbon*, **48**, 1626-1635.
- [48] **Yang, H., Han, Z., Li, Y. Chen, D., Zhang, P., To, A.T.** (2012). Heat welding of non-orthogonal X-junction of single-walled carbon nanotubes, *Physica E*, **46**, 30–32
- [49] **Wang, M., Wang, J., Chen, Q., Peng, L-M.** (2005). Fabrication and electrical mechanical Properties of Carbon Nanotube Interconnections. *Adv. Funct. Mater.*, **15**, 1825-1831.
- [50] **Dimaki, M., Bøggild, P., Svendsen, W.** (2007). Temperature response of carbon nanotube networks, *J. Phys.: Conf. Ser.*, **61**, 247–251.
- [51] **Rahatekar, S.S, Koziol, K.K., Kline, S.R., Hobbie, E.K., Gilman, J.W., Windle, A.H.** (2009). Length-dependent mechanics of carbon-nanotube networks, *Adv. Mater.* **21**, 874–878.
- [52] **Gorrasi, G., Lieto, R.D., Patimo, G., Pasquale, S.D., Sorrentino, A.** (2011) Structure-property relationships on uniaxially oriented carbon nanotube/polyethylene composites, *Polymer*, **52**, 1124–1132.
- [53] **Chen, L., Ozisik, R., Schadler, L.S.** (2010). The influence of carbon nanotube aspect ratio on the foam morphology of MWNT/PMMA nanocomposite foams, *Polymer*, **51**, 2368–2375.
- [54] **Slobodian, P., Riha, P., Lengalova, A., Saha, P.** (2011). Compressive stress-electrical conductivity characteristics of multiwall carbon nanotube networks, *J. Mater.Sci.*, **46**, 3186–3190.
- [55] **Zavodchikova, M.Y., Nasibulin, A.G., Kulmala, T., Grigoras, K., Anisimov, A.S., Franssila, S., Ermolov, V., Kauppinen, E.I.** (2009). Novel carbon nanotube network deposition technique for electronic device fabrication, *Phys. Stat. Sol.*, **245**, 2272–2275.
- [56] **Cassell, A.M, McCool, G.C., Ng, H.T., Koehne, J.E., Chen, B., Li, J., Han, J. Meyyappan, M.** (2003). Carbon nanotube networks by chemical vapor deposition, *Appl. Phys. Lett.*, **82**, 817–819.
- [57] **Jang, E.Y., Kang, T.J., Im, H.W., Kim, D.W., Kim, Y.H.** (2008). Single-walled carbon-nanotube networks on large area glass substrate by the dip-coating method, *Small*, **12**, 2255–2261.
- [58] **Lee, H.S., Yun, C.H., Kim, S.K., Choi, J.H., Lee, C.J., Jin, H.J., Lee, H., Park, S.J., Park, M.** (2009). Percolation of two-dimensional multiwall carbon nanotube networks, *Appl. Phys. Lett.*, **95**, 134104.
- [59] **Snow, E.S, Novak, J.P., Campbell, P.M., Park, D.** (2003). Random networks of carbon nanotubes as an electronic material, *Appl. Phys. Lett.*, **82**, 2145–2147.

- [60] **Snow, E.S, Novak, J.P., Lay, M.D. Houser, E.H. Perkins, F.K., Campbell, P.M.** (2004). Carbon nanotube networks: nanomaterial for macroelectronic applications, *J. Vac. Sci. Technol. B*, **22**, 1990–1994.
- [61] **Jaber-Ansari, L., Hahm, M.G., Kim, T.H., Somu, S., Busnaina, A. Jung, J.Y.** (2009). Largescale highly organized single-walled carbon nanotube networks for electrical devices, *Appl. Phys. A-Mater.*, **96**, 373–377.
- [62] **Tu, Y., Lin, Y., Yantasee, W., Ren, Z.** (2004). Carbon nanotubes based nanoelectrodearrays: fabrication, evaluation, and application in voltammetric analysis, *Electroanalysis*, **17**, 79–84.
- [63] **Novak, P.J., Lay, M.D., Perkins, F.K., Snow, F.K.** (2004), Macroelectronic applications of carbon nanotube networks, *Solid State Electron*, **48**, 1753–1756.
- [64] **Tai, N.H., Yeh, M.K., Liu, J.H.** (2004). Enhancement of the mechanical properties of carbon nanotube/phenolic composites using a carbon nanotube network as the reinforcement, *Carbon*, **42**, 2735–2777.
- [65] **Li, C., Chou, T.W.** (2008). Modeling of damage sensing in fiber composites using carbon nanotube networks, *Compos. Sci. Technol.*, **68**, 3373–3379.
- [66] **Thostenson, E.T., Chou, T.W.** (2006). Carbon nanotube networks: sensing of distributed strain and damage for life prediction and self healing, *Adv. Mater.*, **18**, 2837–2841.
- [67] **Coluci, V.R., Dantas, S.O., Jorio, A., Galvao, D.S.** (2007). Mechanical properties of carbon nanotube networks by molecular mechanics and impact molecular dynamics calculations, *Phys. Rev. B*, **75**, 075417.
- [68] **Coluci, V.R., Pugno, N.** (2010). Molecular Dynamics Simulations of Stretching, Twisting and Fracture of Super Carbon Nanotubes with Different Chiralities: Towards Smart Porous and Flexible Scaffolds, *Journal of Computational and Theoretical Nanoscience*, **7**, 1294–1298,
- [69] **Li, Y., Qiu, X., Yang, Yin, Y., Fan, Q.** (2009). Stretching-dominated deformation mechanism in a super square carbon nanotube network, *Carbon*, **47**, 812-819.
- [70] **Liu, X., Yang, Q.S., He, X.Q., Mai, Y.W.** (2011). Molecular mechanics modeling of deformation and failure of super carbon nanotube networks, *Nanotechnology*, **22**, 475701-475711.
- [71] **Xie, B., Liu, Y. Ding, Y., Zheng, Q., Xu, Z.** (2011). Mechanics of carbon nanotube networks: microstructural evolution and optimal design, *Soft Matter*, **7**, 10039-10047.
- [72] **Li, Y., Qiu, X., Yin, Y., Yang, F., Fan, Q.** (2009). The specific heat of carbon nanotube networks and their potential applications, *J. Phys. D: Appl. Phys.* **42**, 155405.
- [73] **Cao. G.** (2004). *Nanostructures & Nanomaterials: Synthesis, Properties & Applications*. Imperial College Press, London.

- [74] **Rogers, B., Pennathu S., Adams, J.** (1977). *Nanotechnology: Understanding Small Systems*, CRC Press, Boca Raton, Florida.
- [75] **Shenderova, O.A., Zhirnov, V.V., Brenner. D.W.** (2002). Carbon Nanostructures. *Critical Reviews in Solid State and Materials Sciences*, **27**, 227–356.
- [76] **Terrones, M., Botello-Méndez, A.R., Campos-Delgado, J., López-Urías, F., Vega-Cantú, Y.I., Rodríguez-Macías, F.J., Elías, A., Sandoval, E.M., Cano-Márquez, A.G., Charlier, J., Terrones, H.,** (2010) Graphene and graphite nanoribbons: Morphology, properties, synthesis, defects and applications. *Nano Today*, **5**, 351–372.
- [77] **Ercolessi, F.** (1997). *A Molecular Dynamics Primer*, Spring College in Computational Physics, ICTP, Trieste.
- [78] **Allen, M.P.** (2004). Introduction to molecular dynamics simulation, *Computational Soft Matter*, **23**, 1-28.
- [79] **Pyrzynska, K.,** (2011) Carbon nanotubes as sorbents in the analysis of pesticides, *Chemosphere*, **83**, 1407–1413
- [80] **Frankel, D., Smit. B.** (1996). *Understanding Molecular Simulation: From Algorithms to Applications*, Academic Press, California.
- [81] **Yao, Z., Zhu, C-C., Cheng, M. Liu, J.,** (2001). Mechanical properties of carbon nanotube by molecular dynamics simulation, *Computational Materials Science*, **22**, 181-184.
- [82] **Griebel, M., Hamaekers, J.** (2004). Molecular dynamics simulations of the elastic moduli of polymer–carbon nanotube composites, *Comput. Methods Appl. Mech. Engrg.*, **19**, 1773–1788.
- [83] **Rappe, A.K., Casewit, C.J., Colwell, K.S., Goddard, W.A., Skiff, W.M.** (1992). A full periodic table force field for molecular mechanics and molecular dynamics simulations, *J Am Chem Soc*, **114**, 10024–10035.
- [84] **Xiao, J.R., Gama, B.A., Gillespie, J.W.,** (2005). An analytical molecular structural mechanics model for the mechanical properties of carbon nanotubes, *Int. J. Solids Struct.*, **42**, 3075–3092.
- [85] **Rossi, M., Meo, M.** (2009). On the estimation of mechanical properties of single-walled carbon nanotubes by using a molecular-mechanics based FE approach, *Composite Science and Technology*, **69**, 1394-98.
- [86] **Meo, M., Rossi, M.** (2006). Tensile failure prediction of single wall carbon nanotube, *Eng. Fract. Mech.*, **73**, 2589–2599.
- [87] **Meo, M., Rossi, M.** (2007). A molecular-mechanics based finite element model for strength prediction of single wall carbon nanotubes, *Materials Science and Engineering A*, **454 -455**, 170-177.
- [88] **Tserpes, K.I., Papanikos, P., Tsirkas, S.A.** (2006). A progressive fracture model for carbon nanotubes, *Composites: Part B*, **37**, 662–669.
- [89] **Tersoff, J.** (1988). New empirical approach for the structure and energy of covalent systems. *Physical review B*, **37**, 6991-7000.

- [90] **Tersoff, J.** (1989). Empirical interatomic potential for Carbon, with applications to Amorphous Carbon, *Physical Review Letters*, **61**, 2879-2882.
- [91] **Brenner, D.W.** (1990). Empirical potential for hydrocarbons for use in simulating the chemical vapor-deposition of diamond films, *Phys.Rev. B*, **42** , 9458–9471.
- [92] **Brenner, D.W.** (1990). Erratum: Empirical potential for hydrocarbons for use in simulating the chemical vapor deposition of diamond films, *Phys. Rev. B*, **42**, 9458.
- [93] **Brenner, D. W., Shenderova, O. A., Harrison, J. A., Stuart, S. J., Ni, B., Sinnott S.B.** (2002). A second-generation reactive empirical bond order (REBO) potential energy expression for hydrocarbons, *J. Phys.: Condens. Matter*, **14**, 783–802.
- [94] **Stuart, S.J., Tutein, A.B., Harrison, J.A.** (2000). A reactive potential for hydrocarbons with intermolecular interactions, *J. Chem. Phys.*, **112**, 6472.
- [95] **Lennard–Jones, J.E.** (1924) The determination of molecular fields: from the variation of the viscosity of a gas with temperature, *Proc Roy Soc* 106A-441.
- [96] **Battezzatti, L., Pisani, C., Ricca F.** (1975). Equilibrium conformation and surface motion of hydrocarbon molecules physisorbed on graphite, *J. Chem. Soc.*, **71**, 1629–1639.
- [97] **Mylvaganam, K., Zhang, L.C.** (2004). Important issues in a molecular dynamics simulation for characterising the mechanical properties of carbon nanotubes, *Carbon*, **42**, 2025–2032.
- [98] **Wernik, J.B., Meguid, S.H.** (2010). Atomistic-based continuum modeling of the nonlinear behavior of carbon nanotubes, *Acta Mech*, **212**, 167–79.
- [99] **Kudin, K.N., Scuseria, G.E., Yakobson, B,I,** (2001). C₂F, BN and C nanoshell elasticity from ab initio computations, *Phys Rev B*, **64**, 235406.
- [100] **Tu, Z., Ou-Yang, Z.** (2002). Single-walled and multiwalled carbon nanotubes viewed as elastic tubes with the effective Young’s moduli dependent on layer number, *Phys Rev B*, **65**, 233407.
- [101] **Giannopoulos, G.I., Kakavas, P.A., Anifantis, N.K.** (2008). Evaluation of the effective mechanical properties of single walled carbon nanotubes using a spring based finite element approach. *Comput. Mater. Sci.*, **41**, 561–569.
- [102] **Gupta, S., Dharamvir, K., Jindal, V.K.** (2005). Elastic moduli of single-walled carbon nanotubes and their ropes, *Phys. Rev. B*, **72**, 65428.
- [103] **To, C.W.S.** (2006). Bending and shear moduli of single-walled carbon nanotubes, *Finite Elem. Anal. Des.* **42**, 404–413.
- [104] **Ávila, A.F., Lacerda, G.S.R.** (2008). Molecular mechanics applied to single-walled carbon nanotubes, *Mater Res*, **11**, 325-333.

- [105] **Zhao, P., Shi, G.** (2011) Study of Poisson's ratios of graphene and single-walled carbon nanotubes based on an improved molecular structural mechanics model. *SL*, **5**, 49-58.
- [106] **Stone, A.J., Wales, D.J.**, (1986). Theoretical studies of icosahedral C₆₀ and some related species, *Chem. Phys. Lett.*, **128**, 501–503.
- [107] **Andzelm, J., Govind, N., Maiti, A.** (2006). Nanotube-based gas sensors – Role of structural defects, *Chemical Physics Letters*, **421**, 58–62.
- [108] **Bryning, M.B., Milkie, D.E., Islam, M.F., Hough, L.A., Kikkawa, J.M., Yodh, A.G.** (2007). Carbon nanotube aerogels, *Adv. Mater*, **19**, 661-664.
- [109] **Pekala, R.W.** (1989). Organic aerogels from the polycondensation of resorcinol with formaldehyde. *Journal of Materials Science*, **24**, 3221–3227.
- [110] **Li, Y., Qiu, X., Yin, Y., Yang, F., Fan, Q.** (2009). The specific heat of carbon nanotube networks and their potential applications, *J. Phys. D: Appl. Phys.* **42**, 155405.
- [111] **Lin, Y., Cai, W., Shao, X.** (2006). Fullerenes connected nanotubes: an approach to build multidimensional carbon nanocomposites, *Chem. Phys.* **331**, 85–91.
- [112] **Reddy, A.L.M., Ramaprabhu, S.**, (2007). Design and fabrication of carbon nanotube-based microfuel cell and fuel cell stack coupled with hydrogen storage device, *Int. J. Hydrogen Energ.*, **32**, 4272–4278.
- [113] **Biro, L.P., Horvath, Z.E., Mark, G.I., Osvath, Z., Koos, A.A., Benito, A.M., Maser, W., Lambin, P.H.** (2004). Carbon nanotube Y junctions: growth and properties, *Diam. Relat. Mater.*, **13**, 241–249.
- [114] **Su, J.W., Fu, S-J., Gwo, S., Lin, K-J.** (2008). Fabrication of porous carbon nanotube network, *Chem. Commun.*, 5631–5632.
- [115] **Chen, Z., Yang, Y., Chen, F., Qing, Q., Wu, Z., Liu, Z.** Controllable Interconnection of Single-Walled Carbon Nanotubes under AC Electric Field, *The Journal of Physical Chemistry B Letters*, **109**, 11420-11423..
- [116] **Menon, M., Srivastava, D.** (1997). Carbon nanotube “T Junctions”: nanoscale metal semiconductor-metal contact devices, *Phys. Rev. Lett.*, **79–22** 4453–4456.
- [117] **Tomblor, T.W., Chongwu, Z., Alxseyev, L., Jing, K., Hongjie, D., Lei, L., Jayanthi, C.S., Meijie, T., Shi-Yu, W.** (2000). Reversible electromechanical characteristics of carbon nanotubes under local-probe manipulation, *Nature*, **405**, 769–772.
- [118] **Zavodchikova, M.Y., Kulmala, T., Nasibulin, A.G., Ermolov, V., Franssila, S., Grigoras, K., Kauppinen, E.I.** (2009). Carbon nanotube thin film transistors based on aerosol methods, *Nanotechnology*, **20**, 085201.
- [119] **Srivastava, D., Wei, C.** (2003). Nanomechanics of carbon nanotubes and composites, *Appl. Mech. Rev.*, **56**, 215–230.

- [120] **Wang, M., Qiu, X., Zhang, X.** (2007). Mechanical properties of super honeycomb structures based on carbon nanotubes. *Nanotechnology*, **18**, 1-6.
- [121] **Baykasoglu C,** (2012). Prediction of mechanical behavior of carbon- based nano structures. *PhD Thesis*, ITU, Istanbul, Turkey.
- [122] **Url-1** <<http://nanoscience.massey.ac.nz/>>, 24.04.2013
- [123] **Url-2** <<http://www.intechopen.com>>, 24.06.2013.
- [124] **Url-3** <<http://www.ndt-ed.org>, 12.07.2013.
- [125] **Url-4** <[https://en.wikipedia.org/wiki/Yield_\(engineering\)](https://en.wikipedia.org/wiki/Yield_(engineering)), 12.07.2013.
- [126] **Url-5** <https://en.wikipedia.org/wiki/Poisson's_ratio, 12.07.2013.
- [127] **Url-6** <<http://lammps.sandia.gov/> 12.07.2013.

APPENDICES

CURRICULUM VITAE



Name Surname: Alper Tunga ÇELEBİ
Place and Date of Birth: Sakarya 15.06.1988
Address: Sarıyer/İSTANBUL
E-Mail: celebial@itu.edu.tr
B.Sc.: Istanbul Technical University, Department of Mechanical Engineering

List of Publications and Patents:

1. **Celebi, A.T.**, Icer, E., Kirca, M., Baykasoglu, C., Mugan, A., 2013. Analysis of Junctions in Carbon Nanotube Networks. “9th NanoTR Conference”, June 24-28, 2013 Erzurum, Türkiye.
2. Icer, E., **Celebi, A.T.**, Kirca, M., Baykasoglu, C., Mugan, A., 2013. Comparison of the strain behavior of nanoporous Cu. “9th NanoTR Conference”, June 24-28, 2013 Erzurum, Türkiye.
3. Baykasoglu, C., **Celebi A.T.**, Icer E., Mugan A., 2013. Nonlinear Fracture Analysis of Carbon Nanotubes with Stone-Wales Defects. 3rd South-East European Conference on Computational Mechanics, June 12-14, 2013 Kos Island, Greece

4. Baykasoglu, C., Icer, E., **Celebi, A.T.**, Mugan, A., 2013. Vibration and Elastic Buckling Analyses of Single-Layer Carbon Nanocones. *3rd South-East European Conference on Computational Mechanics*. June 12-14, 2013 Kos Island, Greece
5. Eren, M.M., Yucel, T., Yildiz, E., **Celebi, A.T.**, Icer, E., Baykasoglu, C., Mugan, A. Influence of Different Luting Cement on the Stress Distribution in Maxillary Central Incisor Restored By Composite Laminate Veneer: A 3D-finite element analysis. *CONSEURO Paris 2013*, May 9-11, 2013 Paris, France.
6. Eren, M.M.,**Celebi, A.T.**, Icer, E., Baykasoglu, C., Yildiz, E.,Mugan, A., 2012. Three-dimensional Finite Element Analysis of Sound Incisor and Porcelain Veneers. *SIMULIA Abaqus Turkey Regional Users Meeting*, November 8-9, 2012 Istanbul, Turkey